זיהוי ואפיון גנים ב *Fusarium oxysporum* המעורבים בפתוגנזה בצמחי מלון

חיבור לשם קבלת תואר דוקטור לפילוסופיה

מאת

יוליה דניסוב

הוגש לסנאט האוניברסיטה העברית, בירושלים

אפריל 2010

עבודה זו נעשתה בהדרכתם של:

פרופ׳ עודד ירדן,

המחלקה למחלות צמחים ומיקרוביולוגיה, הפקולטה לחקלאות, מזון וסביבה ע״ש רוברט ה. סמית,

האוניברסיטה העברית בירושלים, רחובות.

ד״ר סטנלי פרימן

המחלקה למחלות צמחים וחקר עשבים, מנהל המחקר החקלאי, בית דגן

תקציר

תת-המין *Fusarium oxysporum* f.sp. *melonis* (FOM) כולל תבדידי פטריות אל-מיניות, פתוגניות שוכנות-קרקע שגורמות למחלת נבילה של צמחי מלון. אחד מארבעת הגזעים המוכרים של הפטרייה, 1,2 קטלני ביותר ופוגע ברוב זני המלון הידועים בשל אופיה הפוליגני של העמידות. בעבודה זו בחרנו להתמקד בגזע ספציפי זה. הדבקה מוצלחת על ידי פטריות הינה תהליך רב-שלבי המבוסס על יחסי גומלין בין הפתוגן לצמח, כאשר הצלחתה כרוכה בהתגברות על תגובות הצמח בכל שלב בין שינוי ביטוי גנים פטרייתיים בהתאם לאותות הצמח. יצור ואפיון של תבדידים מותמרים גנטית בעלי פתוגניות פחותה הינה שיטה אטרקטיבית ביותר המסייעת בחקר תהליך הפתוגנזה. מחקר זה נועד לאתר ולאפיין גנים הקשורים לתהליך הפתוגני של פטריית FOM. להשג המטרה זו שומשו שתי אסטרטגיות מחקר: א) אפיון מוטנט UV לא פתוגני של FOM; ב) יצירה ואפיון של תבדידים מותמרים גנטית בעלי פתוגניות פחותה על ידי שימוש בשיטת ה *Agrobacterium tumefaciens*-mediated transformation (ATMT).

בחלק הראשון של עבודת המחקר אופיין מוטנט ה-UV הלא פתוגני (מוטנט 4/4), שהוצע בעבר לשמש כמדביר ביולוגי. במסגרת המחקר, על ידי שימוש במקורות פחמן שונים, ערכנו מבחן השוואתי של קצב גידול, הנבגה, הצטברות ביומאסה והפרשת אנזימים חוץ תאיים, ונמצא כי המוטנט 4/4 מעוכב בכל הפרמטרים ההתפתחותיים הללו לעומת תבדיד הבר. תוספת של תמצית שמרים, אדנין (adenine) או היפוקסנתין (hypoxanthine), אבל לא גואנין (guanine) למצע הגידול הביאו להגברת קצב הגידול, הפרשת אנזימים צלוליטיים והגברת פעילותם עד לרמות הדומות לאלו של תבדיד הבר. לפיכך הסקנו שהמוטנט 4/4 הינו מוטנט חסר באדנין. בנוסף, נמצא כי הדגרת נבגים של המוטנט 4/4 בתמיסת אדנין לפני הדבקה צמחי מלון, משלימה חלקית את הפתוגניות. למרות שהגורם המגביל הספציפי שמקשר בין דרישה לאדנין לפתוגניות טרם זוהה, החשיבות של נתיב ביוסינטתי בסיסי הודגמה כרלוונטית לתהליך הפתוגני של FOM.

בהמשך העבודה, יצרנו אוסף של כ- 2000 טרנספורמנטים של FOM באמצאות ATMT. לאחר סריקתם על צמחי מלון נמצאו שישה תבדידים בעלי פתוגניות פחותה, שהפגינו בנוסף לכך עיקוב בהופעת סימנים ראשוניים והאטה כללית של המחלה. שימוש בשיטת thermal asymmetric interlaced (TAIL)-PCR איפשר לאתר מחדרים בדנ"א הגנומי (הן באזורים המקודדים והן ב אזורי 5'-UTR) של התבדידים הנבחרים. בשיטה זו אותרו ארבעה גנים (*pex7*, *hop78*, *cdc48*, ו *snt2* שמקודדים לגורם ביוסינתתי של

פרוקסיסומות (peroxisomes) 7, טרנספוזאז ממשפחת mutator, חלבון המעורב בחלוקת תאים ומוות תאי מתוכנן וגורם שיעתוק, בהתאמה). האפיון הראשוני של התבדידים בעלי הפתוגניות הפחותה מגלה הבטים חדשים הקשורים למעורבותם של תהליכים כמו ביוסינתזה של פרוקסיסומות ומוות תאי מתוכנן בתהליך פתוגני של *F. oxysporum*. אחד התבדידים הנבחנים שכונה D122, נמצא פגום בגן המקודד לגורם שיעתוק SNT2 ההומולוגי לגורם שיעתוק שתואר ב *Schizosaccharomyces pombe*. מוטנט D122 גורם ל 20% תמותת שתילים ולהאטה משמעותית של הופעת הסימנים הראשוניים של מחלת הנבילה במלון בהשוואה לתבדיד הבר ועקב כך נבחר המוטנט D122 לעמוד במוקד המחקר. מעורבותו של *snt2* בפתוגנזה של FOM הוכחה על ידי שיבוש מכוון של הגן. בדיקת real time PCR (qRT-PCR) של ביטוי *snt2* ברקמת הפונדקאי הראתה מעורבותו של הגן בשלב התחלתי של התהליך הפתוגני. חלבון ה-SNT2 של FOM נושא חמישה אזורים שמורים: bromo-adjacent domain (BAH), שלושה plant homeodomain Zn fingers (PHD) ו Zn-finger מסוג GATA. נוכחותם של אזורים BAH ו PHD מאפיינת את SNT2 כגורם שעתוק שמעורב בדיכוי השעתוק דרך מעורבות בהתמרת כרומטין. בעבודה זו אופיינו, פנוטיפית, תבדידי Δ*snt2* של שתי פטריות השייכות למחלקת ה-Ascomycota – FOM ו *Neurospora crassa*. בשתי הפטריות שיבוש הגן *snt2* גרם לשילוב תסמינים דומה, כולל הפחתה בייצור נבגים, האטה בגידול וגטטיבי והצטברות ביומאסה. כמו כן, התגלו חריגות במיקום מחיצות ובתבניות צביעה בתאי התפטיר על ידי Congo red. תכונה נוספת שנצפתה במוטנט Δ*snt-2* של *N. crassa*, מעידה על מעורבותו של *snt2* בהתרבותה המינית של הפטרייה, מכיוון שהמוטנט Δ*snt-2* לא יצר גופי פרי בשלים, אלה פרוטופריתציות בלבד. על מנת לפענח את רשת הגנים המבוקרים על ידי *snt2*, נעשה שימוש בשיטה Suppression subtractive hybridization (SSH), משולבת עם בדיקת ביטוי qRT-PCR. ארבעה גנים (*idi4*, induced during incompatibility; *pdc*, pyruvate decarboxylase; *msf1*, transporter of the major facilitator family and *eEF1G*, eukaryotic translation elongation factor 1-gamma) מתוך ארבעה עשר שהתגלו בשיטת SSH, ידועים כמבוקרים על ידי נתיב בקרה שמור TOR (target of rapamycin) בפתוגן של אורז *Fusarium fujikuroi*. בדיקות qRT-PCR זיהו שינוי משמעותי בביטוי של שני גנים – *idi4* ו *pdc* במוטנט Δ*snt2* של FOM. בנוסף ב *N. crassa*, שיבוש מכוון של *snt-2* גרם לביטוי יתר של גן *idi-4*, הידוע כמקושר לתהליכי אוטופגוציטוזה. אחרים הראו

ש *idi4* הינו גן ייחודי לפטריות, שמעורב בתגובה למצבי עקה, ומושרה על ידי הרעבה ואי-התאם זוויגי, הגן מבוקר על ידי TOR קינאז והמבקר הגלובלי של מטבוליזם חנקני AreA. לפיכך בחנו את מעורבותו של *snt2* במטבוליזם של חנקן ואוטופגוציטוזה. מבחני גידול במוטנטים של *snt2* ב FOM על מקורות חנקן כמו ניטראט ואמוניה לא חשפו הבדלים מובהקים בהשוואה לתבדיד הבר. לעומת זאת, גידול מוטנטים של *snt2* על גלוטמאט היה מעוקב מזה של תבדיד הבר. אך למרות זאת, ביטויים של שלושה גנים המקודדים למבקרים ראשים של מטבוליזם חנקני בפוזאריום, כולל גלוטמין סינטאז (glutamine synthase) (*glnA*), האחראי על ניצול של גלוטמאט, *fnr1* – הומולוג של *areA* ב *F. oxysporum*, ו *nit4* – הומולוג של מבקר מטבוליזם חנקני ב *N. crassa*, לא השתנה בעקבות שיבוש בגן *snt2*. יתרה מכך, העובדה שהתבדידים הנבחנים לא ניצלו כלוראט, וגדלו על היפוקסנתין, מוכיחה העדר פגמים במסלול חיזור חנקן. ייתכן ש *snt2* אינו נחוץ לניצול חנקן, ועיקוב כללי בגידול של מוטנטים *snt2* ב FOM ו *N. crassa*, כנראה מעובר דרך מסלולים אחרים. במחקר זה מצאנו שתוספת של רפאמיצין עיקבה גידול של מוטנטים *snt2* ושל תבדיד הבר של FOM באופן דומה, כמו כן, ביטוי של *snt2* לא הושפע מתוספת רפאמיצין. לאור התוצאות הסקנו ש *snt2* אינו מבוקר על ידי TOR קינאז. יתרה על כך, הופעה מוגברת של אוטופגוסומים, מלווית במוות תאי מוגבר נצפתה במוטנטים של *snt2* ב FOM. בנוסף נמצא כי גם מוטנט *snt-2* Δ של *N. crassa* מאופיין במוות תאי מוגבר. לפיכך שערנו ששילוב בין ביטוי יתר של גן *idi-4* עם הופעה מוגברת של אוטופגוסומים, מוות תאי מוגבר ופגמים מורפולוגיים הכוללים אי-סדירות במיקום מחיצות בין תאים ותבנית צביעה של תאי תפטיר על ידי Congo red מעידים על מצב עקה בו נתונים המוטנטים בעקבות פגיעה ב *snt2*. בהמשך העבודה, נבחנה הרגישות למצבי עקה על ידי ניטור תגובה של *snt2* מוטנטים לרדיקלים חופשיים של חמצן (reactive oxygen species - ROS). רגישות זו נבחנה על ידי ניטור פעילותה של קבוצת האנזימים superoxide dismutases (SOD) וביטוי הגנים המקודדים לאנזימים אלה לאחר תוספת מי חמצן. בתבדידי הבר של FOM ו *N. crassa* נצפתה עלייה בפעילות של SOD בעקבות העקה החמצנית, בניגוד ל *snt2* מוטנטים שאופיינו בחוסר תגובה. בנוסף לכך, נמצא כי תוספת מי החמצן גרמה לעליה בביטוי גנים המקודדים לתת-קבוצה של אנזימי SOD (*fe,mn sod*), במוטנטים של *snt2* הן ב- FOM והן ב- *N. crassa*. ביטוי גנים שמקודדים לתת-קבוצה שנייה של SOD (*cu,znsod*), לא השתנה לאחר מתן עקה חמצנית. התוצאה הדגישו

לא רק את אופן הבקרה של אנזימי Fe,MnSOD המתרחשת, ככל הנראה, בשלב שלאחר השעתוק (post-transcriptional regulation), אלא גם הצביעו על פגם אפשרי בתפקוד המיטוכונדריה שנגרם בעקבות שיבוש של *snt2*. התיפקוד המיטוכונדריאלי נבדק על ידי ניטור צריכת החמצן. ואכן, התגלה כי ב- FOM וב- *N. crassa*, שיבוש של *snt2* השפיע על מערכת החמצון הראשית, תלוית ציטוכרום (cytochrome-dependent) הוביל לצריכת חמצן מופחתת, עובדה המקשרת בין פעילות הגן לבין בקרת הנשימה האירובית הפטרייתית. תהליך זה היה מלווה גם בביטוי יתר של הגן *aod1* המקודד ל alternative oxidase, וככל הנראה מצביע על המנגנון המפצה, או אפילו על קשר ישיר בין *snt2* ורגולציה של alternative oxidation. היחסים בין הנשימה המיטוכונדריאלית וייצור ROS מורכבים ועדיין לא מובנים במלואם. בעבודה זו אנו מדווחים כי שיבוש *snt2* בשתי פטריות חוטיות גורם לירידה בנשימה המיטוכונדריאלית ומשפיע על תגובת SOD לעקה חמצנית ברמת החלבון והדנ״א. זוהי לדעתינו עדות נוספת המחברת בין שני התחומים הפונקציונאליים. גן נוסף, ייחודי ל FOM, בעל תפקיד לא ידוע שכונה (*rbs1*) regulated by *snt2* התגלה בסריקת SSH. הביטוי שלו נמצא ירוד משמעותית, במוטנטים *snt2* של FOM.

לסיכום, כמתואר במחקר זה, שיתוף בקרה בין *snt2* ל TOR קינאז מייצג אלמנט נוסף להבנת נתיבים רגולטוריים בפטריות חוטיות. ״החפיפה״ הרגולטורית הינה שכיחה בביולוגיה ומספקת בסיס חזק לשרידות תאית. במחקר זה, שוער כי יכולתה הירודה של הפטרייה לנטרל רעלני ROS המיוצרים באופן טבעי במיטוכונדריה מוביל לנזק תוך תאי, שגורם לעלייה בביטוי גנים מעורבים בעקה ולירידה בנשימה. הנשימה הירודה יכולה בהמשך להוביל להצטברות ROS נוספת ולמוות של תאים, בעוד אוטופגיה משמשת כמערכת הגנה. אנו מניחים שפגמים במערכת תגובה ל ROS תורמים לפתוגניות מופחתת במוטנטים *snt2* של FOM.

גילוי ואפיון גורם השעתוק הפטרייתי SNT2 שופך אור על מנגנוני הפתוגנזה, ומדגים את מעורבותו בתהליכים תאיים כגון צמיחה, רבייה מינית, נשימה, תגובה למצבי עקה ופותח אפשרויות למחקר עתידי הבוחן את מעורבותו במסלולים גנטיים הקשורים לתהליך הפתוגני בפטרייה FOM.

Identification and characterization of *Fusarium oxysporum* genes involved in pathogenicity on muskmelon

Thesis submitted for degree of
"Doctor of Philosophy"
By

Youlia Denisov

Submitted to the Senate of the Hebrew University of Jerusalem
April 2010

This work was carried out under the supervision of:

Prof. Oded Yarden,

The Department of Plant Pathology and Microbiology, The Robert H. Smith Faculty of Agricultural, Food and Environment, Hebrew University of Jerusalem, Rehovot, Israel

Dr. Stanley Freeman,

The Department of Plant Pathology and Weed Research, Agricultural Research Organization - The Volcani Center, Bet-Dagan, Israel

ABSTRACT

The soilborne, asexual fungus *Fusarium oxysporum* f.sp. *melonis* (FOM) is a causal agent of muskmelon wilt disease. One of the four races, 1,2 of FOM, is the most virulent of the four known races affecting most commercial cultivars due to polygenic nature of host resistance. We therefore chose to focus our studies on this race. A successful infection by *F. oxysporum* fungi is a multi-staged pathogen-host interaction process, which involves overcoming the host reaction at each stage by altering fungal gene expression according to some of the host signals. Generation and characterization of tagged reduced-pathogenicity mutants is an attractive method to explore fungal pathogenesis. The aim of the present work was to identify and characterize genes of *Fusarium oxysporum* involved in pathogenicity on muskmelon. This goal was achieved by application of two independent strategies: 1) characterization of a previously UV-generated non-pathogenic isolate; 2) generation and characterization of reduced pathogenicity mutants of FOM, by utilizing tagged *Agrobacterium tumefaciens*-mediated mutagenesis (ATMT).

The UV-induced non-pathogenic mutant (strain 4/4) of FOM was previously identified as a potential biological control agent. During comparative analysis of vegetative growth parameters using different carbon sources, mutant strain 4/4 showed a delay in development and secretion of extracellular enzymes, compared to the wild type strain. Amendments of the growth medium with yeast extract, adenine or hypoxanthine, but not guanine, complemented the growth defect of strain 4/4, as well as secretion and partial activity of cellulases and endopolygalacturonases, indicating that the strain is an adenine auxotroph. Incubation of strain 4/4 conidia in an adenine solution, prior to inoculation of muskmelon plants, partially restored pathogenicity to the mutant strain. Even though the specific limiting factor in adenine

requirement that determines pathogenicity has yet to be identified, the importance of a basic biosynthetic pathway was demonstrated to be highly relevant to FOM pathogenicity.

Using ATMT, we produced 2000 tagged FOM mutants. Utilizing the pathogenicity assay, we identified six reduced pathogenicity mutants which also exhibited a delay in initial wilt symptom appearance and slower disease progress, when compared to the wild type. Using thermal asymmetric interlaced (TAIL)-PCR the inserted tag was detected within the coding or 5-UTR regions of four pathogenicity-related genes (*pex7, hop1, cdc48* and *snt2*, coding to peroxisome biogenesis factor 7; *mutator* superfamily transposase; apoptosis-related cell division protein and transcription factor, respectively). This preliminary characterization of tagged reduced-pathogenicity mutants provides interesting prospects of involvement of apoptosis and peroxisome biogenesis in pathogenesis of *F. oxysporum.* The tagged mutant D122**,** which was impaired in the gene encoding an *snt2*-like transcription factor (TF) of *Schizosaccharomyces pombe*, caused delayed appearance of initial wilt disease symptoms as well as a marked reduction in pathogenicity, was chosen as the focus for this study. Involvement of *snt2* in pathogenesis and its requirement for the host colonization ability of *F. oxysporum* were confirmed by targeted disruption. Quantitative real time (qRT) PCR analysis of the *snt2 in planta* identified this gene as expressed specifically during early stage of pathogenesis. The FOM SNT2 protein contains five conserved domains: a bromo-adjacent domain (BAH), three plant homeodomain Zn fingers (PHD) and a GATA-type Zn-finger. Presence of BAH and PHD domains characterize SNT2 as transcription factor involved in transcriptional repression through involvement in chromatin modifications. During this work phenotypical characterization of Δ*snt2* mutants of two Ascomycota fungi – FOM and

Neurospora crassa was performed. In both fungi, disruption of the *snt2* gene caused similar sets of morphological abnormalities, including a reduction in conidia production, slower vegetative growth and biomass accumulation. Moreover, abnormalities in hyphal septation of FOM and *N. crassa snt2* mutants were observed. An additional trait, linking *snt2* to fungal sexual development was detected in Δ*snt-2 N. crassa* mutants that were unable to produce mature perithecia. An attempt to identify a *snt2* genetic network was performed using suppressive subtraction hybridization (SSH) following qRT-PCR gene expression analysis. Four genes (*idi4*, induced during incompatibility; *pdc*, pyruvate decarboxylase; *msf1*, transporter of the major facilitator family and *eEF1G*, eukaryotic translation elongation factor 1-gamma) out of the fourteen detected by the SSH-screen were previously found in association with the target of rapamycin (TOR) kinase pathway in the rice pathogen *Fusarium fujikuroi*. Using qRT-PCR, two of the genes – *idi4* and *pdc* were shown to be over-expressed in Δ*snt2* FOM mutants. In addition, the disruption of *snt-2* causes a significant over-expression of an *idi-4* gene in *N. crassa*. Others have shown that *idi4* is a fungal-specific, stress-responsive gene that is induced during starvation, incompatibility and autophagy and regulated by the TOR kinase and the global nitrogen regulator AreA TF, and therefore the involvement of *snt2* in nitrogen metabolism and autophagy was examined. Use of sole nitrogen sources such as nitrate and ammonia detected no difference between wild type and *snt2* mutants of FOM. The only observed significant delay was during growth on medium containing glutamate as a sole nitrogen source. Nevertheless, expression of three master nitrogen regulators, including glutamine synthetase (*glnA*), which is involved in glutamate processing, *fnr1* (a homolog of *are*A in *F. oxysporum*) and *nit4* (a homolog of pathway-specific nitrogen regulator of *N. crassa*) did not differ significantly in the

Δ*snt2* mutant, when compared to the wild type isolate. Moreover, all the examined isolates were not able to utilize chlorate and were able to grow on hypoxanthine, confirming the absence of defects in the nitrate reduction pathway. Therefore, it is likely that *snt2* is not required for utilization of nitrogen and the general delay of hyphal growth in *snt2* mutants of FOM and *N. crassa* is conveyed through other pathways. It was also found that rapamycin inhibited growth of all tested FOM isolates in a similar manner and did not affect expression of *snt2*, thus excluding *snt2* from a long list of TOR kinase downstream targets. Furthermore, an excessive appearance of mature autophagosomes was observed in FOM *snt2* mutants and was accompanied by increased cell mortality. Interestingly, *N. crassa* the Δ*snt-2* mutant also demonstrated significantly increased cell death rates. This suggests that a combination of the over-expression of the stress-inducible *idi-4* gene along with excessive appearance of autophagosomes, increased cell death, and morphological abnormalities, such as frequent cell wall deposition are indicative of a stress-caused state. Susceptibility to stress was further evaluated by monitoring the reactive oxygen species (ROS) scavenging ability of Δ*snt2* mutants. To do so, activity of superoxide dismutases (SOD) and expression of SOD-coding genes was measured following hydrogen peroxide induction. In the wild type isolates of FOM and *N. crassa*, enzymatic activity of SOD proteins was induced by hydrogen peroxide, in contrast to Δ*snt2* mutants, which were characterized by lack of such a response. In addition, expression of *fe,mn sod* genes of FOM and *N. crassa* Δ*snt2* mutants, but not that of wild type isolates was up-regulated following hydrogen peroxide induction. Expression of Cu,Zn SOD-coding genes of all tested FOM isolates was not affected by hydrogen peroxide. These findings pointed out a possible defect in mitochondrial function caused by *snt2* disruption, which was further studied by testing oxygen

consumption. Indeed, it was detected that in FOM and *N. crassa*, *snt2* disruption affected activity of cytochrome-dependent oxidation leading to reduced oxygen consumption, thus, linking this transcription factor-encoding gene to regulation of fungal aerobic respiration. This was accompanied by up-regulation of the *aod1* gene, coding an alternative oxidase and suggesting the presence of a compensatory mechanism, or even a potential direct link between *snt2* and regulation of alternative oxidation. The relationships between mitochondrial respiration and ROS production are complex and not fully understood. Here we reported that disruption of *snt2* in two filamentous fungi caused reduced cytochrome-dependent respiration and a defect in SOD-dependent response to oxidative stress, providing an additional link between respiration and ROS response. An additional gene, unique to *F. oxysporum*, with so far unknown functions, designated regulated by *snt2* (*rbs1*) was identified during the SSH-screen. Its expression was found to be significantly down-regulated in *snt2* mutants of FOM.

Overall, the displayed shared regulation between *snt2* and TOR kinase is a novel addition to our understanding of regulatory circuits in filamentous fungi. Such regulatory "overlapping" is quite redundant in biology and provides a stronger basis for organism survival. In this study, we hypothesized that the decreased ability to properly detoxify naturally produced ROS in mitochondria leads to mitochondrial and cell damage, leading to up-regulation of stress-related genes and decreased respiration. The latter can subsequently lead to further ROS accumulation and cell death, while autophagy plays a protective role. A damaged ROS-responsive system is also presumed to contribute to the reduced virulence of the FOM *snt2* mutants.

The discovery and characterization of a fungal transcriptional regulator, SNT2, sheds light on pathogenesis, unravels its involvement in cellular processes

such as growth, sexual reproduction, respiration and stress-response, and opens new horizons for identification and research of a novel genetic network.

CONTENTS

8.1. Denisov, Y., Yarden, O. and Freeman, S. Impaired purine biosynthesis affects pathogenicity of *Fusarium oxysporum* f. sp. *melonis.* 2005. *Eur. J. Plant Pathol.* 112:293-297.

8.2. Denisov, Y., Freeman, S. and Yarden, O. Inactivation of Snt2, a BAH/PHD-containing transcription factor, impairs pathogenicity and increases autophagosome abundance in *Fusarium oxysporum.* 2010. *Mol. Plant Pathol.* (Accepted)

List of abbreviations

aa	Amino acids
ATMT	*Agrobacterium tumefaciens*-mediated transformation
CMC	Carboxymethylcellulose
dNTP	Dideoxy nucleotide triphosphate
endoPG	Endopolygalacturonase
EtOH	Ethanol
FLC	Fusarium liquid medium
FMM	Fusarium minimal medium
h	Hour
LSD	Least significant difference
min	Minute
MS	Mass spectrometry
NaPG	Sodium polygalacturonate
O/N	Overnight
PAGE	Polyacrylamide gel electrophoresis
PDA	Potato dextrose agar
rpm	Round per minute
ROS	Reactive oxygen species
RT	Room temperature
RT-PCR	Reverse transcription polymerase chain reaction
SD	Standard deviation
SDS	Sodium dodecyl sulfate
SE	Standard error
SM	Synthetic medium
SOD	Superoxide dismutase
Tris	2-Amino-2-hydroxymethyl-propane-1,3-diol
UV	Ultraviolet
YE	Yeast extract

INTRODUCTION

Fusarium is perhaps the most important genus of plant pathogenic fungi. Together three annotated Fusarium species, *F. oxysporum, F. verticillioides* and *F. graminearum* cause economically important disease on nearly every species of cultivated plants and pose a threat to human health and food safety due to production of mycotoxins. The current research is focused on expanding our knowledge of pathogenicity processes of *F. oxysporum* causing Fusarium wilt disease of over 120 cultivated plant species (Beckman, 1987).

1.1. Fusarium wilt disease of muskmelon

The soilborne, asexual fungus *Fusarium oxysporum* f. sp. *melonis* Snyder & Hansen (FOM) (Nelson *et al.*, 1981) causes vascular wilt disease of melon (*Cucumis melo* L). This phytopathogen is highly-host specific and four physiological races (0, 1, 2, and 1,2) of the pathogen have been identified, according to their reaction with differential melon genotypes (Risser *et al.*, 1976). Resistance to race 1 and race 2 *in planta* is conferred by single dominant genes, *Fom-2* (Joobeur *et al*. 2004) and *Fom-1* (Brotman *et al*. 2002), respectively. Both genes also confer resistance to race 0. Race 1,2 of FOM, initially identified in Israel in 1989, is the most virulent of the four known races affecting most commercial cultivars (Cohen *et al.*, 1989) due to polygenic nature of host resistance (Perchepied and Pitrat, 2004). Fusarium wilt is a monocyclic disease, and a source of primary inoculum is resilient chlamydospores that survive in soils for extended periods of time. After planting, *F. oxysporum* chlamydospores germinate and adhere to the host root surface, penetrate the epidermis and then invade xylem vessels through pits. Host colonization occurs in xylem vessels, where secondary conidiation takes place in order to further penetrate the stem, causing disease symptom, expressed as necrotic lesions, chlorosis and wilting,

leading to eventual plant mortality (Zvirin *et al.,* Doi: 10.1111/j.1365-3059.2009.02225). A successful infection by *F. oxysporum* fungi is a multi-staged pathogen-host interaction process, which involves overcoming the host reaction at each stage by altering fungal gene expression according to some of the host signals. Recently, *F. oxysporum* has been reported as an emerging human pathogen, causing opportunistic mycoses (Nir-Paz, *et al.,* 2004). Furthermore, *F. oxysporum* has been proposed to be used as a model organism for research of fungal virulence mechanisms in both plants and mammals (Ortoneda *et al.*, 2004), and therefore the importance of identification and characterization of its pathogenicity-related genes.

1.2. Identification of pathogenicity-related genes in *Fusarium oxysporum*

Identification of pathogenicity genes is performed mostly by forward or reverse genetics approaches. Diverse methodologies that have been used to explore fungal functional genomics, in general, and pathogenesis, in particular, are comprehensively described in a recent review (Weld *et al.,* 2006). One of the uses of forward genetics is generation of mutants, which are further screened for pathogenicity on host plants. Generation of such isolates is usually performed by random mutagenesis, either chemical (ethyl methanesulfonate [EMS]), radiation (Ultra-violet [UV]) or insertional (restriction enzymes-mediated integration [REMI], *Agrobacterium tumefaciens*-mediated transformation [ATMT] or transposon-arrayed). Use of non-pathogenic UV-mutants was demonstrated in different fungal plant pathogens, such as *F. oxysporum* (Freeman *et al.,* 2002) and *Colletotricum magna* (Freeman and Rodriguez, 1993). However, the major obstacle in characterization of such mutants is location of the mutation, due to the nature of UV irradiation that causes a wide range of DNA defects, including deletions, rearrangements of single and multiple nucleotides to loss of chromosomal fragments. In *F. oxysporum*,

insertional mutagenesis has been also instrumental in the identification of fungal genes involved in pathogenesis by efficient utilization of REMI (Inoue *et al.,* 2001) or ATMT (Mullins *et al.,* 2001). For tagged mutagenesis, ATMT has several advantages as an alternative tool to REMI. For example, ATMT generates a high percentage of transformants with a single insert of T-DNA in the fungal genomes (Mullins *et al.,* 2001), that assists in the subsequent isolation of tagged genes, especially from fungi lacking a sexual stage. Recently, using this technique, a large-scale mutagenesis of the tomato-specific pathogen *F. oxysporum* f.sp. *lycopersici* was performed, identifying more than one hundred reduced-pathogenicity mutants, and verifying five novel pathogenicity-related genes (Michielse *et al.,* 2009).

Utilization of these transformation techniques has led to the detection of twenty nine pathogenicity-related genes of *F. oxysporum* over the last two decades (Michielse and Rep, 2009), which participate in various cellular functions, such as cell wall degradation, signal transduction, transcription and gene expression regulation. Plant colonization is a critical stage for the success of the disease cycle and several genes were found to play an important role in this process. At least six pathogenicity-related genes of *F. oxysporum* involved in root penetration and colonization have been discovered to date. *fow1*, encoding a mitochondrial carrier protein, is required specifically for colonization (Inoue *et al.,* 2002); a $Zn(II)_2Cys6$ transcription factor encoding *fow2* is required for invasive growth of FOM (Imazaki *et al.,* 2007); *frp1,* encoding an F-box protein, is involved in root penetration and colonization (Duyvestejin *et al.,* 2005); *fmk1*, a MAPK encoding gene, is required for root attachment and host-invasive growth (Di Pietro *et al.,* 2001); a *six1* gene encoding a small, cysteine-rich protein that is secreted by *F. oxysporum* during colonization of the xylem of its host, tomato (Rep *et al.,* 2005) and a recently

identified transcriptional regulator-encoding gene *sge1*, is required for parasitic growth (Michielse *et al.,* 2009). The requirement of functional fungal genes involved in fundamental biosynthetic pathways for pathogenicity has been established over the last decade. In FOM, disruption of an arginine biosynthesis gene *arg1*, which converted a wild type strain into an auxotroph, led to reduced pathogenicity (Namiki *et al.,* 2001), while in the rice blast fungus *Magnaporthe grisea* two amino acid auxotrophic mutants (histidine and methionine) were impaired in their pathogenic ability as well (Sweigard *et al.,* 1998; Balhadére *et al.,* 1999). An additional strategy for elucidating pathogenesis mechanisms is by studying mutants impaired in transcription factors (TFs). TFs control biological processes by regulating the expression of multiple genes, thus, their disruption may reveal novel regulatory pathways, especially in cases when redundancy is present in downstream effectors. Recently, several genes encoding TFs involved in pathogenicity of *F. oxysporum* have been studied. In addition to the earlier mentioned TF FOW2, the virulence factor *ftf* was found to be expressed only *in planta* (Ramos *et al.,* 2007), the pH responsive TF PacC was demonstrated to be a negative pathogenicity regulator of *F. oxysporum* (Caracuel *et al.,* 2003) and *xlnR* was reported as a regulator of three xylanase genes involved in pathogenicity of *F. oxysporum* (Calero-Nieto *et al.,* 2007).

1.3. Functional role of reactive oxygen species (ROS) in fungal biology and host-pathogen interactions

The most biologically important reactive molecules of reduced dioxygen include the superoxide anion (O_2^-)**,** hydrogen peroxide (H_2O_2), hydroxyl radical (OH^-) and a singlet oxygen. In both plants and fungi, intracellular ROS are routinely generated at low levels in non-stressed cells in chloroplasts and mitochondria as inevitable by-products of successive one-electron reduction of molecular oxygen

during energy production cascades. Low amounts of intracellular ROS serve as molecules of cell signaling and regulatory processes in a variety of organisms (Thannickal and Fanburg, 2000). In mitochondria, electrons can be misdirected from the respiratory pathway and reduce oxygen molecules to produce superoxide radicals. In the presence of even trace amounts of ferric iron these radicals react with hydrogen peroxide to produce hydroxyl radicals via the Fenton reaction. Hydroxyl radicals are extremely toxic and are known to cause DNA mutations, protein denaturation, and lipid peroxidation. Most cells have also acquired the relevant protective mechanisms to maintain the lowest possible levels of ROS inside the cell (Scandalios, 1993). In some cases, especially under stress conditions (i.e. temperature extremes, osmotic stress and starvation) as well as upon recognition of fungal pathogens by the host, these protective mechanisms are overridden by the rapid production of huge amounts of ROS, mostly hydrogen peroxide and superoxide anion, namely the oxidative burst (Wojtaszek, 1997). Being not very reactive and electrically neutral, hydrogen peroxide is able to pass through cell membranes and reach cell locations remote from the site of its formation. This oxidative burst might induce cell death of both pathogen and host by direct damaging or induction of several host-pathways (Fig. 1) **(**Torres *et al.*, 2006**)**.

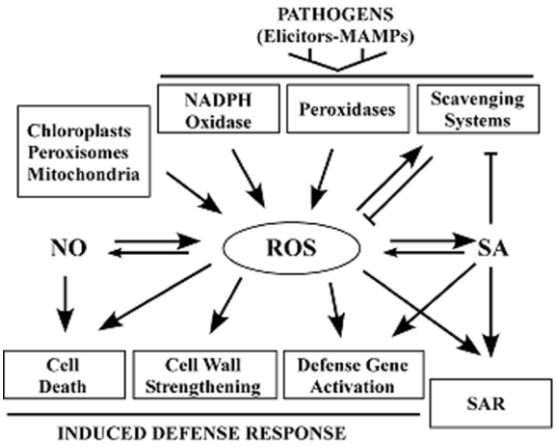

Figure 1. Plant ROS production and functions in response to pathogens (Torres et al., 2006).

Therefore, the ROS functions are diverse, for example, at low concentration they are vital for routine organism function (Takemoto *et al.,* 2007), while at higher concentrations they may serve as a stress response and/or defense mechanism, endangering survival of an organism when failure to manage oxidative stress (independent of its source) inevitably leads to cell death (Lin *et al.,* 2009). Thus, preserving an intracellular ROS equilibrium is vital for organism function and survival. A battery of ROS detoxifying enzymes, including superoxide dismutases (SODs), catalases (CATs) and peroxidases is involved in controlling this delicate balance. Hydroxyl radicals are too active to be easily detoxified therefore cells protect themselves from these molecules by removing the precursor superoxides and hydrogen peroxides. SODs are ubiquitous multimeric metalloproteins that catalyse dismutation of superoxide to produce oxygen and hydrogen peroxide, which can then be removed by catalase and peroxidase (Scandalios, 1993). SOD proteins have three main isoforms, depending on their metal cofactor: manganese- (MnSOD), iron- (FeSOD) or copper/zinc (Cu/ZnSOD). Additional group of CuZnSOD-related proteins is the copper chaperones that transport copper to the enzyme core. Mn- and Fe-SODs share similar sequence and structure however FeSOD is typically the major form in anaerobic prokaryotes and MnSOD is found both in eukaryotes and in aerobic prokaryotes, but are unrelated to Cu/ZnSOD (Fréalle *et al.,* 2005). Other defense mechanisms that protect cells against oxidative stress and have been widely studied in yeasts and mammals include the ubiquitin-proteasome system (Grune *et al.,* 2003) and autophagy (Kiffin *et al.,* 2006).

1.4. Autophagy in filamentous fungi

In filamentous fungi the term "autophagy" is used to describe a non-selective (or marco-) process that involves random uptake of portions of the cytoplasm in the

vacuole/lysosome for recycling (Meijer *et al.,* 2007). Non-selective autophagy is a process which supports cell survival under nutrient-limiting conditions (Levine and Klionsky, 2004). Nutrient sensing as well as mediation of cell growth in response to nutrient availability is regulated in eukaryotes by the well-conserved target of rapamycin (TOR) kinase pathway (Rohde *et al.,* 2001). Repression of the TOR pathway occurs during nutrient-limiting conditions, heterokaryon incompatibility or treatment with rapamycin, following by activation of downstream processes, one of which is autophagy (Pinan-Lucarre, *et al.,* 2007; Schönig *et al.,* 2008). In filamentous fungi, autophagy was demonstrated to be necessary for normal developmental processes, such as growth and differentiation in *Podospora anserina* (Pinan-Lucarre *et al.,* 2002), *Aspergillus oryzae* (Kikuma *et al.,* 2006) and *M. grisea* (Liu *et al.,* 2007). Autophagy also plays an essential role during pathogenesis in the rice pathogen *M. grisea* (Veneault-Fourrey *et al.,* 2006; Kershaw and Talbot, 2009) and the bean pathogen *Colletotrichum lindemuthianum* (Dufresne *et al.,* 1998).

As was previously mentioned, autophagy can be activated by starvation. Throughout the life cycle and pathogenesis, fungi experience a variety of external signals which affect their development. Nutrient availability is one of the forces of host environment that are needed to be overcome by fungi during infection. Involvement of fundamental biosynthetic pathways in fungal pathogenicity was mentioned before (section 1.2). Significant attention has been given to genes involved in nitrogen assimilation, with emphasis on the involvement of GATA-type TFs in nitrogen regulation, some of them have been linked to pathogenicity (Bolton and Thomma, 2008). In *F. oxysporum*, targeted disruption of the GATA-type global nitrogen regulator *fnr1* (an AreA homolog) affected nitrogen utilization as well as pathogenicity on tomato plants (Divon *et al.,* 2006). In *F. verticillioides*, the AreA

nitrogen regulator was shown to be involved in fumonisin production and colonization of corn kernels (Kim and Woloshuk, 2008). One of the factors involved in regulation of AreA is TOR kinase, which was shown to activate the AreA cascade during nitrogen-limiting conditions in *F. fujikuroi* (Teichert *et al.*, 2006). The link between autophagy and programmed cell death (PCD) is a central topic of current investigations. Involvement of autophagy in conflicting processes such as survival and PCD raises a lot of questions, especially in filamentous fungi where research on autophagy is still in its infancy (Pollack *et al.*, 2009). Tsujimoto and Shimizu (2005), reviewing mammalian cells studies, questioned evidence that the mechanism of autophagic death actually exists. However, existence of vegetative incompatibility - strictly typical for filamentous fungi, demonstrated a possible connection between PCD and autophagy (Fedorova *et al.*, 2005). This non-self recognition system is especially important to preserve biological integrity in filamentous fungi (organisms that are able to form chimeras) hence the incompatibility reaction has to be precisely regulated and spatially restricted in order to enable organism survival. Cell death by incompatibility is triggered, when strains bearing different genetic loci (termed *het*) interact on solid medium. Fungal proteins of *F. oxysporum, M. grisea, P. anserina* and *Neurospora crassa* that harbor the HET domain are numerous (over 70) and could be involved in other functions in addition to their function in incompatibility (Pinan-Lucarré *et al.*, 2007). In *P. anserina*, an additional group of genes termed *idi* (induced during incompatibility) is associated with the incompatibility reaction. In this model organism six *idi* genes have been identified so far. The *idi1, -2* and *-3* genes encode small putative cell wall proteins of unknown functions. The *idi-4* gene encodes a transcription regulator, harboring a basic leucine zipper domain (bZIP), which positively regulates its own expression as well as expression of two *idi* genes

(*idi-2* and *idi-7*). Other than the incompatibility reaction *idi-4* is induced by different stress conditions, such as amino acid starvation, osmotic or oxidative stress (Dementhon *et al.,* 2003). The *P. anserina* mutant constitutively overexpressing the TF-encoding gene *idi-4* was characterized by both increased production of autophagosomes and increased cell death, indicating the link between autophagy and PCD (Dementhon *et al.,* 2004). Two additional *idi* genes (*idi-6/pspA* and *idi-7/ATG8*) were found to be involved in both vegetative incompatibility system and autophagy. *idi-6/pspA* encodes for a vacuolar protease, involved in degradation of autophagic bodies in *Podospora* (Dementhon *et al.,* 2003), however it is not conserved among filamentous fungi. *idi-7,* on the other hand, encodes for a highly conserved protein (Mejer *et al.,* 2007), homologous to the yeast ATG8 and the human LC-3 autophagy proteins involved in autophagosome formation (Pinan-Lucarré *et al.,* 2007). Despite this connection, the relationships between autophagy and PCD in filamentous fungi are much more complicated, since it was later demonstrated with Δ*idi-7/atg8* and Δ*atg1* autophagy mutants of *Podospora,* that autophagy was not the cause of cell death by vegetative incompatibility. On the contrary, autophagy was found to be induced during cell death and played a protective role against it (Pinan-Lucarré *et al.,* 2007). Fungal database searches indicated *idi* homologous genes in genome of both the *F. oxysporum* and *N. crassa*.

Existence of additional, less characterized elements in the TOR/AreA-controlled gene network, have been recently discovered (Schönig *et al.,* 2008; Teichert *et al.,* 2006). Interestingly, several genes, including the autophagy regulator *idi4*, were found to be both nitrogen-independent and TOR/AreA-dependent, suggesting existence of other regulatory elements.

1.5. Role of mitochondria in fungal development and pathogenesis

Mitochondria are high efficient energy-producing organelles, developed during eukaryotic evolution, following accumulation of oxygen in the Earth's atmosphere. Incorporation of mitochondria into eukaryotic organisms has extremely benefited their energy production, yielding 38 ATP molecules with breakdown of one molecule of glucose via oxidative phosphorylation (OXPHOS), but also at the cost of oxidative stress and generation of ROS. OXPHOS is a cytochrome-dependent and cyanide-sensitive pathway. In contrast to mammals, fungi possess diverse electron transport pathways, involving alternative redox centers. This additional, cyanide-resistant and salicylhydroxamic acid (SHAM)-sensitive energy pathway, called alternative oxidation (AOX) pathway also occurs in inner mitochondrial membranes (Fig. 2). AOX is a nonphosporylating process that bypasses complexes III and IV in the cytochrome-mediated pathway and transfers electrons directly from ubiquinon to oxygen (Kaneko and Ishii, 2009). Incubation under anaerobic conditions, favored the persistence of AOX (Sandor *et al.*, 2003), which in *F. oxysporum* is mediated by a single enzyme. An additional type of mitochondrial nitrate-respiration (denitrification) occurring under hypoxic conditions and involves cytochrome oxidase, was discovered in *F. oxysporum* (Kobayashi *et al.*, 1996). In anoxic conditions *F. oxysporum* uses ammonia fermentation, which is similar to anaerobic respiration of bacteria. The ammonia fermentation is a process of the reduction of nitrate to ammonium coupled with the catabolic oxidation of electron donors to acetate and substrate-level phosphorylation (Zhou *et al.*, 2002).

Mitochondria are the major sites of intracellular ROS production, with 2–4% of oxygen consumption being converted at complexes I and III of the respiratory chain (Forman and Boveris, 1982). The most sensitive organelle exposed to ROS

damage is the mitochondrion, due to its natural involvement in cellular respiration, since mitochondrial (mt) DNA is more sensitive to ROS than nuclear DNA.

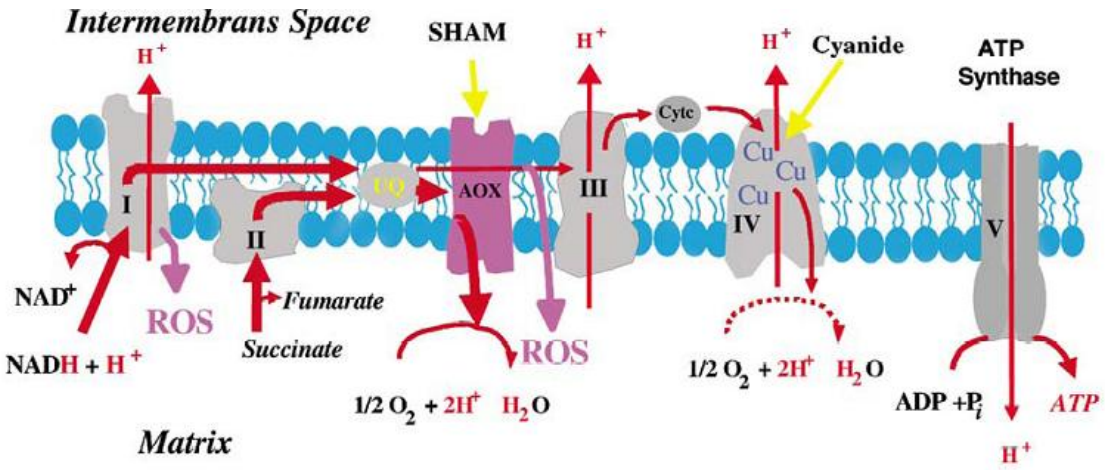

Figure 2. Schematic representation of the fungal respiratory chain (from Osiewacz, 2002). Complex I: NADH dehydrogenase, complex II: succinate dehydrogenase, complex III: cytochrome *bc1*, complex IV: cytochrome *c* oxidase, complex V: ATPase, Q: ubiquinone pool, AOX: alternative oxidase, *c*: cytochrome *c*, Ext1 and Ext2: external NAD(P)H dehydrogenase. The cyanide (CN)-sensitive cytochrome pathway utilizes complexes I, II, III and IV. The electron transfer activity of complexes I, III and IV is used to pump protons across the inner membrane, from the matrix into the intermembrane space. The resulting proton gradient drives the synthesis of ATP complex V. If electron flow through the cytochrome pathway is compromised, it is diverted towards the CN-resistant and salicylhydroxamic acid (SHAM)-sensitive AOX branched at the level of ubiquinone. When the AOX is exclusively used, electron flow and pumping are coupled only for electrons entering by complex I.

Numerous human diseases, as well as normal aging processes and age-related diseases, have been associated with ROS-related damage of mtDNA (Kirkinezosa and Moraes, 2001). Since the superoxide anion, as a charged molecule, does not easily diffuse through the mitochondrial membrane, it has to be scavenged within/through the mitochondrial matrix. However, damaged mitochondria are characterized by increased membrane permeability, which leads to further exposure to ROS molecules. The mitochondrial respiratory chain is the main producer of these toxic byproducts and to minimize damage of oxidation a range of ROS-scavenger antioxidant enzymes (see section 1.3) have evolved. In fungal genomes, redundancy of *sod*-s is more evident of all ROS-scavenger encoding genes. The two SOD groups also differ in

cellular location: Cu,Zn SODs are mainly cytosolic enzymes, while Fe/Mn SODs are located in the inner mitochondria space and in peroxisomes. Group of mitochondria-located Fe/MnSOD has been the subject of particular interest, as they efficiently scavenge superoxide anions produced as by-products of OXPHOS; and hence protect mitochondrial DNA and proteins involved in the citric acid cycle and respiratory chain from ROS damage (Raha and Robinson, 2000). In general, the connection between mitochondrial morphogenesis and fungal development is evident due to its involvement in vital processes such as energy and heme metabolism. In addition, the role of mitochondria in fungal and mammalian pathogenesis has been extensively studied. Different fungal developmental processes such as hyphal elongation (Fuchs *et al.,* 2002), germination (Stade and Brambl, 1981) and aging (Osiewacz, 2002) are dependent upon mitochondrial dynamics. Mitochondrial dysfunction in the chestnut blight fungus *Cryptonectria parasitica* caused by virus-induced mutations in mtDNA led to hypovirulence of the mutant strains (Allen and Nuss, 2004). Involvement of SODs in fungal pathogenicity has not been widely explored due to their functional redundancy. It was shown that Cu,Zn SOD of the phytopathogen *Claviceps purpurea* is dispensable for pathogenicity (Moore *et al.,* 2002). The *sod1:sod2* double mutants in *S. cerevisiae* are defective in sporulation, hypersensitive to oxygen, have an elevated mutation rate, and are aerobically auxotrophic for lysine and methionine (Liu *et al.,* 1992). *N. crassa sod-1* mutants were sensitive to superoxide and hyperbaric oxygen and display increased rates of spontaneous mutation (Chary *et al.,* 1994). In addition to oxidative stress response, mitochondrial MnSOD enzymes, encoded by *sod2*, are involved in general stress reactions. For example, in human and mice, MnSOD expression was found highly inducible by alcohol (St. Clair, 2004; Wheeler *et al.,* 2001). In the fission yeast *S. pombe*, *sod2* was required for tolerance to external

sodium due to functioning of the enzyme as Na^+/H^+ antiporter; interestingly, this mechanism does not exist in the baker's yeast *S. cerevisiae* (Hahnenberger *et al.*, 1996). In the phytophathogen *Colletotrichum graminicola, sod2* was found to be up-regulated during conidiogenesis (Fang *et al.*, 2002). In the human pathogen *Cryptococcus neoformans*, a *sod2* knockout mutant exhibited reduced pathogenicity and impaired growth at elevated temperature. This mutant also accumulated significantly more ROS, during growth at 37°C, suggesting that SOD2 protein is involved in the primary defense of *C. neoformans* against the superoxide anion in the mitochondria. Δ*sod2* was also highly susceptible to redox-cycling agents, high salt and nutrient limitations (Narasipura *et al.*, 2005). A similar picture was observed in evolutionary distant systems. Recently, the Sod2 mutant mouse, which is sensitized to mitochondrial stress was proposed as an ideal model mutant for studying the role of oxidative stress in a diverse range of complications arising from mitochondrial dysfunction and diminished antioxidant defense (Lee *et al.*, 2010). In *Drosophila*, *sod2* null mutations severely reduced life span and increased sensitivity to the oxidative stress (Duttaroy *et al.*, 2003).

Furthermore, two additional unrelated to oxidative stress response mitochondria-located genes were reported to be linked with fungal pathogenicity. First is a carnitine acetyltransferase (*cat*) gene of *M. grisea*, located in peroxisomes and mitochondria and required by for complete pathogenicity (Sweigard *et al.*, 1998). Second, is a mitochondrial carrier protein, *fow1* of *F. oxysporum*, which was found to be involved in invasive growth within muskmelon plants as well as in complete pathogenicity (Inoue *et al.*, 2002).

Interaction between plant hosts and fungal pathogens has evolved in a polyphyletic manner (Ma *et al.*, 2010), involving multiple fungal and host genes,

including different biosynthetic and transduction pathways. Pathogenicity genes are of interest, not only to enrich our knowledge of disease progress as well as of fungal physiology, but also to detect new potential targets for disease management. Even though phytopathologists have been studying pathogenicity processes for decades, only limited number of the definite pathogenicity-related genes has been identified. In particular, study of transcriptional factors, may assist in discovering novel regulatory pathways of pathogenesis. As new genes are being discovered, our understanding of the pathogenicity network takes new turns, for example, not so long ago, involvement of ROS in a variety of aspects of fungal functioning was discovered and only recently, importance of autophagy and programmed cell death for pathogenicity was revealed (Kershaw and Talbot, 2009; Kim *et al.*, 2008). The current research provides an additional point of view on pathogenicity of *F. oxysporum* by identifying novel pathogenicity-required genes and pathways, and exposing their physiological and genetic input.

2. RESEARCH OBJECTIVES

2.1. To characterize phenotypically and genetically a UV-induced non-pathogenic isolate of FOM.

2.2. To generate reduced pathogenicity mutants of FOM, by utilizing a forward genetics approach using tagged *Agrobacterium tumefaciens*-mediated mutagenesis (ATMT), and characterize them phenotypically and genetically.

2.3. To determine the mechanistic nature, by which analyzed genes regulate development and pathogenicity.

3 . METHODOLOGY

3.1. Strains, media and growth conditions

Available list of fungal strains used throughout this study is presented in Table 1.

Table 1. Fungal strains used in this study*

Strain	Description	Organism	Genotype	Source
1,2	wild type	FOM§	race 1,2	Cohen *et al.*, 1989
4/4	UV-induced non-pathogenic	FOM	race 1,2	Freeman *et al.*, 2002
74-ORS-6a (FGSC 4200)	wild type	NC‡	a	FGSC†
FGSC 15052	Targeted gene disrupted in ku80 background	NC	Δ*snt2::hph* a	FGSC

*Complete collection of reduced-pathogenicity *Agrobacterium tumefaciens*-mediated transformants (ATMT) strains generated and characterized in this study (see below) are not presented; §= *Fusarium oxysporum* f.sp. *melonis;* ‡= *Neurospora crassa*; † FGSC= Fungal Genetics Stock Center.

Routinely, *Fusarium* isolates were cultured in Petri dishes containing potato dextrose agar (PDA) (Difco, Detroit, MI) amended with chloramphenicol (0.25 mg/L) (Sigma, St. Louis, MO). Transgenic isolates of *Fusarium oxysporum* f. sp. *melonis* (FOM) were grown on PDA supplemented with hygromycin B (75 μg/mL) (Cayla, Toulouse, France). For conidia production, plugs of mycelia were cultured in 50 ml of *Fusarium* liquid culture (FLC) medium, containing $MgSO_4 \cdot 7H_2O$ - 0.25 g, KH_2PO_4 - 1.5 g, KNO_3 - 2 g, yeast extract – 10 g, sucrose – 20 g and 1 ml trace element solution ($Na_2B_4O_7$ - 0.865 g, $FeCl_2 \cdot 6H_2O$ - 4.82 g, $(NH_4)_6Mo_4O_{24} \cdot 4H_2O$ - 0.129 g, $Cu(NO_3)_2 \cdot 3H_2O$ - 0.378 g, $ZnSO_4 \cdot 7H_2O$ - 4.43 g per 100 ml of water), per 1 L distilled water (Freeman *et al.,* 2002). Induction of extracellular enzyme production was performed essentially as described by Di Pietro and Roncero (1996) on synthetic medium (SM), containing $MgSO_4$ - 0.2 g, $(NH)_4NO_3$ - 1 g, KH_2PO_4 - 0.4 g, KCl - 0.2 g, $FeSO_4$ - 0.01 g, $MnSO_4 \cdot 7H_2O$ - 0.01 g, $ZnSO_4$ - 0.01 g per 1 L distilled water, supplemented with 1 % of the appropriate carbon sources. For analysis of nutritional requirements, strains

were grown on *Fusarium* minimal medium (FMM), containing: 20 ml ×50 FMM solution [$NaNO_3$ – 40 g, KH_2PO_4 – 20 g, $MgSO_4 \cdot 7H_2O$ – 10 g, KCl – 10 g per 400 ml of water], 60 µl of trace element solution [citric acid – 5 g, $ZnSO_4 \cdot 7H_2O$ – 5 g, $FeSO_4 \cdot 7H_2O$ – 4.75 g, $Fe(NH_4)_2SO_4 \cdot 6H_2O$ – 1 g, $CuSO_4 \cdot 5H_2O$ – 0.25 g, $MnSO_4 \cdot H_2O$ – 0.05 g, H_3BO_3 – 0.05 g, $Na_2MoO_4 \cdot 2H_2O$ – 0.05 g per 95 ml water], 30 g sucrose and 1.5 % agar (Difco), per 1 L of distilled water (Correll *et al.,* 1987). For auxotrophy tests, the following amendments were used: vitamins (choline, nicotinamide, riboflavin, biotin, thiamine, and pyridoxine), amino acids mixture as well as purines and pyrimidines (Sigma). All the amendments were applied at a final concentration of 100 µg ml^{-1}. The following carbon sources were used as inducers of cellulases and polygalacturonases: carboxymethylcellulose (CMC) (BDH Chemicals Ltd, Poole, England), D-galacturonic acid (GA), polygalacturonic acid from orange (PGA) and sodium polygalacturonate (NaPG), all of which were purchased from Sigma. *Neurospora crassa* isolates were maintained on Vogel's N medium (Davis and de Serres 1970), if required, hygromycin B was added at concentration of 100 µg/mL.

For tagged and targeted mutagenesis GV3101 and EHA105 strains of *Agrobacterium tumefaciens* were used throughout this research. Both the *A. tumefaciens* strains were routinely maintained on LB agar plates, containing 40 µg/ml Rifampicin, addition of 100 µg/ml Gentamycin was required for GV3101 strain growth. DH5α strain of *E. coli* was used for all standard DNA molecular manipulations (Sambrook *et al.,* 1989). Kanamycin (at a concentration 50 µg/ml) or ampicillin (100 µg/ml) were used as selective antibiotics for plasmid growth within *A. tumefaciens* or *E. coli* strains, respectively. All antibiotics were purchased from Sigma.

3.2. Plant inoculation assays

3.2.1. Inoculation technique

A cultivar of muskmelon (cv. Ein Dor), susceptible to race 1,2 of FOM was used throughout this study (Zeraim Gedera, Israel). Plant inoculation assays were conducted in a greenhouse under controlled conditions at 25±1°C and 16 hr light photoperiod (Freeman *et al.*, 2002). Melon plants were inoculated by dipping roots for 30 min in the conidial suspensions (at concentrations 1.5×10^6 or 5×10^5 conidia/mL), followed by transfer to water or soil medium.

3.2.2. Influence of adenine on pathogenicity

Influence of adenine and yeast extract on pathogenicity of mutant strain 4/4 was determined as follows: conidia of strains 4/4 and 1,2 of FOM, at a concentration of 1.5×10^6 conidia/mL, were resuspended in 5 mg/mL adenine solution or in 0.5 % (w/v) yeast extract solution and preincubated at 25°C for 24 h (Namiki *et al.*, 2001). Subsequently, melon plants were inoculated by dipping roots for 30 min in the conidial suspensions and transferred into glass tubes containing 30 ml of water or 0.1 mg/mL adenine solution. The symptoms of vascular wilt disease were assessed over six-day period.

3.2.3. Pathogenicity assays for isolation of reduced-pathogenicity mutants

Tagged mutants were tested for their ability to cause wilt disease. A two-staged pathogenicity assay was applied, three replicate groups of thirty five-day-old melon plants were inoculated in a conidial suspension (dipping method) and following by incubation in tubes containing 40 ml of sterile water. Isolates causing disease symptoms (wilting or/and stem lesions) of less than 50% of inoculated plants were subjected to two additional rounds of the rapid screen. At the second stage,

suspected transformants were screened on plants in soil medium following a standard protocol (section 3.2.1.) (Freeman *et al.*, 2002).

3.3. Statistical analysis

All experiments were conducted at least three times. Data (apart from results of Real-time PCR) were analyzed using the JMP software (version 3.2.6; SAS Institute, Inc. Cary, NC, USA). All values were subjected to ANOVA, then mean comparisons of calculated values were performed using LSD, according to the Tukey Kramer multiple comparison test ($P \leq 0.05$) and were analyzed.

3.4. Fungal transformation

Tagged mutagenesis of FOM was performed by *Agrobacterium tumefaciens*-mediated transformation using plasmids pBHt2 and pKHt, following standard protocol (Mullins *et al*. 2000), with the following modifications: 200 μL of mixed bacteria cells and conidia per plate, at a concentration of 10^5 conidia/mL were plated directly on 12 ml of co-cultivation medium, following incubation at 25°C for 48 hours. Twelve ml of selection medium containing 100 μg/mL hygromycin B and cefotaxime (Sanofi Aventis Laboratory, Paris, France), were overlaid on each plate and incubated at room temperature for 5-7 days. Hygromycin-resistant transformants were isolated and subjected to further characterization. A collection of 2000 mitotically stable transformants were screened for pathogenicity on melon plants.

3.5. DNA modifications and cloning procedure

The fungal transformation vector ks:hph (Horowitz *et al.*, 2006), containing the *E. coli* hygromycin phosphotransferase (hph) gene regulated by promoter and terminator elements from the *trp*C gene of *Aspergillus nidulans* were used. The gene replacement construct pDΔ*snt2* was assembled as follows: a 1.7 kb fragment of *snt2* was amplified with primers homFGF1-*SdaI*/ homFGR1-*MunI*, introducing *SdaI* and

MunI cloning sites. The resulting fragment was cloned into pGEM-T Easy (Promega) and its 335 bp fragment was replaced with the 2.13 kb hphB/trpC cassette from the vector ks:hph, using *Acc65*I/*Bgl*II restriction. The resulting 3.8 kb *snt2::*hphR *Sda*I/*Mun*I-digested construct was transferred into *EcoRI/PstI*-digested pDHt (Mullins *et al.*, 2001). Gene knockout was confirmed by Southern blot analysis on *Acc65I/Bsp1407I (Bs)* digested genomic DNA, using a 1.4kb fragment PCR-amplified with primers inHPH-rev2/homFG1R as a probe.

3.6. Isolation and analysis of nucleic acids from *F. oxysporum* f.sp. *melonis*

3.6.1. DNA isolation

High molecular weight genomic DNA was extracted as previously described by Möller, *et al.* (1992) with minor modifications. Briefly, 1 g of lyophilized mycelia was ground with liquid nitrogen, transferred to 12 ml polyethylene tubes and mixed with 3 ml of TES buffer [100mM Tris, pH=8.0, 10mM EDTA, 2% SDS], and 100µg of Proteinase K (AppliChem GmbH, Darmstadt, Germany). The tubes were incubated in a water bath at 60°C for 1 h, with gentle shaking. The salt concentration was adjusted to 1.4 M using 5 M NaCl; 0.1V of 10% CTAB was added as well and the mix was incubated for 10 min at 65°C. An equal volume of chloroform: isoamylalcohol (24:1) (CIA) was added to pre-chilled tubes, incubated for 30 min on ice and centrifuged for 10 min at 4°C, 10,000 rpm. The supernatant was transferred to fresh tubes and nucleic acids were precipitated with 0.2 vol. of 5 M ammonium acetate following incubation on ice for at least 30 min. After additional centrifugation, the supernatant was precipitated with 0.55 vol. isopropanol and immediately centrifuged for 5 min. The pellet was washed twice with cold 70% EtOH, air-dried and dissolved in TE.

3.6.2. RNA isolation

Prior to total RNA extraction, the harvested samples (fungal and plant) were treated with RNAlater® solution (Ambion Inc., Austin, TX, USA), following the manufacturer's protocol and stored at -20°C. Total RNA was extracted from lyophilized mycelia of germinated conidia using the SV RNA Isolation System Kit (Promega, Madison, WI, USA). Total RNA from melon plants was extracted using a CTAB-based protocol, previously described by Chang *et al.*, 1993. Briefly, 1 g of tissue was ground in liquid nitrogen using a mortar and pestle then incubated in 5 ml of extraction buffer [2% CTAB, 2% polyvinylpyrrolidne, 100 mM Tris-HCl (pH 8.0), 25 mM EDTA, 2 M NaCl and 2% ß-mercaptoethanol] at 65°C for 10 min. The samples were cooled to room temperature and an equal volume of CIA was added. The mixture was homogenized and separated by centrifugation at 8000 rpm for 30 min at RT. The supernatant was transferred to fresh tubes and extracted with an equal CIA volume; the mRNA was purified using DynaBeads® (Invitrogen, Carlsbad, CA, USA). The complete sequence of *snt2* gene was obtained from gemonic DNA of the wild type of FOM race 1,2 isolate by using the Universal Genome Walker kit (Clontech Laboratories, Palo Alto, CA, USA), combined with TAIL-PCR. Amplified fragments were cloned into pGEM-T easy, sequenced (Macrogen Inc, Seoul, Korea) and manually annotated. Sequence details of the primers are presented in Table 2.

Table 2. Primers used throughout this study

Primer	***Sequence (5' to 3')***	***Use***
	TAIL-PCR	
AD1	wagtgnagwancanaga	Degenerative primer for TAIL-PCR*
LB1	agggttcctatagggtttcgctcatg	Left Ti border, primary TAIL-PCR
LB2	ccatgtgttgagcatataagaaaccct	Left Ti border, secondary TAIL-PCR
LB3	gaattaattcggcgttaattcagt	Left Ti border, tertiary TAIL-PCR
RB1	ggcactggccgtcgttttacaac	Right Ti border, primary TAIL-PCR
RB2	aacgtcgtgactgggaaaaccct	Right Ti border, secondary TAIL-PCR
RB3	cccttcccaacagttgcgca	Right Ti border, tertiary TAIL-PCR
	Real time PCR	
798tubRT_F	cccctcttacggcgatctta	NC**, tubulin, 3'-end

923tubRT_R	gggaagggaaccatgttgac	NC, tubulin, 5'-end
ACS1 qRT-for1	tgacatcacctacctcctc	ATP-citrate synthase subunit 1, 3'-end
ACS1 qRT-rev1	cgccttatttcttcctttcc	ATP-citrate synthase subunit 1, 5'-end
AraTR qRT-for1	gaggacgagagcccatac	Glutamine amidotransferase-like, 3'-end
AraTR qRT-for1	accaccaagtcgcatagc	Glutamine amidotransferase-like, 5'-end
EF qRT-for1	ctcatccgcaacaccttc	Elongation factor 1G 5'-end
EF qRT-rev1	cttctcagcaacctcagc	Elongation factor 1G 3'-end
idi4 qRT-for1	aacgctctggatacgaatac	Induced during incompatibility 4, 5'-end
idi4 qRT-rev1	ggagtgcttgatgttgagg	Induced during incompatibility 4, 3'-end
MFS qRT-for1	cggcattcactgggcttcttc	Multidrug resistance transporter, 5'-end
MFS qRT-rev1	cggattgagcggcgaacttg	Multidrug resistance transporter, 3'-end
PDC qRT-for1	acctcgtcagcgtcttcg	Pyruvate decarboxylase, 5'-end
PDC qRT-rev1	agcagcgttgaactccttg	Pyruvate decarboxylase, 3'-end
qRT 01738 SOD F1	tccctagatccgcatttg	Fe,Mn SOD (1), 5'-end
qRT 01738 SOD R1	acaccctcagaatagtcg	Fe,Mn SOD (1), 3'-end
qRT 04389 SOD F1	aggaggcattcaagaagac	Fe,Mn SOD (2), 5'-end
qRT 04389 SOD R1	tgatccttcgtcgtaacaatac	Fe,Mn SOD (2), 3'-end
qRT FO_00474 for1	tgcctcttgtcaggttggagacaa	Cu,ZnSOD (2), 5'end
qRT FO_00474 rev1	acaaaggaccggttgccaaagt	Cu,ZnSOD (2), 3'end
qRT FO 03076-for1	cgaatctgcccctaccaccatc	Cu,ZnSOD (1), 5'end
qRT FO 03076-rev1	ttgaagtgaggaccagcggaag	Cu,ZnSOD (1), 3'end
qRT FO 13757-for1	ctccaagcaccaccagacctac	Fe,Mn SOD (3), 5'-end
qRT FO 13757-rev1	accaccgcccttgccattg	Fe,Mn SOD (3), 3'-end
qRT FO_11513-for1	cctctttgctgttccgctgtc	Cu,ZnSOD (3), 5'end
qRT FO_11513-rev1	ggtccttcaagttgccttccac	Cu,ZnSOD (3), 3'end
qRT cpc1-for2	tgtctgcacctaactcctcagcat	Cross-pathway control 1, 5'-end
qRT cpc1-rev1	tgccgaagtttggagacacatcgt	Cross-pathway control 1, 3'-end
qRT fnr1-for1	tcgcctatcaactttgcgtctcct	*Fusarium* nitrogen regulator, 5'-end
qRT fnr1-rev1	gcgatggttctttgcgggatttga	*Fusarium* nitrogen regulator, 3'-end
qRT fnt NC F1	atggcgattatctttggttatgg	NC, formate-nitrate transporter, 5'-end
qRT fnt NC R1	gccattcgggaacaacttg	NC, formate-nitrate transporter, 3'-end
qRT fnt1-for1	gttgtcgccaatatgttctac	Formate-nitrate transporter, 5'-end
qRT fnt1-for1	atgccaccgccaataatg	Formate-nitrate transporter, 3'-end
qRT FoAOX F	acagttggcgactatacag	Alternative oxidase (*aod1*), 5'-end
qRT FoAOX R	tggtcttgtcggatttctg	Alternative oxidase (*aod1*), 3'-end
qRT GAPHD for1	tcaacgagaacaagtacgacggct	Glyceraldehyde-3-phosphate dehydrogenase, 5'-end
qRT GAPHD rev1	aacttgtcgttgatgaccttggcg	Glyceraldehyde-3-phosphate dehydrogenase, 3'-end
qRT gln1 for1	tcatcgttcttgctgagtgctgga	Glutamine synthetase, 5'-end
qRT gln1 rev1	tgtccataaccttcacgcagtcgt	Glutamine synthetase, 3'-end
qRT idi7 for1	cttgtccccgccgatttg	Autophagy-related ATG8, 5'-end
qRT idi7 rev1	cctcgtcaacgaagatgaagatg	Autophagy-related ATG8, 3'-end
qRT NC aod-1 F	gggaagcggacgatgaag	NC, alternative oxidase (*aod-1*), 5'-end
qRT NC aod-2 R	cctccttctggtccaaattg	NC, alternative oxidase (*aod-1*), 3'-end
qRT NC cpoxIII-F	cacctacatttccatcat	NC, coproporphyrinogen oxidase III, 5'-end
qRT NC cpoxIII-R	gttgaactcgacatactt	NC, coproporphyrinogen oxidase III, 3'-end
qRT NC idi-4 F	acaacaacatgggctacag	NC, induced during incompatibility 4, 5'-end
qRT NC idi-4 R	gaagtggagccagaagattg	NC, iduced during incompatibility 4, 3'-end
qRT NCU01213 F1	gggtagttttgacgagttc	NC, Fe,Mn SOD (SOD2), 5'-end
qRT NCU01213 R1	cttctcggcagtagactc	NC, Fe,Mn SOD (SOD2), 3'-end
qRT NCU09560 F1	ccaaccaggaccctgttac	NC, Fe,Mn SOD, 5'-end
qRT NCU09560 R1	tactctgccttcctgttctcatac	NC, Fe,Mn SOD, 3'-end
qRT nit4 for1	gaagacgacgtgttgggcattgtt	Pathway-specific nitrogen regulator, 5'-end
qRT nit4 rev1	tcattagccaacggaactgtcggt	Pathway-specific nitrogen regulator, 3'-end
qRT SNT2-F7	caaacccacggacacaac	*Snt2*, 5'-end
qRT SNT2-R7	tgaggagcaggataagcc	*Snt2*, 3'-end
RBS qRT-for2	gggttgatttcgggcttagtcc	Regulated by *snt2* -1, 3'-end
RBS qRT–rev2	ggcggcggcacatttctg	Regulated by *snt2*-1, 5'-end
Tub qRT-for1	ttgactggtcgcaagatg	Tubulin, 5'-end

Tub qRT-rev1	cggaacaagtgaggtatcg	Tubulin, 3'-end
Vector construction and other uses		
homFG1F	gaatgacagcagcaaacccgt	*snt2* partial amplification, 5'-end
homFG1R	cggcataaagctaccacacgc	*snt2* partial amplification, 3'-end
homFG1F-SdaI	Acttaacctgcagggaatgacagcagcaaacccgt	*snt2* knockout vector construction, 5'-end
homFG1R-MunI	Taaggatccaattgcggcataaagctaccacacgc	*snt2* knockout vector construction, 3'-end
inHPH-for2	tgtcgaacttttcgatcagaa	Hygromycin phosphotransferase, 5'-end
inHPH-rev2	agtactcgccgatagtggaaac	Hygromycin phosphotransferase, 3'-end
SNT2-del.-For	acgcactcgactacgacgaca	*snt2*, confirmation of gene disruption, 5'-end
SNT2-del.-Rev	gggaggtatccacatgcgagt	*snt2*, confirmation of gene disruption, 3'-end
SNT2outer-F3	aggagcaacagtcgggcagtt	*snt2*, identification of knockout mutants, 5'-end
SNT2outer-R2	tggccacagactgcacaaggc	*snt2*, identification of knockout mutants, 3'-end

* Primers are designed for *Fusarium oxysporum*, unless stated otherwise; **NC=*N. crassa*

3.6.3. Southern hybridization

For Southern hybridization, 10 µg of genomic DNA was treated with appropriate restriction enzymes, resolved in 1% agarose gel, transferred to nylon membranes (Hybond N^+; Amersham, Little Chalfont, UK) and analyzed following standard protocols (Sambrook *et al.,* 1989) using a digoxigenin-based labeling kit (Roche, Mannheim, Germany).

3.7. Location of inserted tag in ATMT mutants

Thermal asymmetric interlaced (TAIL)-PCR (Liu and Whittier, 1995) was used to locate inserted tags in reduced-pathogenicity ATMT mutants. The right border primers (RB-1, -2, and -3), the left border primers (LB-1, -2, and -3) and the arbitrary degenerate (AD-1) primer used (Table 2) were designed such that their melting temperatures (*Tm*'s) would ensure maximum thermal asymmetric priming (Mullins *et al.,* 2001). The TAIL-PCR amplification was performed following a previously published protocol (Table 3) (Mullins *et al.,* 2001). A thermal cycler (PTC-100; MJ Research Inc., Watertown, MA) was used for the TAIL-PCR. The tertiary TAIL-PCR product of selected transformant showing the highest intensity was purified from gels, cloned and sequenced (Macrogen Inc, Seoul, Korea).

Table 3. Conditions used for thermal asymmetric interlaced (TAIL)-PCR

Primary PCR	***Secondary PCR***	***Tertiary PCR***
92°C: 2 min	94°C: 10 s***	94°C: 10 s
95°C: 1 min	66°C: 1 min***	94°C: 15 s****
94°C: 30 s*	72°C: 2 min***	42°C: 1 min****
66°C: 1 min*	94°C: 10 s***	72°C: 2 min****
72°C: 2 min*	66°C: 1 min***	72°C: 5 min
94°C: 30 s	72°C: 2 min***	
30°C: 3 min	94°C: 10 s***	
Ramp to 72°C over 3 min	44°C: 1 min***	
72°C: 2 min	72°C: 2 min***	
94°C: 5 s**	72°C: 5 min	
44°C: 1 min**		
72°C: 2 min**		
94°C: 5 s***		
66°C: 1 min***		
72°C: 2 min***		
94°C: 5 s***		
66°C: 1 min***		
72°C: 2 min***		
94°C: 5 s***		
44°C: 1 min***		
72°C: 2 min***		
72°C: 5 min		

*, **, ***, **** represent ×5, ×10, ×15 and ×30 cycles, respectively.

3.8. Molecular analysis of targeted gene-disruption mutants

In order to identify the *snt2* knockout event, genomic DNA of 200 independent targeted transformants was amplified by specific PCR amplification using two pairs of primers. The first set consisted of the inHPH-for2, located within the Hyg cassette, and outerSNT2-F3, based on endogenous *snt2* sequence which is not present in the gene-replacement construct. Amplification of a ~2.8kb fragment, using primer pair, provided evidence for the disruption event. Amplification with the second set of primers (SNT2-del.for1/rev1) originated from a 0.3kb fragment of the *snt2* which was replaced with the hygromycin resistance cassette, verified an ectopic integration of the gene-replacement construct (Table 1 and Fig. 9B).

3.9. Gene expression analysis

3.9.1. Gene expression analysis by RT-PCR

Reverse transcription (RT) was carried out on 1 μg total RNA treated with Turbo DNase (Ambion) using Verso™ RTase (ABgene, Epsom, UK) and an

anchored oligo-dT primer. cDNA was stored at −20 °C. For RT-PCR experiments, amplification was performed in 25-µL reactions with the following components: 5 µL cDNA, 2.5 U Taq DNA polymerase, X1 Taq polymerase buffer, 0.1mM $MgCl_2$, 0.2 mM dNTP and sense and antisense primers to final concentrations of 1 µM. RNA samples were tested for the presence of genomic DNA contamination by using extracted treated RNA directly as a PCR template, prior to cDNA synthesis, under the same PCR conditions.

3.9.2. Gene expression analysis by quantitative real-time (qRT)-PCR

Total or/and messenger RNA was extracted from cultured mycelia, germinated conidia, grown on FMM or from infected seedlings (at 24-h intervals from 1 to 5 days after inoculation and from non-inoculated control plants). cDNA dilutions were used as templates for calibration curves. For qRT-PCR, reverse transcription was carried out in a 15 µL volume, using 4 µL cDNA, X1 DyNamo Flash Master SYBR green Mix (FinnEnzymes, Finland), with 1 µL sense and antisense primers at concentration of 0.03 mM. Real-time (qRT) PCR amplification was performed in a Rotor-Gene 3000 machine (Corbett Research, Sydney, Australia). qRT-PCR analyses of selected genes were performed using RNA, extracted from inoculated and non-inoculated muskmelon seedlings as well as mycelia, grown on FMM. For estimation of *snt2* expression *in planta*, cDNA obtained from 2-day post-inoculation plants (dpi) was used as a reference (at dpi 1, no expression of housekeeping fungal genes was detected). Relative quantification of a target transcript was analyzed using REST-2005© program, which is based on the mean CP deviation of control and sample group, normalized by a reference (β-tubulin) transcript (Pfaffl *et al.*, 2002). This method is also based on efficiency-corrected calculation of qRT-PCR amplification. The Pair Wise Fixed Reallocation Randomization Test© (Pfaffl *et al.*, 2002) was used

to analyze the mean of at least three technical if two independent biological repeats, detecting the relative quantification, and the level of significance.

3.9.3. Suppression subtractive hybridization (SSH)

Direct SSH analysis (Diatchenko *et al*. 1996) was carried out using the Clontech PCR Select-Subtraction cDNA kit (Clontech), according to the manufacturer's protocol. For subtracted cDNA library construction, 500ml flasks containing 25ml of FMM was inoculated with the wild type and D122 strains of FOM at a concentration of 10^6 conidia/ml, for 14 hr, on an orbital shaker at 25°C at 100 rpm. Conidia were harvested at initial germination stage by centrifugation at 10,000 rpm, for 15 min. cDNA was synthesized from 2mg of mRNA using SuperScript® II Reverse Transcriptase (Invitrogen). The “tester” and the “driver” samples contained cDNA populations isolated from germinated conidia of the wild type and D122 mutant, respectively, cloned into pGEM-T Easy (Promega) and sequenced (Macrogen Inc). The obtained sequences were used to search the available databases of *Fusarium* (http://www.broad.mit.edu) and the National Center for Biotechnology Information (NCBI).

3.10. Protein-related methodologies

3.10.1. Extracellular protein extraction

Extracellular cellulases and polygalacturonases (endoPGs) were purified from liquid cultures supplemented with 1% of CMC, GA, NaPG or PGA. Initially, the medium was inoculated with 10^6 conidia/mL and then after 96 h of shaking at 150 rpm, 500 ml of the cultures were filtered on no. 3 Whatman paper (Maidstone, England). The filtrate was then passed through a 0.2 μm filter (Nalgene, USA). The filtrates were concentrated using rotary evaporation (Rotavapor R, Büchi, Germany) at 37°C to a volume of approximately 5 ml and then centrifuged for 10 min at 10,000

rpm for 15 min, at 4°C. The supernatant was dialyzed against 10 L of ddH_2O for cellulase purification or 5 L of 25 mM sodium acetate and then 5 L of 10 mM sodium acetate for endoPG purification (Prusky *et al.*, 1989). All dialyses were performed at 4°C for 24 h.

3.10.2. Intracellular protein extraction

Fungal mycelia were frozen in liquid nitrogen and then ground with a mortar and pestle and subsequently homogenized in ratio 1:1 (w/v) in the presence of extraction buffer [1mM DTT, 0.1mM EGTA, 0.1mM EDTA and 50mM Tris-HCl, pH 7.5]; one tablet of Complete™ Protease Inhibitor (Roche) was added to 50ml of the extraction buffer. Then, samples were incubated on ice for 1h, with vortexing each 10min. The homogenate was centrifuged for 40 min at 12,000 rpm and 4°C; supernatants were separated and kept at -20°C prior to superoxide dismutase and NADPH-oxidase activity assays. Protein quantities were determined by NanoDrop™ spectrophotometer (Thermo Scientific, Wilmington, DE) using Bradford staining (Sigma) with bovine serum albumin standard solution (BioRad Laboratories, Hercules, CA), as a reference.

3.10.3. Native and SDS polyacrilamyde gel electrophoresis (PAGE)

Proteins were resolved in diluted 1:2 in × 3 Laemmli loading dye [2.4 ml 1M Tris-Cl pH 6.8, 3 ml 20% SDS, 3 ml glycerol, 1.6ml β-mercaptoethanol and 6mg bromophenol blue per 10ml], resolved in 12 % SDS-PAGE in × 1 Laemmli buffer [×10 buffer contains 30.3 g Tris base, 144 g glycine, 10 g SDS per 1L of dH_2O] and stained with Coomassie blue (Sigma) for visualization. Stained protein bands were removed from gels and subjected to partial amino acid sequencing by mass spectrometry (MS-MS), which was conducted using a Q2-TOF device (Hadassah Ein Kerem Medical Center, Jerusalem, IL).

3.10.4. Spectrophotometrical methods of estimation of enzymatic activity

Endogluconase activity was assayed in 50 mM sodium acetate buffer, pH 5.5, containing 0.5 % Na carboxymethylcellulose (CMC). Activity was determined after 30 min of incubation at 37°C (Eshel *et al.,* 2000). Quantification of hydrolysis products was determined calorimetrically, as described by Nelson (1945). Products were analyzed by measuring the OD at 660 nm. Specific enzyme activity was expressed in nanokatals (nkat) - the amount of enzyme that released 1 nmol of D-glucose equivalent per second at the mentioned above conditions per mg. Polygalacturonase (PG) activity was determined by measuring the release of reducing groups from polygalacturonate. Routinely, PG activity assays were performed in 50 mM sodium acetate buffer (pH 5.5) containing 1 % PGA (w/v) and various amounts of the enzyme preparation. After incubation for 30 min at 30°C, the reducing sugar component was determined. Reduced monomers were analyzed by measuring the OD at 500 nm, and then compared to a standard curve, prepared using D-galacturonic acid standards.

3.10.5. Detection of total superoxide dismutase (SOD) and NADPH-oxidase (NOX) activity

The total SOD activity was determined by specific negative staining of native intracellular proteins, separated in 8-10% Discontinuous-PAGE according to Beauchamp and Fridovich (1971) by soaking gels for 30 min in 50 ml of the detection buffer [37 mg EDTA, 1.25 mg riboflavin, 20 mg nitroblue tetrazolium (NBT), and 250 µl N,N,N′,N′-tetramethylethylenediamine (TEMED) in 100ml of 0.1 M phosphate buffer pH 7.8]. Activity bands were observed after illumination with fluorescent light for 5 to 15 min and documented. Relative *in vitro* NOX activity was determined on the basis of a procedure described by Lopez-Huertas (1999).

3.11. Gas chromatography

Oxygen uptake was detected by monitoring relative production of carbon dioxide (CO_2) per total accumulated dry biomass (mg) by gas chromatography (GC) analysis using Gow-Mac® flow chromatography device (Bethlehem, PA, USA). Conidial suspensions of the wild type and *snt2* mutants of FOM and *N. crassa*, were incubated in 20ml minimal medium, at concentration of 10^6 conidia/mL for 24 hr. Flasks were then sealed with rubber plugs and then incubated for 1 hr 25°C, followed by GC analysis of 10ml of the chamber air. Inhibitors of oxidative phosphorylation and the alternative oxidase pathway - potassium cyanide (KCN) and salicylhydroxamic acid (SHAM), were added prior to incubation, at a concentration of 1mM and 100μg/ml, respectively. Statistical analysis of three independent experiments was conducted using LSMeans Difference Tukey HDS test (at $P \leq 0.05$) comparatively to the wild type isolate and separately for each fungus.

3.12. Fungal cell staining methods and microscopy

For microscopic analyses, *Fusarium* mycelia were cultured on FMM medium medium for 48 h. *N. crassa* isolates were grown on cellophane film (BioRad), over Vogel's medium. The mycelium was examined using inverted laser scanning confocal microscope (Olympus IX 81, Japan). For vitality staining, 0.1% Evans Blue solution was applied for 5min, following by a rinse of distilled water (Dementhon *et al.*, 2003). Fungal cell wall staining was performed using 0.1% (w/v) Congo red solution in 150 mM NaCl water solution, following by a rinse of 150 mM NaCl. Autophagosome staining was performed with acidotropic dye monodansyl cadaverine (MDC) (Sigma) at concentration of 0.05 mM (Biederbick *et al.*, 1995). One mM of protease inhibitor phenylmethanesulphonylfluoride (PMSF) (Sigma) was used to emphasize autophagosome appearance. Ten mM of the specific autophagosome inhibitor 3-

methyladenine (Pollack *et al.*, 2009), combined with PMSF was applied, prior to MDC staining.

4. RESULTS

4.1. Impaired purine biosynthesis affects pathogenicity of *Fusarium oxysporum* f. sp. *melonis* (FOM)

Strain 4/4, which was derived by UV-mutagenesis from FOM race 1,2, was characterized as non-pathogenic on melon and watermelon plants (Freeman *et al.*, 2002). The mutant was capable of penetrating and colonizing stem vessels of the host plants, but did not cause vascular wilt disease symptoms. The 4/4 mutant was proposed as a biocontrol agent and therefore a thorough characterization of the isolate was required. Furthermore it was assumed, that characterization of the 4/4 mutant strain might be helpful for further understanding pathogenicity processes in Fusarium wilt.

4.1.1. Growth and development of the non-pathogenic mutant strain 4/4.

Growth analysis experiments were conducted comparing the two FOM isolates, wild type and mutant strain 4/4, which were cultured on complete (FLC) medium. Vegetative growth rates were not significantly different when both isolates were grown on solid PDA medium (Fig. 3).

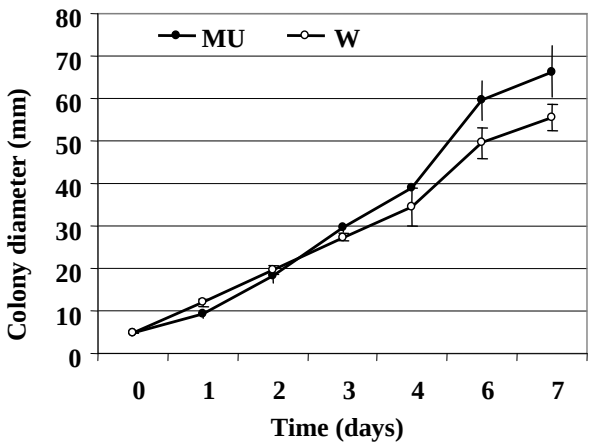

Figure 3. Comparison of vegetative growth between wild type 1,2 (W) and mutant 4/4 (MU) strains of *Fusarium oxysporum* f. sp. *melonis*. Both strains were cultured on PDA medium for six days; three replicates per isolate. Radial growth (mm) of the strains were measured daily over a week period. Bars represent standard error of the means of the three replicates. Data were analyzed by Student's test (α=0,05).

Furthermore, both isolates exhibited similar levels of biomass accumulation and conidia production when incubated in FLC (Table 4). When growth and development

parameters (biomass accumulation, conidial production and vegetative growth rate) of mutant strain 4/4 were examined on minimal synthetic medium (SM), containing pectin or sodium polygalacturonate (NaPG) as sole carbon sources, a delay in all the tested parameters was observed (Table 4).

Table 4. Evaluation of developmental parameters of wild type (WT) and mutant 4/4 (MU) strains of *Fusarium oxysporum* f.sp. *melonis* during growth on different carbon sources*

	FLC	SM	SM+CMC	SM+NaPG	SM+Pectin
	Conidia production, $\times 10^6$ conidia per ml				
WT	91±7 a†	45±7 a	151±13 a	14±1 a	95±13 a
MU	80±6 a	10±4 b	11±5 b	1±0.2 b	9±4 b
	Biomass, mg				
WT	198±18 a	37±13 a	43±2 a	66±1 a	46±3 a
MU	186±11 a	41±4 a	38±4 a	5±1 b	21±2 b

*Minimal synthetic medium (SM) was amended with 1% (w/v) of the following carbon sources: carbomethylcellulose (CMC), sodium polygalacturonate (NaPG) and pectin. † Means of three independent experiments were compared by LSMeans Tukey HDS test, between WT and MU isolates, separately for each treatment. Values presented in the table are mean ± SE, different letters indicate level of significance, at $P \leq 0.05$.

4.1.2. Effect of nutritional amendments on development, secretion and activity of extracellular hydrolytic enzymes of mutant 4/4

In order to examine the possibility that a mutation leading to nutritional defects might be the cause of differential development of strain 4/4 under the tested conditions, yeast extract was used to supplement the growth medium.

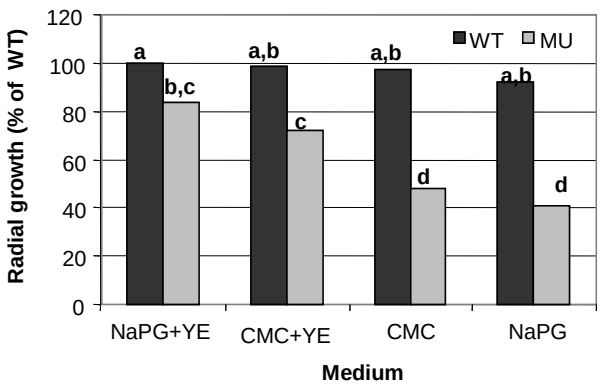

Figure 4. Effect of yeast extract (YE) amendment on utilization of different carbon sources by mutant 4/4. Growth rate of wild type (WT) and mutant 4/4 (MU) strains was evaluated, when the strains were grown on synthetic medium (SM) with 1% of carbomethylcellulose (CMC) or sodium polygalacturonate (NaPG) as sole carbon source, with or without 1% YE. Results of three independent experiments were analyzed by LSMeans Differences Tukey HSD test ($P \leq 0.05$), indicating differences (marked by different letters) between the strains.

Addition of yeast extract significantly increased the growth of mutant strain 4/4,

compared to non- amended medium. Moreover, addition of yeast extract to medium containing NaPG increased growth rate of the mutant to rates similar to that of the wild type (Fig. 4).Strain 4/4 was further characterized by studying its ability to utilize different carbon sources by monitoring the level of extracellular enzyme secretion. Addition of yeast extract to synthetic medium (SM), supplemented with carbomethylcellulose (CMC) or galacturonic acid (GA) as the sole carbon source, resulted in increased extracellular enzyme production by the mutant strain 4/4. Mass spectrometry (MS-MS) analysis of the two predominant proteins was performed, identifying them as exocellulase (Fig. 5A) and endopolygalacturonase (endoPG) (Fig. 5B), identical to those secreted by wild type strain 1,2.

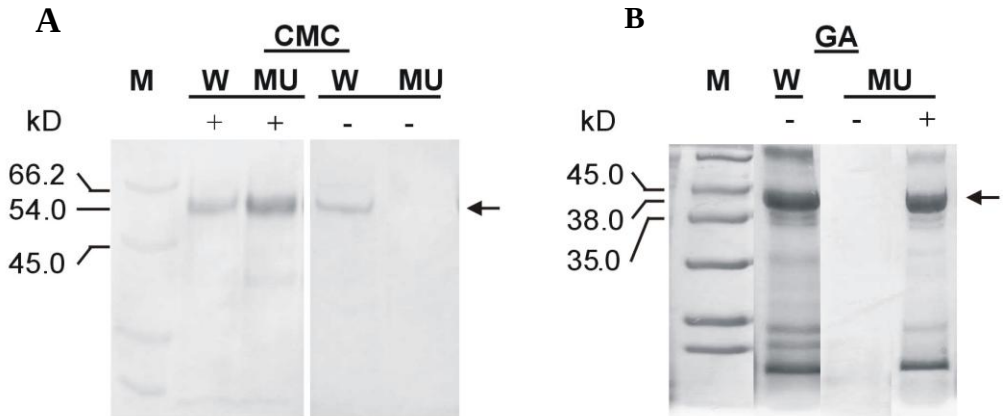

Figure 5. Effect of yeast extract on extracellular enzyme production by wild type, 1,2 (W) and mutant 4/4 (MU) strains of *Fusarium oxysporum* f. sp. *melonis* (FOM). Extracellular enzyme patterns from culture filtrates of the FOM isolates, grown on SM supplemented with 1 % of carboxymethylcellulose (CMC) (A) or galacturonic acid (GA) (B), with (+) and without (-) yeast extract (YE). Five µg of protein were resolved on 12 % SDS-PAGE and stained with Coomassie blue. In presence of YE both W or MU secreted proteins with molecular weights of 54 kD in (A) or 38 kD in (B) (arrows), were sequenced and identified as cellobiohydrolase (A) and endopolygalacturonase (B). M represents protein weight marker in kilo Dalton (kD).

Specific activity of total cellulases in the mutant increased to similar levels of that of the wild type strain 1,2 (1.10±0.08 and 1.03±0.13 nkat/mg protein for strains 1,2 and 4/4, respectively). Specific activity of endoPG, purified from pectin or NaPG

containing medium, of mutant strain 4/4 increased significantly – to 23.06±2.67 and 0.81±0.10 nkat/mg protein, respectively, when supplemented with yeast extract.

Hence, it was concluded that growth as well as specific activity of cellulases and endoPG of mutant strain 4/4 increased significantly with addition of yeast extract to the growth medium. Based on these data it was assumed that at least one of the components of the yeast extract had an influence on the mutant strain 4/4 and therefore the effect of amendments such as amino acids, vitamins and nitrogen bases (purines and pyrimidines) were tested on the growth parameters.

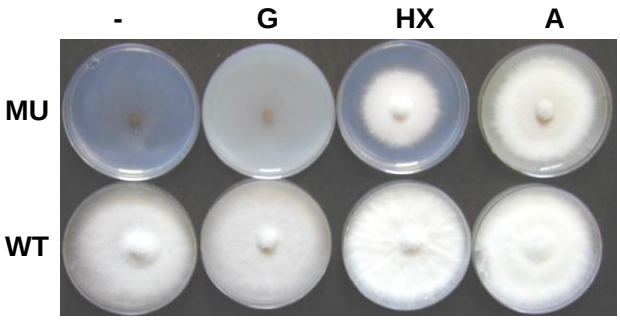

Figure 6. Complementation of growth of mutant strain 4/4 of *Fusarium oxysporum* f. sp. *melonis* by adenine and hypoxanthine amendments. Plugs of the wild type 1,2 (W) and 4/4 mutant (MU) strains, were grown on minimal medium (FMM), amended with 0.1 mg/ml of guanine (G), hypoxanthine (HX) or adenine (A). The cultures were incubated at 20°C for 5 days. Nonamended (-) medium was used as a negative control.

Various combinations of amendments were added to minimal medium (FMM) to determine whether strain 4/4 behaved as an auxotrophic mutant. Growth was partially restored by complementation with two of the three tested purines: adenine, hypoxanthine (Fig. 6), but not guanine. Moreover, addition of 10-25 mM of adenine induced and increased germination of the mutant strain 4/4 to approximately the same levels of the wild type (Fig. 7). Furthermore, effect of adenine on vegetative growth of the 4/4 mutant strain was not concentration dependent.

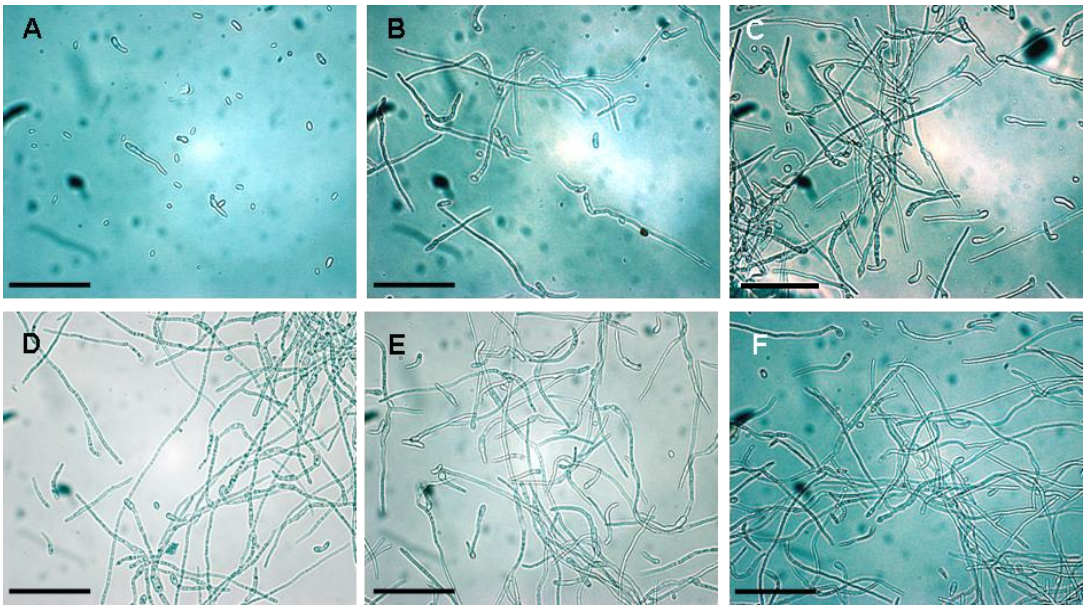

Figure 7. Complementation of germination of 4/4 mutant (MU) of *Fusarium oxysporum* f. sp. *melonis* by adenine. Addition of adenine to FMM (A) at concentrations of 10 mM (B) or 25 mM (C) induced germination of MU and increased it to levels similar to that of wild type isolate (D, E and F, respectively). Bar represents 50µm.

4.1.3. Effect of adenine supplements on pathogenicity of mutant strain 4/4

In order to determine the effect of nutritional supplements on growth of mutant strain 4/4 *in vitro* and *in planta,* pathogenicity tests were performed. Addition of adenine, but not yeast extract, partially restored pathogenicity of mutant strain 4/4 on melon plants, as determined by plant inoculation experiments conducted.

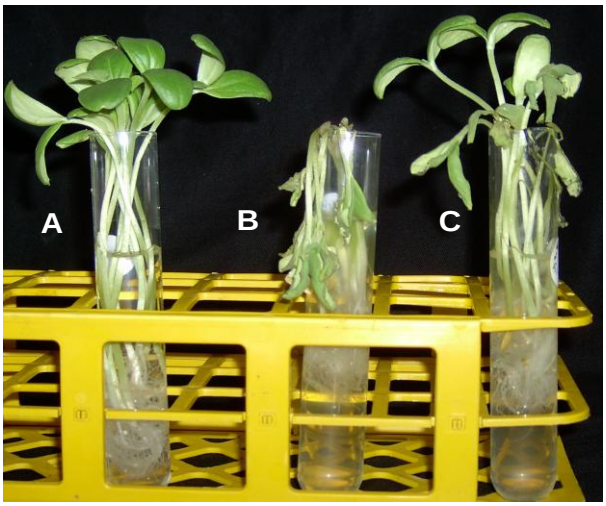

Figure 8. Effect of adenine on pathogenicity of mutant strain 4/4 of *Fusarium oxysporum* f. sp. *melonis*. Melon seedlings were inoculated with (A) conidial suspension of mutant strain 4/4 (1.5×10^6 conidia/mL); (B) mutant 4/4 conidia incubated in a 5 mg/mL adenine solution prior to incubation, transferred to water or 0.1 mg/mL adenine solution and (C) conidial suspension of wild type strain 1,2 (1.5×10^6 conidia/mL). No mortality was observed when plants were exposed to 0.1 mg/mL adenine solution, mutant strain 4/4 or water controls.

Pathogenicity was restored only after pre-incubation of the conidial suspension in the adenine solution for 24 h at 25°C. The effect of adenine on pathogenicity was

concentration dependent. When adenine was applied at 0.1 mg/mL, pathogenicity of mutant strain 4/4 was partially restored.

4.1.4. The nature of the UV-induced defect in mutant 4/4

BLAST analysis indicated a high degree of conservation of purine biosynthetic enzymes in filamentous fungi such as *N. crassa* (Galagan *et al.*, 2003), *M. grisea*, *A. nidulans*, *F. graminearum* and *F. oxysporum* (http://www.broad.mit.edu). Since adding histidine and tryptophan (precursors of purine biosynthetic pathway) did not have an effect on growth of mutant strain 4/4, the defect is likely located in the purine biosynthetic pathway, between 5-phosphoribosyl pyrophosphate (PRPP) amidotransferase (first step) and inosine monophosphate (IMP) cyclohydrolase (tenth step) (Fig. 9).

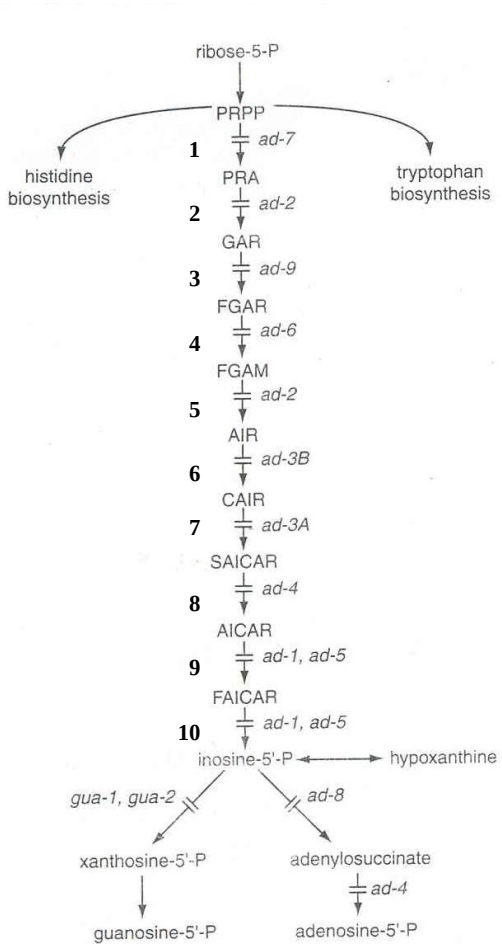

Figure 9. The 4/4 mutant strain of *Fusarium oxysporum* f. sp. *melonis* is defective in purine biosynthetic pathway*. Precursors of purine biosynthetic pathway - histidine and tryptophan did not affect growth of mutant strain 4/4. Addition of hypoxanthine complemented mutant's growth, therefore the defect is likely located in the purine biosynthetic pathway, between 5-phosphoribosyl pyrophosphate (PRPP) amidotransferase (first step) and inosine monophosphate (IMP) cyclohydrolase (tenth step). * The highly conserved purine biosynthetic pathway of *Neurospora crassa* (Perkins *et al.*, 2001).

As strain 4/4 was impervious to DNA-mediated transformation, it was not possible to perform genetic complementation of the located mutation therefore we proceeded with a forward genetics approach in order to generate additional reduced-pathogenicity strains.

4.2. Identification of pathogenicity-related genes of *Fusarium oxysporum* f. sp. *melonis* (FOM) using *Agrobacterium tumefaciens*-mediated tagged mutagenesis

4.2.1. Generation of reduced-pathogenicity mutants of FOM

In order to identify novel pathogenicity related genes in FOM, we employed a tagged mutagenesis approach on the basis of *Agrobacterium tumefaciens*-mediated transformation (ATMT). Screening of 2000 stable transformants harboring an insert of the pBHt2 and pKHt plasmids resulted in the recovery of six reduced-pathogenicity mutants. Utilization of the pathogenicity assay detected not only reduction of total plant mortality, but also a delay in initial wilt symptom appearance and slower disease progress, when comparing the mutants to wild type (Table 5, Fig. 10).

Table 5. Analysis of pathogenicity of five selected mutants of *Fusarium oxysporum* f. sp. *melonis*

Isolate	Plant mortality, (%)*	Seedling mortality 50%, (dpi) †	Apparent infection rate (r) ‡
Wild type, 1,2	96.2±4.0 a §	6.8 a	1.44 a
D122	27.1±6.0 c	32.7 c	0.36 b
D510	66.8±12.8 b	13.0 b	0.74 b
D663	56.9±2.4 b	13.6 b	0.34 b
K705	59.3±18.2 b	11.3 b	0.71 b
K993	81.4±12.0 a	11.1 b	0.59 b

dpi=day post-inoculation; * Plant mortality was evaluated over a three-week period, results represent mean (±standard error) values of three independent experiments; † Values for 50% seedling mortality (dpi-days post-inoculation) were calculated based on regression equation of disease progress; ‡ Apparent infection rate (r) over the first week of infection was calculated by regression a logit disease severity (Logit severity=ln((% mortality+0.1)/(100.1-% mortality)) in time (7-day period); § Values with different letters represent level of significance accordingly to LSMeans Difference (LSD) Tukey-Kramer multiple comparison ($P \leq 0.05$)

Differences in onset of the disease between the selected mutants and wild type isolate were detected by using a logit function (Fig. 10), evaluated using the following equation: Logit severity=ln[(% mortality + 0.1)/(100.1 - % mortality)]. Differences in slope, expressed through the respective apparent infection rate (r) (1.44 compared to

0.34-0.74), between the wild type and mutants indicate slower rates caused by reduced-pathogenicity strains (Table 5, Fig. 10).

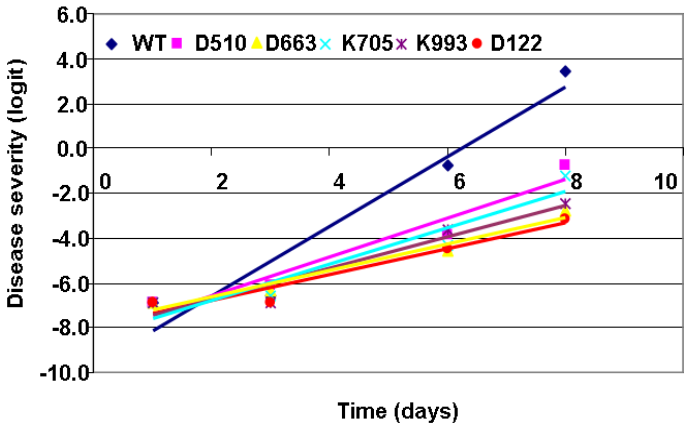

Figure 10. Wilt disease severity of selected mutants of *Fusarium oxysporum* f. sp. *melonis* in time. Severity of disease was evaluated using logit function over a seven-day period. Differences in slopes between the wild type and reduced-pathogenicity mutants indicate slower rate of disease progress of the generated strains compared to wild type (WT).

4.2.2. Location of inserted tags in the reduced-pathogenicity transformants of FOM

The number of inserts in genomic DNA of the transformants was detected by Southern blot analysis, confirming the presence of a single insert in five of the six tested transformants. In transformant D625 the presence of two inserts was detected (Fig. 11).

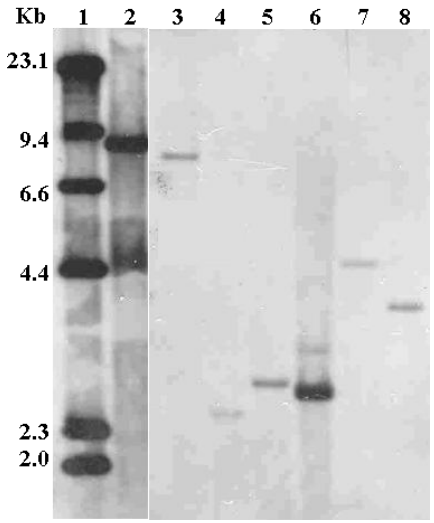

Figure 11. Detection of number of insertion tags in genomic DNA of reduced-pathogenicity mutants of *Fusarium oxysporum* f. sp. *melonis*. Genomic DNA of six selected transformants was digested with *Pdm*I and hybridized with pBHt2/*Hind*III as a probe. Lanes 3-8 contain genomic DNA of K993 (lane3), D122 (lane 4), D510 (lane 5), D625 (lane 6), D663 (lane 7) and K705 (lane 8), respectively. DNA size marker (Kb) and pBHt2/*Hind*III positive control are presented in lanes 1 and 2, respectively.

Thermal asymmetric interlaced (TAIL)-PCR was used to identify the location of the inserted tag in each of the five (K993, D122, D510, D663, K705) transformants harboring a single tag (Table 6).

Table 6. Location of inserted tag in reduced pathogenicity transformants of *Fusarium oxysporum* f. sp. *melonis*

Name	Impaired gene	Sequence description	Locus/accession number *	Location of insert
K705	*pex7*	Peroxisome biogenesis factor 7	FOXG_08573	298bp upstream
D663	*hop78*	*Mutator* superfamily transposase	AAP31248†	244bp upstream
D510	*cdc48*	Cell division protein Cdc48	FOXG_09364	220bp upstream
K993	*cdc48*	Cell division protein Cdc48	FOXG_09364	coding region (257bp)
D122	*snt2*	*Schizosaccharomyces pombe snt2*-like transcription factor	FOXG_01993	coding region (1326 bp)

* Accession numbers are according to the Broad Institute /http:www.broad.mit.edu/ and NCBI databases. † Chalvet *et al.*, 2003.

Based on the fact that D122 exhibited the most significant reduction in pathogenicity, we focused our efforts on further characterization of this mutant.

4.3. The *snt2* transcription factor-like coding gene is involved in development and pathogenesis of *Fusarium oxysporum* f. sp. *melonis* (FOM)

The tagged mutant D122**,** which caused delayed appearance of initial wilt disease symptoms as well as marked reduction of pathogenicity, was chosen as the focus for this study. The D122 mutant was shown to be impaired in the *snt2* gene encoding a transcription factor, hence it was assumed that further characterization of the mechanistic nature of *snt2* may contribute to the understanding of pathogenesis and development of FOM.

4.3.1. D122 is affected in a *snt2*-transcription factor-like coding gene

The D122 mutant was shown to be affected in a gene, which demonstrated a similarity to the *snt2* gene of *Schizosaccahromyces pombe*, therefore this gene was designated as *snt2*. The complete genomic DNA sequence of FOM s*nt2* was determined after its amplification using a genome walking procedure and its coding region was found to be 5202 bp in length, containing five short introns (172bp, 67bp, 104bp, 105bp and 53bp) and encoding a protein of 1567 amino acids. The FOM *snt2* open reading frame was deduced by comparing it to the sequence of *F. oxysporum* f. sp. *lycopersici* FOXG_019932.2 (www.broad.mit.edu) and to a 3.1kb partial cDNA sequence of FOM *snt2*, amplified by RT-PCR with primers BAHfom1F/2R. The FOM SNT2 protein contains five conserved domains: a bromo-adjacent domain (BAH) located at position 205-324 amino acids, three plant homeodomain Zn fingers (PHD) at positions 362-410, 752-793 and 1074-1144, and a GATA-type Zn-finger at position 925-971 (Fig. 12A). Multiple alignment analysis of SNT2 showed that FOM SNT2 is 96%, 79% and 63% identical to proteins from *F. oxysporum* f.sp. *lycopersici* (FOL) (FOXG_019932.2), *F. graminearum* (FGSG_06833.3) and *F. verticillioides*

(FVEG_05152.3), respectively. The N and C termini of the protein displayed a lower percent of similarity to the listed proteins. It was also found that FOXG_019932.2 contains a 60bp 5-UTR region, however in *snt2* of FOM this fragment was capable of being translated, similar to that in FGSG_06833.3 of *F. graminearum*. Another significant difference between FOM *snt2* and its *F. oxysporum* f. sp. *lycopersici* homologue resides in the 84 bp shorter annotated third intron of the FOM gene compared with FOL, which results in an additional PHD finger (Fig 12A, B).

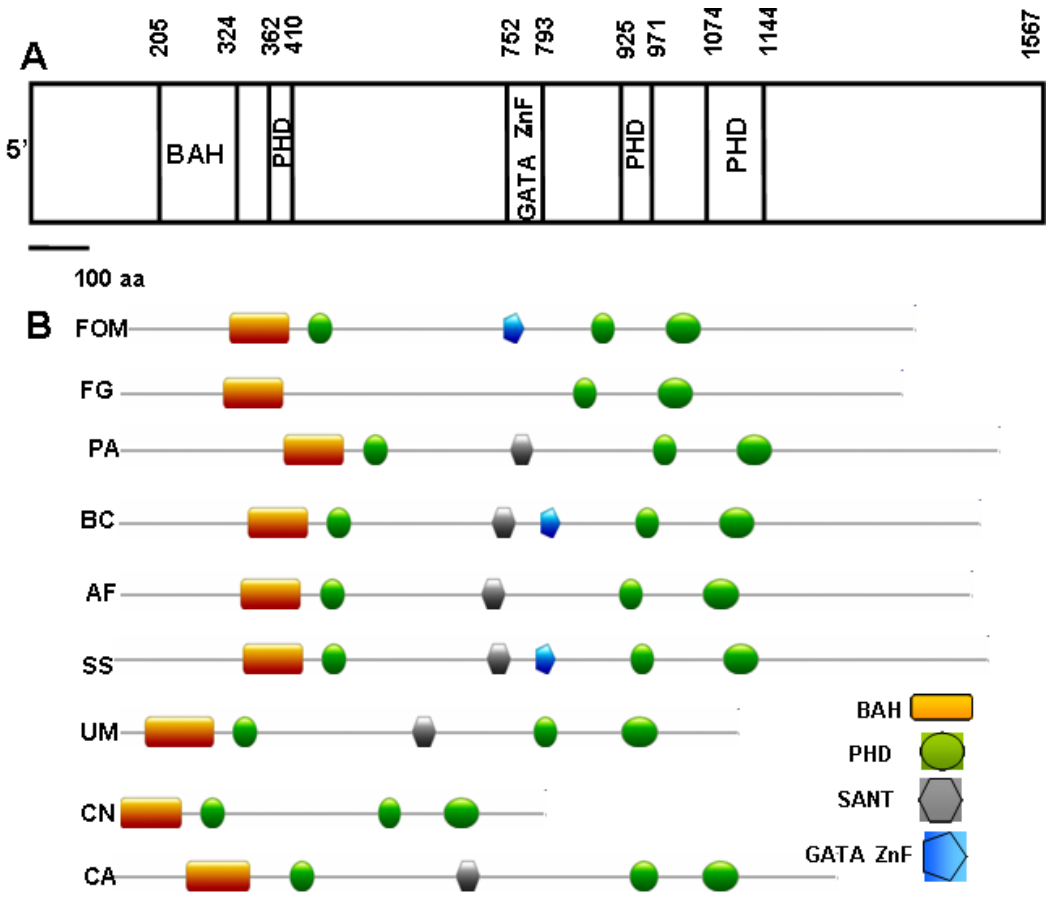

Figure 12. SNT2 protein structure. (A) The SNT2 protein of *Fusarium oxysporum* f.sp. *melonis* harbors five conserved domains: bromo-adjacent domain (BAH) at position 205-324 amino acids, three plant homeodomain Zn fingers (PHD) at positions 362-410, 752-793 and 1074-1144, and a GATA-type Zn-finger at position 925-971. Bar indicates a 100 amino acid-sized fragment. (B) Comparison of the structural domain of SNT2 proteins between different fungi (BAH, rectangle; PHD, circle; GATA Zn-finger, pentagon; SANT, hexagon). Sequences shown: SNT2, *Fusarium oxysporum* f.sp. *melonis* (FOM); XP_387009, *Fusarium graminearum* (FG); XP_001908700, *Podospora anserina* (PA); XP_001549253, *Botritis cinerea* (BC); XP_750273, *Aspergillus fumigatus* (AF); XP_001584831, *Sclerotinia sclerotiorum* (SS); XP_716567, *Candida albicans* (CA); XP_761724, *Ustilago maydis* (UM), and AAN75722 (ZNF1), *Cryptococcus neoformans*.

The presence of the third PHD finger of SNT2 is found in different filamentous fungi (Fig. 12B); in *Fusaria* it is found in the SNT2 proteins of FOM and *F. verticillioides*, but not in *F. graminearum*. The GATA-Zn finger was only found in *F. oxysporum* and in two necrotrophic fungi, *Sclerotinia sclerotiorum* and *Botrytis cinerea,* but not in other fungi with annotated genomes (Fig. 12B).

4.3.2. Verification of *snt2* function by targeted gene disruption

In order to verify the significance of *snt2* in development and pathogenicity, and due to the fact that in D122 the mutating cassette was integrated downstream of the 5'-coding region start site, targeted gene disruption of *snt2* in the wild type isolate was carried out. The targeted mutagenesis was performed by use of ATMT and resulted in recovery of approximately 200 stable, Hygromycin B-resistant transformants (Fig. 13A).

However, based on initial PCR analysis of the transformants' DNA, the majority of the transformants appeared to harbor ectopic integration events and only 1% of the isolates were disruptants at the *snt2* locus (Fig. 13B). Southern blot analysis confirmed the presence of a single integration of the *snt2::hphR* construct at the *snt2* locus, verifying targeted mutagenesis (Fig. 13C). The transcript of *snt2* was undetectable in the Δ*snt2* isolate (as well as in the D122 strain), as determined by RT-PCR (Fig. 13D). Interestingly, expression of *snt2* within mycelium was found to be much lower than that of the β-tubulin gene.

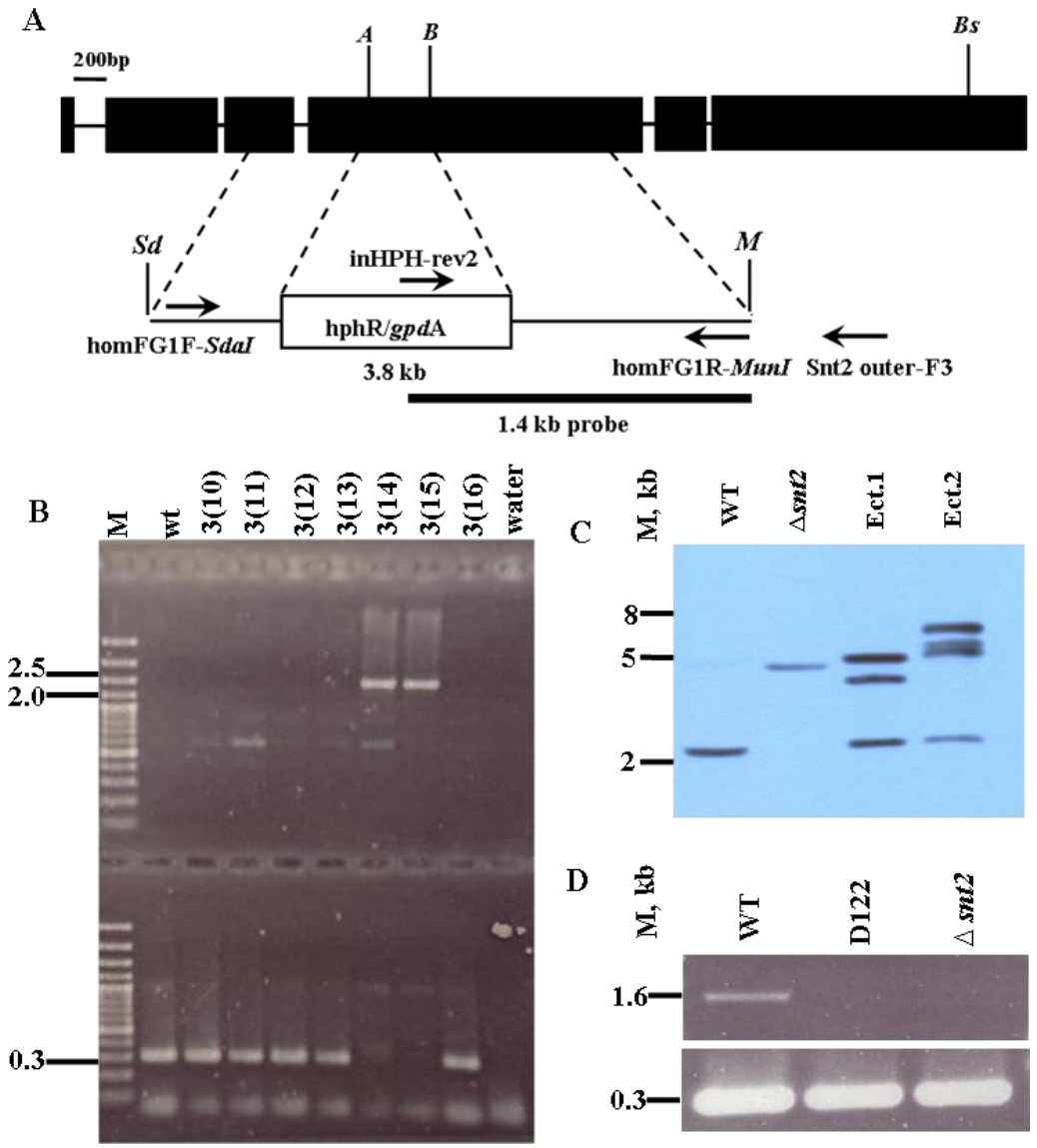

Figure 13. Targeted disruption of *snt2* in *Fusarium oxysporum* f.sp. *melonis*. (A) Knockout vector construction was performed by introducing a 2.13 kb hygromycin B resistance cassette between the *Acc65*I*(A)* and *Bgl*II*(B)* sites of a 1.6 kb fragment of FOM *snt2*, which was first amplified with primers homFG1F/R and cloned into pGEM-T easy, subsequently creating a 3.8 kb *snt2::hphR* cassette. The *Sda*I *(Sd)*/*Mun*I *(M) snt2::hphR* cassette was transferred into the *EcoR*I/*Pst*I binary vector pDHt in order to perform *Agrobacterium tumefaciens*-mediated transformation. (B) PCR detection of *snt2*-disruptants, using two pairs of primers (i) for amplification of a 2.2kb flanking region between *snt2::hphR* cassette and outer 5'-end of *snt2* (inHPH-for2/outerSNT2-F3) (ii) for amplification of a 0.3kb fragment, which was deleted in *snt2::hphR* cassette, but present in DNA of wild type isolate or ectopic transformants (SNT2-del.for1/SNT2-del.rev1). (C) Southern blot analysis using a 1.4 kb fragment of *snt2::hphR* amplified with inHPH-rev2/homFG1R as a probe (see A) was performed on *Acc65*I*/Bsp1407*I *(Bs)* digested genomic DNA, detecting a disruption of *snt2* in one transformant (designated Δ*snt2*). Ectopic transformants (Ect. 1 and Ect. 2) with several insert copies and a wild type (WT) with an original *snt2* copy. (D) RT-PCR analysis of *snt2* transcripts with the ß-tubulin gene used as a control. M denotes a DNA size marker.

Plant pathogenicity assays with the Δ*snt2* mutant showed that the mutants exhibited impaired pathogenicity, as evident from the significant delay in initial symptom appearance, compared to the wild type isolate. Furthermore, inoculation of muskmelon plants by Δ*snt2* led to approximately 50% reduction in plant mortality compared to the wild type isolate (Fig. 14). In addition, the Δ*snt2* mutant demonstrated reduced upper and lower stem colonization (27±8% and 59±11%, respectively), compared to the wild type isolate.

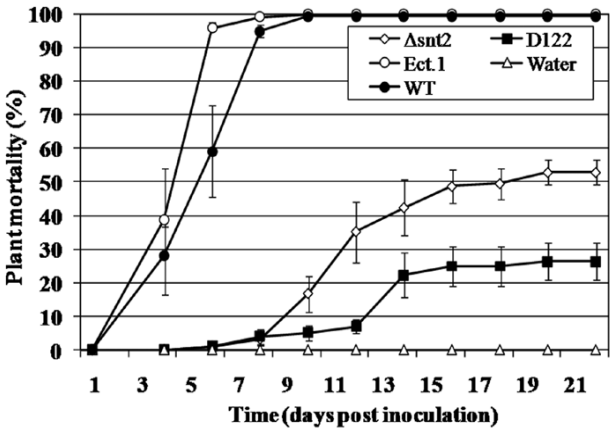

Figure 14. Disruption of *snt2* impairs pathogenicity of *Fusarium oxysporum* f.sp. *melonis* on muskmelon plants. One-week old muskmelon seedlings were inoculated by dipping roots in a conidial suspension (5×105 conidia/ml). Plants were assessed for symptoms of vascular wilt disease over a 3-week period. The mean (±SE) were calculated from three independent experiments and compared using the Turkey-Kramer test ($P<0.05$). Treatments:Δ*snt2*, targeted *snt2* mutant; D122, tagged *snt2* mutant; Ect. 1, ectopic transformant; WT, wild type; water control

Similarly, the D122 mutant was impaired in its colonization ability and exhibited significantly lower colonization of upper plant stems (38±8%), when compared to the wild type isolate. Based on these results, it appears that *snt2* is important for invasive pathogen growth and is essential for full pathogenicity of FOM.

4.3.3. *In planta* expression of *snt2*

To determine the timing of *snt2* expression *in planta,* transcript levels of *snt2* in inoculated muskmelon plants were examined using qRT-PCR over a six day post inoculation (dpi) period. The *snt2* transcript amounts reached detectable levels at 2 dpi, likely due to low amounts of the fungal biomass within plant tissue at 1 dpi. At

day 3 the expression of *snt2* was 5-fold higher (than day 2), while at day 5 *snt2* expression was significantly lower (100-fold reduction) and by day 6 its expression was undetectable (Table 3). Interestingly, first significant wilt symptoms in wild type-inoculated plants appeared at 4 dpi and at 6 dpi plant mortality was over 90%. In contrast, after inoculation with the D122 mutant no wilt symptoms were detected until 6 dpi. Thereafter, wilt symptoms and mortality caused by D122 were evident (Fig. 14). These results confirmed the importance of *snt2* for invasive growth within the host and rapid colonization of muskmelon plants.

Table 3. Expression of the *snt2* during pathogenesis of *Fusarium oxysporum* f.sp. *melonis* on muskmelon plants

Treatment, days post-inoculation	*snt2* relative gene expression*
1	BDT
2	1
3	4.96 ± 2.33†
4	0.35 ± 0.35
5	0.01 ± 0.06†
6	BDT
water	BDT

* cDNA was synthesized from 0.5 µg of mRNA, isolated from infected plants. All samples were analyzed in triplicate. Transcripts levels at dpi 2 were used as a reference. Averaged CP values were normalized to the endogenous control gene, ß-tubulin. Expression *snt2* levels with standard error of two independent experiments were evaluated using the REST© program (Pfaffl *et al.*, 2002). BDT = below detection threshold. †= significantly different results.

4.3.4. *snt2* is required for fungal growth and development

In addition to the reduction in pathogenicity, cultures of both D122 and Δ*snt2* mutants of FOM also exhibited defects in growth and development.

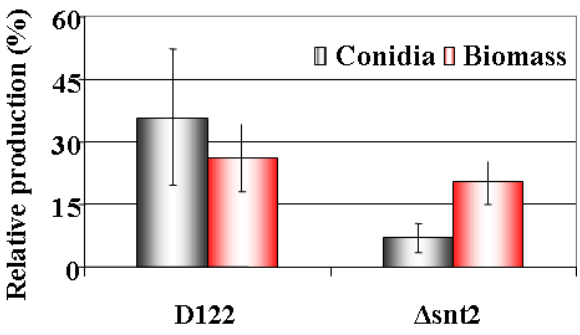

Figure 15. Effect of disruption of *snt2* on conidia and biomass accumulation in *Fusarium oxysporum* f. sp. *melonis*. Mean (±SD) amount of conidia (on PDA medium) and biomass accumulation (liquid FMM medium) of three independent experiments were analyzed using Tukey-Kramer test ($P<0.05$). Both the *snt2*-mutants demonstrated significant reduction of the tested parameters, when compared to wild type isolate (100%).

Among the affected parameters were reduced growth rates, conidiation (6.9±3.9, 1.3±0.8×10^6 conidia/plate) on PDA medium, and biomass accumulation on minimal liquid medium (33.9±10.4 and 26.4±6.8 mg) for D122 and Δ*snt2* (respectively), compared to the wild type (which produced 19.8±6.4 conidia/plate and 77.0±16.6 mg of biomass). Relative conidial and biomass production by the different strains is summarized in Fig. 15.

4.3.4.1. Phenotypic characterization of the *Neurospora crassa* Δ*snt-2* strain

In order to evaluate whether the involvement *snt2* in gene expression regulation is restricted to FOM, or can be observed in another species, a partial characterization of the phenotypic consequences of *snt-2* disruption was assessed in the model fungus *N. crassa*.

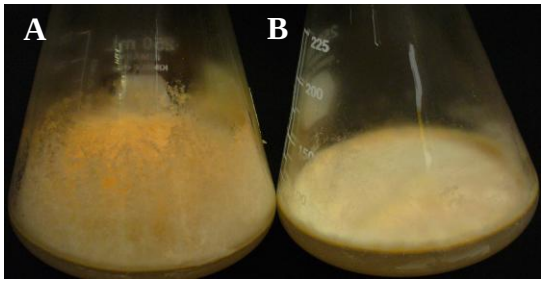

Figure 15. Phenotypical differences between the wild type (A) and Δ*snt-2* mutant (B) strains of *Neurospora crassa*. On solid medium the Δ*snt-2* mutant developed thicker, slower growing mycelium, with little aerial hyphae, reduced numbers of conidia, and therefore less pronounced orange color of the culture, compared to the corresponding wild type.

The disrupted *snt-2* strain was made available as a result of the effort of the *Neurospora* Functional Genomics Project (http://www.fgsc.net/ncrassa.html) that is involved in generation of an extensive collection of gene-disrupted mutants. During growth on solid medium, the Δ*snt-2* strain (NCU07412.2) produced a thick, significantly slow growing (1.65±0.38 mm/hr) mat of hyphae with little aerial hyphae, when compared to the normal growth attributes (2.23±0.14 mm/hr) of the wild type isolate (Fig. 16). Macroconidia production of the Δ*snt-2* strain was only 10 % of the wild type strain (0.28±0.04 and 2.19±0.37×10^9 conidia/flask, respectively), which explains the less pronounced orange color of its mycelium. In this model organism disruption of *snt-2* also affected perithecia formation, since the Δ*snt-2* mutant strains

were unable to produce mature protoperithecia, indicating involvement of *snt-2* in sexual development of *N. crassa* (data not shown).

4.3.5. Disruption of *snt2* causes increased hyphal septation in FOM and *Neurospora crassa*.

In light of the fact that the *snt2* mutants exhibited slower linear growth, cell wall morphology was examined. Congo red staining, which binds a cell wall chitin monomer - *N*-acetyl glucosamine, was employed for this purpose, enabling the detection of irregularities in hyphal septation. Distances between septa along the hyphal cells of Δ*snt2* FOM mutant were markedly shorter, than in the wild type strain (Fig. 17). This was also observed in the D122 strain (data not shown).

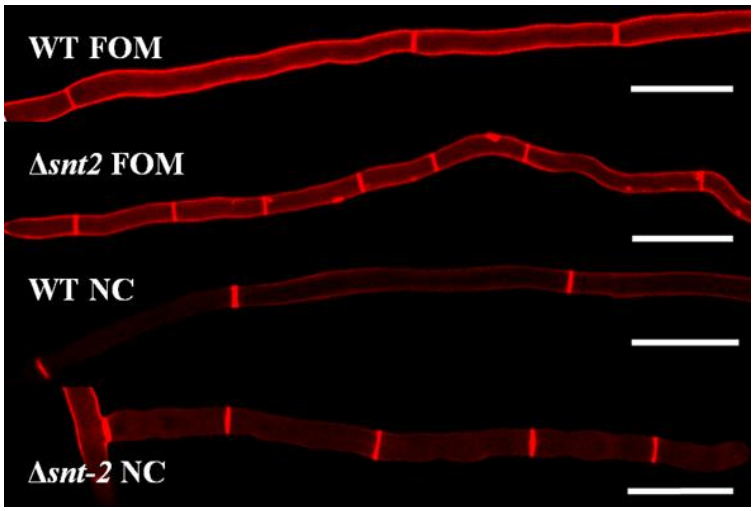

Figure 17. *snt2*-disruption leads to abnormalities of hyphal septation in *Fusarium oxysporum* f. sp. *melonis* (FOM) and *Neurospora crassa* (NC). Congo red staining detected irregularities in cell wall deposition, detecting shorter hyphal stretches between septa and a patchy staining pattern of cell walls in Δ*snt2* mutants of FOM and NC, compared to their respective wild type strains. Bar=50μm.

4.3.6. *In vivo* viability staining detected increased cell death in *snt2* mutants of FOM and *Neurospora crassa*

As the appearance of the *snt2* mutants in both FOM and *N. crassa* was indicative of stress-related conditions, Evans blue staining was used to provide an assessment of viability of the hyphal cells (Fig. 18).

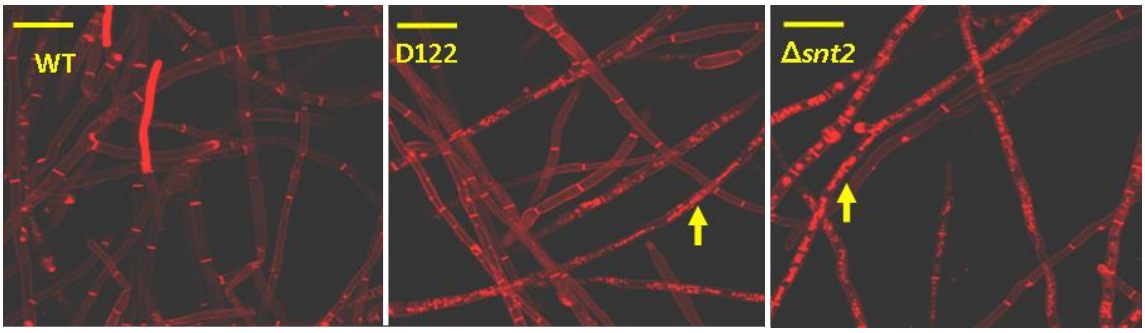

Figure 18. Increased cell mortality was observed in *snt2* mutants of *Fusarium oxysporum* f.sp. *melonis* (FOM), as detected by Evans blue staining. Evans blue staining of mycelial cells detected decreased viability of the cells in mutants D122 and Δ*snt2* of FOM (marked by arrows), compared to the wild type isolate. Bar indicates 50μm.

Based on comparison of the staining pattern and evaluated percentage of stained (dead) hyphal cells, a significant increase in cell death was evident in the Δ*snt2* mutants of FOM and *N. crassa*, when compared to the wild type isolate (5.3±1.9 and 19.6±6.4 %; 1.0±0.3 and 13.9±1.4% in wild type strains and Δ*snt2* mutants of FOM and *N. crassa*, respectively) (Fig. 19). The tagged D122 mutant of FOM also displayed increased cell death (15.9±4.7%) (*data not shown*).

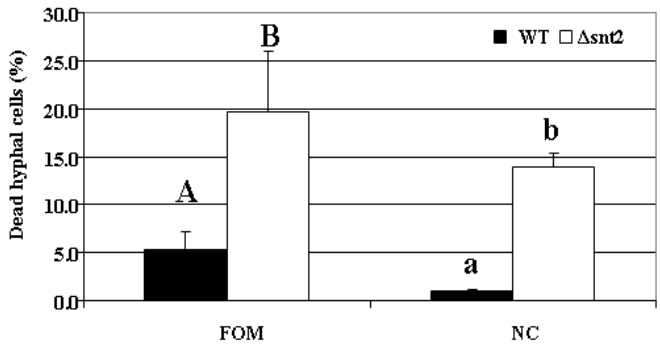

Figure 19. *snt2* mutation leads to increased cell death in *Fusarium oxysporum* f.sp. *melonis* (FOM) and *Neurospora crassa* (NC). Percentage of dead cells in both the Δ*snt2* mutants of FOM and NC, compared to their respective wild type (WT) isolates among 10^3 cells was estimated. Results represent the mean of three independent experiments, analyzed separately for each fungal species by Tukey-Kramer multiple comparison test ($P \leq 0.05$) and levels of significance are marked with different letters.

4.3.7. Analysis of differentially expressed genes between the wild type and tagged D122 *snt2*-mutant isolates of FOM.

Suppressive subtraction hybridization (SSH) was carried out in order to detect differentially expressed genes between the wild type and D122 isolates. To identify

downstream target genes of *snt2*, mRNA was extracted from both isolates, at a developmental stage characterized by absence of visible morphological differences (i.e. initial germination). mRNA populations of the wild type and D122 mutant isolates were used for synthesis of "tester" and "driver" cDNAs, respectively. Sequences of 200 random clones were analyzed, identifying fourteen putative differentially expressed genes (Table 6). The majority (41%) of identified genes belong to primary metabolism. Gene regulation/signal transduction, membrane transport and housekeeping genes were represented by 2, 5 and 0.5% of the sequences, respectively. Over fifteen percent of the submitted sequences did not match those in existing databases.

Table 6. Differentially expressed genes in the cDNA population of the D122 FOM mutant, detected by suppressive subtraction hybridization

No.	*Sequence description*	*Seq. Name*	*Accession or Locus number*	*Organism*
	Gene regulation and signal transduction			
1	b-Zip Transcription Factor-coding	IDI-4	FOXG_04081.2	*Fusarium oxysporum**
2	ATP-family AAA domain containing protein	AAA	FOXG_04199.2	*F. oxysporum*
3	Glutamine amidotransferase (GATase1)-like protein	GAT1-like	FOXG_06249.2	*F. oxysporum*
	Housekeeping			
4	Elongation factor 1-gamma	EEF1G	FOXG_01492.2	*F. oxysporum*
	Membrane transport			
5	Formate/nitrate transporter	FNT	FOXG_10116.2	*F. oxysporum*
6	Multi-drug resistance transporter	MSF	FOXG_09760.2	*F. oxysporum*
	Miscellaneous			
7	Basic proline-rich protein	PRP	NP_001092050	*Sus scrofa*
8	Predicted protein		FOXG_06645.2	*F. oxysporum*
9	Hypothetical protein	UK1	FVEG_07593.2	*F. verticillioides*
10	Predicted protein	RBS1	FOXG_14252.2	*F. oxysporum*
	Primary metabolism			
11	Pyruvate decarboxylase	PDC	BAE98181.1	*F. oxysporum*
12	Coproporphyrinogen oxidase III	CPOXIII	XP_390915.1	*Gibberella zeae*
13	ATP-citrate synthetase subunit 1	ACS1	XP_001228353.1	*Chaetomium globosum*
14	Glyceraldehyde-3-phosphate dehydrogenase	G3PDH	XP_386433.1	*Gibberella zeae*

* Loci names are according to sequence database of *Fusarium oxysporum* f. sp. *lycopersici:* http://www.broadinstitute.org/annotation/genome/fusarium_group. Accession numbers are according to the NCBI Database.

An association between four of the SSH-detected genes (*idi4*, induced during incompatibility; *pdc*, pyruvate decarboxylase; *msf1*, transporter of the major facilitator family and *eeF1G*, eukaryotic translation elongation factor 1-gamma) and the highly conserved target of rapamycin (TOR) serine/threonine kinase pathway has been previously reported (Teichert *et al.*, 2006). The TOR pathway controls numerous cellular processes, including regulation of cell growth through nutrient sensing. Quantitative (q)RT-PCR was used to further investigate expression of the four genes. Three of the mentioned genes (*idi4*, which is discussed in the next chapter, *pdc* and *rbs1*), exhibited a significant change in transcript levels in both D122 and Δ*snt2*, when compared to the wild type isolate (Table 7). During the SSH gene screen, a unique *F. oxysporum* gene, designated regulated by snt2 (*rbs1*), was found. Its expression was significantly reduced in the D122 and Δ*snt2* mutants (-6.78±0.37 and -6.75±0.15-fold), when compared to the wild type. *rbs1* is similar to a FOXG_14252.2, a unique gene found in *F. o.* f.sp. *lycopersici*. This gene encodes a short 170 amino acid protein with yet unknown function. The *pdc* gene encodes a pyruvate decarboxylase, a key enzyme in pyruvate assimilation; its expression was found to be negatively regulated by TOR kinase in *F. fujikuroi* (Teichert *et al.*, 2006). A 20.78±7.04-fold increase in expression of *pdc* was observed in Δ*snt*2, compared to the wild type isolate, however in D122 *pdc* expression did not differ significantly from the wild type isolate (0.90±0.13-fold), even though this gene was detected in the D122 suppression library. Another gene encoding a transporter of the major facilitator superfamily (*mfs*) is known to be negatively regulated by the global nitrogen regulator AreA (Schönig *et al.*, 2008). However, its relative expression in the D122 and Δ*snt2* mutants was not different from that of the wild type (1.32±0.62 and 1.60±0.86-fold, respectively).

Furthermore, expression of an additional SSH-detected gene, *eEF1G*, encoding a translation elongation factor, which is negatively-regulated by TOR kinase, was not significantly different in Δ*snt2*, when compared to the wild type isolate (Table 7). Relative expression of additional SSH-detected genes, unrelated to the regulatory network of the TOR pathway, encoding a coproporphyrinogen oxidase III (CPOXIII), a formate/nitrate transporter (FNT), an ATP-citrate synthetase subunit 1 (ACS1), a glutamine amidotransferase (GATase1)-like protein, a glyceraldehyde-3-phosphate dehydrogenase and an ATPase-family AAA domain containing protein, were also evaluated, however no difference in their expression was found (Table 7).

Table 7. Differentially expressed genes in the D122 FOM mutant as detected by suppression subtractive hybridization

Description	Protein name	Relative gene expression in D122, (fold change)[a]	Relative gene expression in Δ*snt2*, (fold change)
Pyruvate decarboxylase†	PDC	0.90±0.13‡	20.78±7.04*
Coproporphyrinogen oxidase III	CPOXIII	0.73±0.36	0.54±0.48
ATP-citrate synthase subunit 1	ACS1	0.81±0.10	nd
Glyceraldehyde-3-phosphate dehydrogenase	GAPDH	nd	0.61±0.08
b-Zip transcription factor †	IDI-4	20.53±2.04*	24.5±2.25*
Formate/nitrate transporter	FNT	nd	2.56±1.71
ATPase-family AAA domain containing protein	AAA	0.75±0.14	nd
Elongation factor 1-gamma †	EEF1G	1.29±0.21	2.84±1.75
Predicted protein	RBS-1	0.15±0.03*	0.15±0.01*
Major facilitator superfamily†	MFS	1.32±0.62	1.60±0.86
Glutamine amidotransferase (GATase1)-like protein	GAT1-superfamily	0.63±0.15	nd

[a] cDNA was synthesized from 1 µg of total RNA, extracted form mycelium grown on minimal (FMM) medium. All samples were analyzed in triplicate. Averaged CP values were normalized to the endogenous control gene, ß-tubulin. Gene expression level and its comparative analysis (‡) of three technical and two independent biological repeats were evaluated using the REST© program (Pfaffl *et al.*, 2002). Significantly different values are marked by an asterisk. † = detected by cross-species hybridization (Schönig *et al.*, 2008) mutants of *F. fujikuroi*. nd = not determined.

4.3.8. The SNT2 transcription factor is involved in regulation of the autophagy-related transcription factor IDI4 and is not necessary for nitrogen utilization

An additional gene detected by SSH analysis, *idi4*, which displayed similarity to the *P. anserina* TF-coding gene *idi-4* was shown to be involved in regulation of autophagy. A significant change in autophagosome staining in the *snt2* mutants, accompanied by significantly elevated expression of the *idi4* gene (20.53±2.04 and 24.5±2.25-fold, in D122 and Δ*snt2*, respectively) was observed, when compared to the wild type isolate (Table 7). Real time PCR analysis also detected an 8-fold elevation in expression of the *idi4* homologue (NCU08055.3) in *N. crassa* Δ*snt-2* mutant (8.36±0.65), suggesting a common regulatory pathway in the two fungal species. In *F. fujikuroi* the expression of *idi4* was demonstrated to be negatively regulated by TOR kinase through AreA (Teichert *et al.*, 2006). To further explore the potential mechanism involved, mycelia were stained with the autophagosome detecting stain - monodansylcadaverine (MDC). Addition of the serine protease inhibitor phenylmethanesulphonylfluoride (PMSF) emphasizes appearance of autophagosomes. In the absence of PMSF, it was evident that D122 (Fig. 20B) and Δ*snt2* (Fig. 20C) contained increased amounts of MDC-stained organelles, presumably mature autophagosomes, when compared to the wild type isolate (Fig. 20A). Addition of PMSF enhanced the appearance of MDS-stained organelles in all observed isolates (D, E and F for wild type, D122 and Δ*snt2*, respectively). To verify the nature of these organelles, 3-methyladenine, a specific inhibitor of autophagosome assembly (Pollack *et al.*, 2009) was applied, prior to MDC staining. As the presence of 3-methyladenine almost eliminated MDC staining in the wild type cells (Fig. 20G), it is suggested that the observed organelles were, in fact, autophagosomes (Fig. 20H).

To detect whether *snt2* is involved in direct regulation of the autophagy process, the expression of a highly conserved gene, *idi7/agt8*, which regulates initial steps of non-selective autophagy was evaluated. Its relative expression in Δ*snt2* and D122 (1.07±0.55 and 0.59±0.35, respectively) was not significantly different from that of the wild type isolate, therefore it is likely that *snt2* is not involved directly in regulation of non-selective autophagy. Based on these data, we suggest that *snt2* is an important factor related to cell survival, whose disruption leads to stress-related symptoms, including increased appearance of autophagosomes.

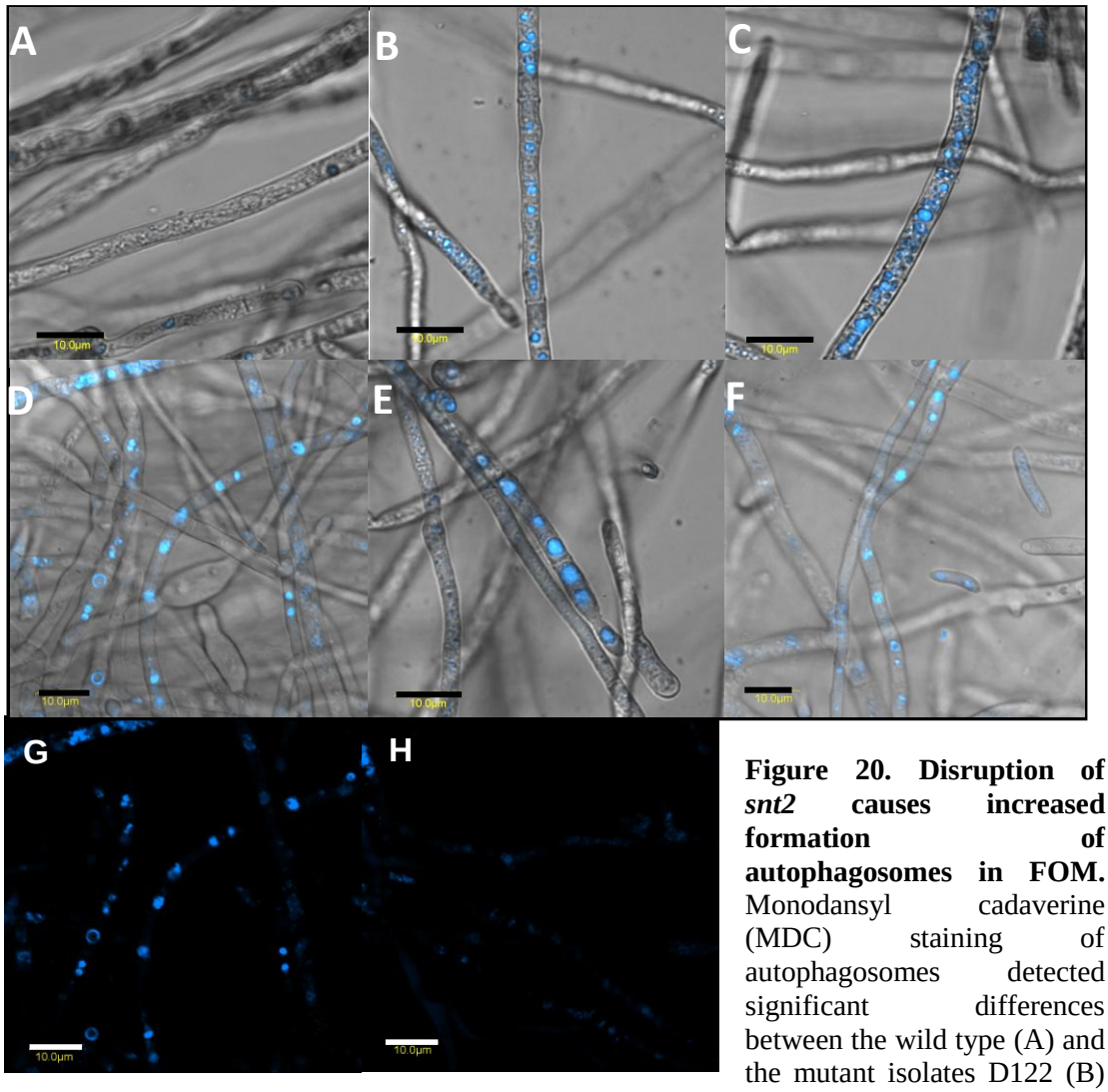

Figure 20. Disruption of *snt2* causes increased formation of autophagosomes in FOM. Monodansyl cadaverine (MDC) staining of autophagosomes detected significant differences between the wild type (A) and the mutant isolates D122 (B) and Δ*snt2* (C). Formation of autophagosomes in the presence of phenylmethanesulphonyl fluoride (PMSF) and stained by MDC in the wild type (D), D122 (E) and Δ*snt2* (F) isolates. Elimination of the MDC staining in PMSF-treated wild type cells (G) after addition of the specific autophagosome inhibitor 3-methyladenine (H). Bar indicates 10µm.

To investigate if *snt2* is involved in nitrogen metabolism and to determine whether it is associated with the TOR kinase pathway, the effect of the specific TOR inhibitor rapamycin on utilization of different sole sources of nitrogen (10mM nitrate, ammonia and glutamate) was examined. During growth on these three nitrogen sources, both the *snt2* mutants grew in an apparently indistinguishable manner compared to the wild type isolate. However, following actual measurement of radial growth it was detected that initially, glutamate slightly delayed vegetative growth of both the *snt2* mutants in the absence of rapamycin and secondly, addition of rapamycin did not delay nitrogen utilization of the Δ*snt2* isolate, as opposed to apparently normal growth of the tagged transformant D122.

As previously demonstrated, *snt2* and *areA* appear to both regulate the expression of at least two common genes, therefore the transcript levels of three master nitrogen regulators: *fnr1* (a homolog of *are*A in *F. oxysporum*), *nit4* (a pathway-specific nitrogen regulator of *N. crassa*), *glnA* (glutamine synthetase) and the *cpc1* (cross-pathway control) gene, which regulates fungal amino acid biosynthesis and are negatively regulated by AreA (Schönig *et al.*, 2008), were examined. However, expression of these genes did not differ significantly in the Δ*snt2* mutant, when compared to the wild type isolate (Table 8).

Table 8. Expression profile of nitrogen metabolism-related genes in the Δ*snt*2 mutant of *Fusarium oxysporum* f. sp. *melonis*

Gene	Locus/accession number	Δ*snt*2 relative gene expression*	Description
Cpc1	FOXG_05954	2.12 ±0.09	Cross-pathway control
Fnr1	DQ387858	1.20±0.15	Global nitrogen regulator
Nit4	FOXG_06396	0.95±0.08	Pathway-specific nitrogen regulator
GlnA	FOXG_05182	4.02±0.50	Glutamine synthetase

* cDNA was synthesized from 1 µg of total RNA. All samples were analyzed in triplicate. Averaged CP values were normalized to the endogenous control gene, ß-tubulin. Gene expression level and its comparative analysis of (‡) were evaluated using the REST© program (Pfaffl *et al.*, 2002). Accession numbers are according to the Broad Institute /http:www.broad.mit.edu/ and NCBI databases.

Growth of both mutant isolates was also not affected by the 3-aminotriazole (3-AT) that induces amino acid starvation along with expression of *cpc1*, supporting results obtained by qRT-PCR. Moreover, all the examined isolates were not able to utilize chlorate (6%) and able to grow on hypoxanthine (0.05%), confirming the absence of defects in the nitrate reduction pathway. In light of these data it is likely that *snt2* is not essential for nitrogen utilization.

4.4. Disruption of *snt2* leads to mitochondrial dysfunction in *Fusarium oxysporum* f.sp. *melonis* (FOM) and *Neurospora crassa.*

The activity of two major groups of ROS-responsive enzymes [superoxide dismutases (SODs) and NADPH-oxidases (NOXs)] was examined in the FOM *snt2* mutants using native PAGE analysis coupled with gel activity assays. No significant visual difference in NOX activity was detected (data not shown).

4.4.1. The *snt2* disruption causes dysfunction of SOD enzymes in FOM and *N. crassa*

Total SOD activity of intracellular proteins extracted from the wild type and D122 mutant strains of FOM, grown on minimal and complete media, was evaluated. The wild type strain demonstrated higher enzymatic activity during growth on complete medium, contrary to the D122 mutant, that showed higher SOD activity when incubated on minimal medium (Fig. 21).

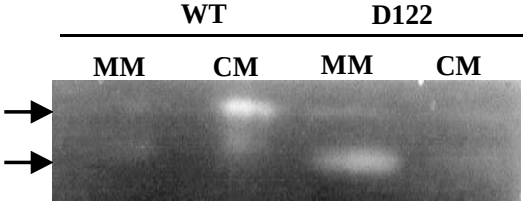

Figure 21. Differences in SOD enzymatic activities, between wild type (WT) and the *snt2* mutant (D122) of *Fusarium oxysporum* f. sp. *melonis* using a native gel activity assay. Total SOD activities of 40μg crude intracellular proteins of the wild type (WT) and D122 mutant was detected. Complete FLC (CM) and minimal FMM (MM) media were used for fungal growth. The upper and lower bands (arrows) relate to Fe,Mn- and Cu,ZnSOD activities, respectively.

In order to identify which SOD type was induced, a cyanide-sensitivity assay was performed, since Cu,ZnSOD is sensitive to KCN, unlike the Fe,Mn-type. Results of this assay confirmed that the upper and lower bands relate to Fe,Mn- and Cu,ZnSOD activities, respectively (data not shown).

The ROS-scavenging ability of the FOM and *N. crassa snt2* mutants was also assessed. Total SOD activity in intracellular protein extracts was evaluated following

hydrogen peroxide (H_2O_2) induction. The H_2O_2 induction led to a time-dependent increase in SOD activity, as detected in the wild type protein extracts. As opposed to the wild type isolate, all the *snt2* mutants exhibited a constant basal level of Cu,ZnSOD activity (lower band) which was independent of the stimulus, whereas both fungal species exhibited lower or undetectable Fe,MnSOD activity (upper band), compared to their respective wild type strains (Fig. 22).

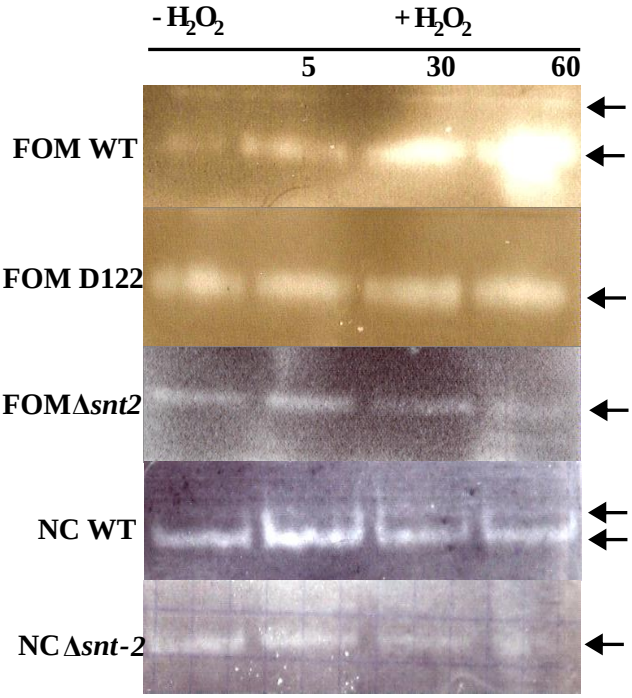

Figure 22. Detection of total superoxide dismutase activity in extracts of *Fusarium oxysporum* f. sp. *melonis* (FOM) and *Neurospora crassa* (NC) with (+) or without (-) hydrogen peroxide (H_2O_2) induction. Prior to total protein extraction, the *snt2* mutants and the wild type isolates of FOM and NC were grown on minimal medium (FMM or Vogel's, respectively) then subjected to the induction treatment (5, 30 and 60 min) with 4mM H_2O_2. Total SOD activity in 40μg crude cellular native proteins of the wild type (WT), D122 and Δ*snt2* of FOM and NC, respectively, was evaluated using native PAGE analysis followed by gel activity assays. Arrows indicate SOD activity bands.

4.4.2. Expression of Fe,MnSOD-encoding genes is deregulated in *snt2* mutants of FOM and *N. crassa*

Using QRT-PCR, expression levels of six (out of seven) putative SOD-coding genes of FOM and two (out of four) SOD-coding genes of *N. crassa* (Fig. 23) were examined. In the FOM Δ*snt2* strain, expression of three Fe,Mn SOD-coding genes was found to be differentially regulated, when compared to the wild type isolate. In both the wild type isolates of FOM and *N. crassa* oxidative stress caused significant down-regulation of four *fn,mn sod* (FOXG_04389, FOXG_13757, NCU01213,

NCU09560) and one *cu,zn sod* (FOXG_03076) genes. In contrast to the wild type strains, in the FOM Δ*snt2* mutant in the *N. crassa* Δ*snt-2* strain, induction by hydrogen peroxide led to over-expression of *fn,mn sod* genes (FOXG_01738, FOXG_13757 and NCU01213 (designated *sod2*)) (Fig. 23).

These results confirm the hypothesis that *snt2* is required for proper regulation of transcription of Fe,MnSOD-coding genes in FOM as well as in *N.*

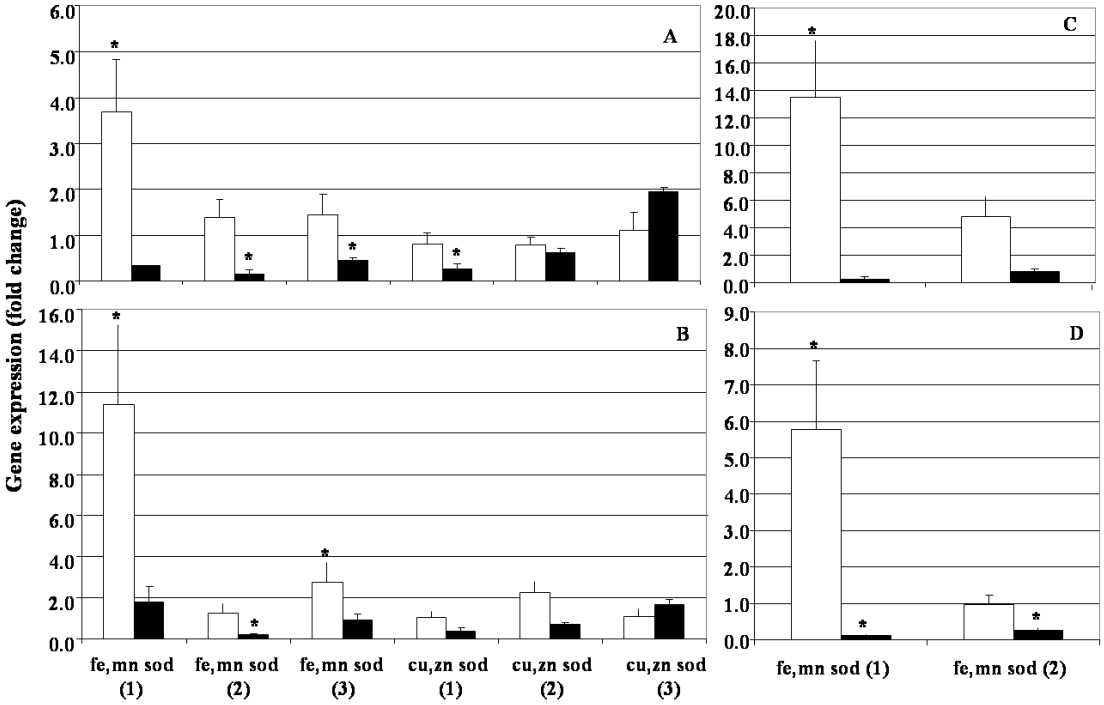

Figure 23. Relative expression* of superoxide dismutases-coding genes of *Fusarium oxysporum* f. sp. *melonis* (FOM) (A, B) and *Neurospora crassa* (C, D).
*cDNA was synthesized from 1 µg of total RNA, extracted from the wild type (wt) and Δ*snt2* mutant isolates grown on minimal medium. Hydrogen peroxide (4mM) was used for induction. Relative expression of each gene was analyzed separately for each isolate at 5 min (A, C) and 30 min (B, D) induction treatments compared to a non-treated control. Mean CP values were normalized to the endogenous control gene, ß-tubulin. Relative expression levels of the following SOD-coding genes† were evaluated: FOXG_01738, FOXG_04389, FOXG_13757 and FOXG_03076, FOXG_00474, FOXG_11513 (fe,mn sod (1), (2), (3) and cu,zn sod (1), (2), (3) respectively) of FOM; NCU01213, NCU09560 (fe,mn sod (1), (2), respectively) of *N. crassa.* Gene expression levels were analyzed (four technical replicates) using the REST© program (Pfaffl *et al.,* 2002). † Gene designations are according to the Broad Institute Database of *F. o.* f. sp. *licopersici* and *N. crassa.*

crassa, as opposed to lack of a detectable change in response to oxidative stress at the protein activity level (Fig. 22). Therefore, it is likely that *snt2* is involved in post-transcriptional regulation of SODs.

The expression of an additional SSH-detected gene, *fnt1*, coding an integral membranal formate-nitrite transporter, was also monitored to determine whether possible changes in H+ transport accompany the deregulation of SOD. Expression of *fnt* in the wild type isolate of FOM decreased drastically following hydrogen peroxide induction (5-fold and 100-fold reduction after 5 min and 30 min of oxidative stress, respectively) (Table 9). In the FOM Δ*snt2* mutant, no change in expression of this gene under oxidative stress was observed. To determine whether the reaction of *fnt* to oxidative stress is conserved, its expression in *N. crassa* was determined, under the same conditions. However, no significant change in *fnt* expression was detected, suggesting that the reaction observed in FOM could be species-specific and/or regulation of the expression in *N. crassa* is independent of *snt2* (Table 9).

Table 9. Relative expression of formate/nirite transporter-encoding genes* of *Fusarium oxysporum* f. sp. *melonis*† (FOM) and *Neurospora crassa*‡(NC) under oxidative stress.

Organism	*Accession number*	*5 min H_2O_2*		*30 min H_2O_2*	
		WT	Δsnt2	WT	Δsnt2
FOM	XP_383338†	0.22 ± 0.10^{down}	0.27±0.07	0.01 ± 0.004^{down}	0.51±0.13
NC	XP_964155‡	1.15±0.54	0.52±0.22	2.33±1.02	0.53±0.26

* cDNA was synthesized from 1 µg of total RNA, extracted from the fungi grown on minimal medium (FMM for FOM and Vogel's for *N. crassa*). Four mM hydrogen peroxide was used for the two-step induction (5 and 30 min). Relative expression of each gene was analyzed separately for each isolate and compared to the non-treated control. All samples were analyzed in triplicate. Mean CP values were normalized to the endogenous control gene, ß-tubulin. Gene expression levels were analyzed for four technical replicates using the REST© program (Pfaffl *et al.,* 2002). Accession numbers are according to the NCBI Database.

Expression of an additional gene, *cpoxIII*, previously detected by our SSH-screening, was also tested (Table 6). The *cpoxIII* gene encodes a coproporphyrinogen oxidase III (CPOXIII), which is located in the intermembrane space of the mitochondrion and catalyzes the third step of heme biosynthesis. The expression of *cpoxIII* in *snt2* mutant strains was not different from that determined in the wild type isolates in both FOM and *N. crassa* (0.54±0.48 and 0.62±0.22, respectively).

4.4.3. *snt2* mutants of *F. oxysporum* and *N. crassa* are impaired in cell respiration

In order to verify whether impairment of *snt2* led to affected mitochondrial function, as expressed in changes in aerobic respiration, both FOM and *N. crassa* mutants were examined. Using gas chromatography, a relative reduction of CO_2 accumulation was detected. The *snt2* mutants of both fungal species were observed to be defective in total respiration ability, expressed in the relative percentage of generated CO_2 per mg of dry biomass (0.101±0.06 and 0.065±0.03 for FOM and *N. crassa*, respectively), compared to their respective wild type isolates (0.174±0.05 and 0.139±0.06 % CO_2/mg) (Fig. 24). Even though *F. oxysporum* possesses more respiratory pathways than the obligatory aerobic fungus *N. crassa*, the predominant respiration ability in both fungi occurs via cyanide-sensitive oxidative phosphorylation, due to this pathway's advantage in energy production (Saraste, 1999). An additional type of respiration is cyanide-resistant, which takes place through an alternative oxidase pathway, which is salicylhydroxamic acid (SHAM)-sensitive. In order to identify which respiratory branch was affected by *snt2*, the effect of potassium cyanide (KCN) and SHAM on oxygen consumption of FOM and *N. crassa* was measured. As expected, addition of KCN (0.124±0.05 and 0.110±0.06 %CO_2/mg), but not that of SHAM (0.129±0.04 and 0.107±0.03 %CO_2/mg) inhibited respiration of the wild type isolates of FOM and *N. crassa*, respectively. When compared to the respective wild type isolates, Δ*snt2* mutants displayed significantly reduced oxygen consumption following KCN (0.080±0.02 and 0.044±0.02 % CO_2/mg), but not SHAM treatment (0.125±0.02 and 0.065±0.02 % CO_2/mg), in FOM and *N. crassa*, respectively. However, contrary to the wild type isolates, respiration in

both the Δ*snt2* mutants was not affected either by KCN or by SHAM (Fig. 24), when compared to the untreated controls.

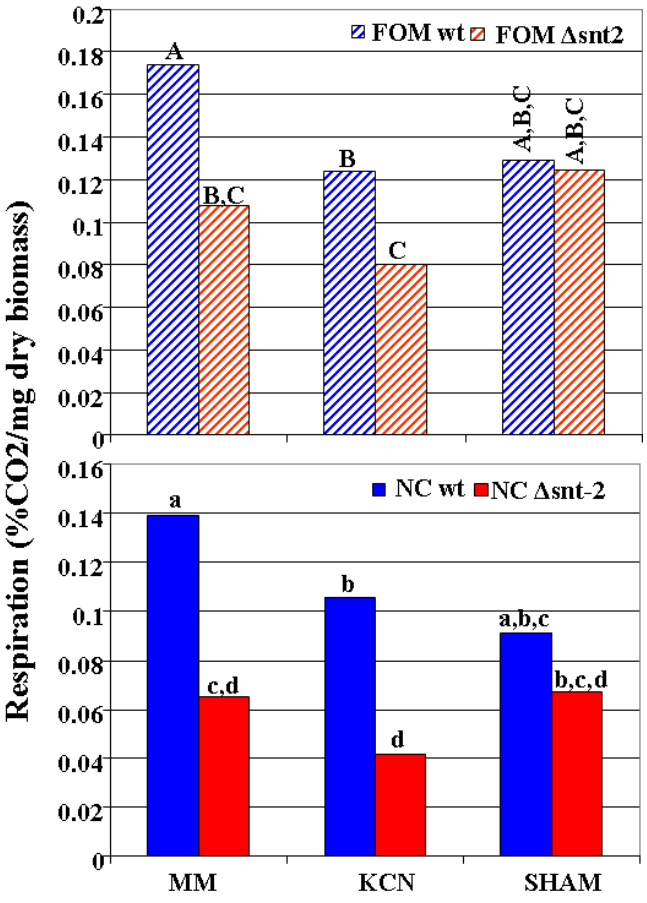

Figure 24. Reduction of cyanide-sensitive respiration following *snt2* disruption in both FOM and *Neurospora crassa* (NCU). Relative production of carbon dioxide per accumulated dry biomass was detected using gas chromatography (GC)-based analysis. Conidial suspensions (10^6 conidia/mL) of the four isolates were incubated on minimal medium (MM) for 24 hr. Flasks were sealed with rubber plugs prior to 1 hr incubation at 25°C, followed by GC analysis of 10ml of the chamber air. Potassium cyanide (KCN) and salicylhydroxamic acid (SHAM) were applied prior to the incubation at concentrations of 1mM and 100μg/ml, respectively. Statistical analysis of four independent experiments was performed using LSMeans Difference Tukey HDS test, separately for each fungus. Values with different letters indicate significant differences between tested isolates, at $P \leq 0.05$.

Thus, it appears that, *snt2* mutants were impaired in general oxygen consumption, providing additional evidence for mitochondrial dysfunction. In particular, only the cyanide-sensitive (OXPHOS) respiratory branch was affected by disruption of the *snt2* gene. Interestingly, both the *snt2* mutants appear to be less responsive to cyanide, displaying an insignificant reduction in oxygen consumption. Alternative oxidation was not affected in the Δ*snt2* mutants. Furthermore, addition of SHAM did not confer a detectable reduction in respiration, probably due to the relatively slight contribution of this pathway to oxygen consumption, in general. To further investigate the link between the *snt2* and the alternative oxidation (AOX) pathway, we evaluated expression of AOX-coding (*aod1* of FOM and *aod-1* of *N.*

crassa) genes, in both fungi. Interestingly, expression of the AOX-coding genes was significantly up-regulated in both *snt2*-disrupted mutants (7.62±0.86 and 3.22±0.44 in FOM and *N. crassa*, respectively), suggesting the presence of a compensatory mechanism, or even a potential direct link between *snt2* and regulation of alternative oxidation.

5. DISCUSSION

5.1. Use of a forward genetics approach for identification of pathogenicity genes

Plant diseases dramatically affect world economy. In the US alone, the estimated damage caused by plant diseases may amount to $33 billion per year. Of all plant pathogens in the US, it was reported that twelve of the nineteen most threatening organisms listed are fungi (Madden and Wheelis, 2003). Thus, study of plant pathogens in general, and understanding the mechanistic nature of fungal pathogenicity, in particular, apart from satisfying pure scientific curiosity, is important for human existence. Over the past two decades the area of fungal functional genomics has significantly progressed, in part, due to development of various transformation techniques. Furthermore, approximately 150 fungal genomes have been sequenced to date, and are available in the public domain. One of the applications of functional genomics may lead to deciphering of pathogenicity-related processes through identification of pathogenicity-related genes in both the host and pathogen, and determining their mechanistic contribution to the process. In order to discover previously unidentified pathogenicity-related genes a forward genetics approach is usually applied. This approach, independent of the technique to be used, has numerous setbacks, including excessive time consumption and uncertain success. For example, the percentage of reduced-pathogenicity isolates of *F. oxysporum* generated by large scale experiments may not exceed 1.5% (Inoue *et al.,* 2001; Michielse *et al.,* 2009; Lopez-Berges *et al.,* 2009). Furthermore, in the current research, the ratio of reduced pathogenicity isolates generated reached only 0.3%. Use of *Agrobacterium tumefaciens*-mediated transformation (ATMT) has been proven as a valuable tool for broad-scale mutational analysis in fungi and has several advantages over conventional transformation methods, such as integration of a single plasmid

copy and high rate of homologous recombination (reviewed by Michielse *et al.*, 2005).

In this study, six reduced-pathogenicity mutants of *Fusarium oxysporum* f. sp. *melonis* (FOM), generated by the forward genetics approach, were characterized; one, non-pathogenic strain (4/4 mutant), which was generated previously by UV irradiation (Freeman *et al.,* 2002) and five additional putative reduced-pathogenicity isolates that were generated by a large-scale insertion mutagenesis using ATMT. The 4/4 mutant was identified as an adenine auxotroph, and addition of adenine restored developmental defects and pathogenicity (Denisov *et al.,* 2005). As purine biosynthesis is important for a wide spectrum of processes (e.g. adenine nucleotides serve as the components of ATP, coenzyme A, FAD and NAD^+), it is likely, that a defect in synthesis can affect different cellular functions, including pathogenicity. The specific limiting factor in adenine requirement that determines pathogenicity has yet to be identified. However, the results presented here demonstrate and re-emphasize the importance of basic biosynthetic pathways for pathogenicity. It has been reported that auxotrophs of different pathogenic fungi exhibited reduced pathogenicity. Studies conducted on *Sclerotinia sclerotiorum* (Miller *et al.,* 1989), *Magnaporthe grisea* (Balhadère *et al.,* 1999) and FOM (Namiki *et al.,* 2001; Inoue *et al.,* 2001) demonstrated that pyrimidine, methionine, arginine and biotin auxotrophic mutants, respectively, were reduced in pathogenicity compared to their respective wild type isolates. Furthermore, an adenine auxotroph of the human opportunistic fungus *Cryptococcus neoformans,* the causal agent of cryptococcal meningitis, was avirulent in the central nervous system model (Perfect *et al.,* 1993).

Molecular characterization of five reduced-pathogenicity ATMT-tagged transformants revealed four putative pathogenicity-related genes. Isolate D122

exhibited the most significant reduction in pathogenicity and was found impaired in the gene encoding a SNT2-like transcription factor (TF) of *Schizosaccharomyces pombe*, which regulates activity of stress related genes in the yeast. A detailed characterization of the D122 mutant isolate was performed in this study and is discussed in the next section. In two independently produced reduced-pathogenicity mutants (K993, D510) the inserted tag was detected in the promoter region or within a gene encoding a protein similar to *cdc48,* respectively. Cdc48p is a member of the AAA-ATPase family and is known to be involved in apoptosis in *S. cerevisiae* (Lu, 2006). This protein is localized in the cytosol, the nucleus and endoplasmic reticulum and in conjunction with different cofactors performs various cellular tasks. The *S. cerevisiae cdc48* mutant was characterized with excessive accumulation of reactive oxygen species (ROS) and subsequent programmed cell death (PCD). In *Arabidopsis thaliana*, the *cdc48* homologue was highly expressed in dividing cells (Feiler *et al.*, 1995). An additional, reduced pathogenicity isolate K705 characterized in this study, was mutated in a promoter region of the peroxisome biogenesis 7 encoding gene (*pex7*). Peroxisomes are single membrane bound organelles possessing multiple metabolic functions in filamentous fungi, including β-oxidation of fatty acids, peroxide detoxification and occlusion of septal pores (Bosch *et al.*, 1992). More than 20 peroxin proteins (PEXs) have been identified in fungi (Kiel *et al.*, 2006). The PEX7 protein functions as a receptor for three amino acids signal located at the C-terminus of peroxisomal proteins, also known as the peroxisomal targeting signal 2 (PTS2). The peroxins PEX7 and PEX5 transport PTS-containing proteins from the cytosol to the peroxisome and then return to the cytolsol. In a recent high throughput study of *F. oxysporum* f.sp. *lycopersici* (FOL) pathogenicity genes (Michielse *et al.*, 2009), four genes encoding peroxisome biogenesis proteins (Pex1, Pex10, Pex12,

Pex26) were identified. Involvement of *pex12* and *pex26* in *F. oxysporum* pathogenesis on tomato plants was confirmed by genetic complementation. *Pex* mutants of FOL were also characterized in this study by their inability to grow on fatty acids, and a similar phenotypic defect was observed when mutant isolate K705 was grown on minimal medium (FMM) containing 1% Tween 20 as a sole carbon source (data not shown). In *Podospora anserina,* PEX7 is needed for normal completion of the sexual cycle and its targeted disruption led to mitochondrial abnormalities (Bonnet *et al.,* 2006). Peroxisomal metabolism has been shown to be critical for pathogenicity of *Cladosporium fulvum* (Segers *et al.,* 2001), *M. grisea* (Ramos-Pamplona and Naqvi, 2006) and *Colletotrichum lagenarium* (Kimura *et al.,* 2001; Asakura *et al.,* 2006). As peroxisomes have been shown to play a role in fungal pathogenesis and are linked with development, it would be interesting to determine the precise mechanism of peroxisome biogenesis and its genetic regulatory environment in the wilt pathogen *F. oxysporum*. Overall, this initial characterization of tagged reduced-pathogenicity mutants provides interesting prospects of involvement of apoptosis and peroxisome biogenesis in pathogenesis of *F. oxysporum*.

5.2. Characterization of the reduced-pathogenicity isolate D122 of *Fusarium oxysporum* f. sp. *melonis* (FOM)

5.2.1. Disruption of *snt2* affects fungal development and pathogenicity in FOM

In this study a novel pathogenicity gene of FOM – *snt2* was identified. Targeted disruption of the *snt2* confirmed its requirement for pathogenicity and complete colonization of muskmelon plants. Interestingly, *Agrobacterium* strain EHA105 was found to be less suitable for targeted disruption in *F. oxysporum* than

strain GV3101, due to a relatively high percentage of false positive transformants obtained when the former was used (Khang *et al.,* 2005).

Expression analysis of *snt2 in planta* identified this gene as essential for early pathogenesis. Only four *F. oxysporum* genes (*fmk1*, *fow1*, *frp1* and *fow2*) have been proven, so far, to be necessary for colonization and host-invasive growth, without affecting vegetative growth and conidiation (Di Pietro *et al.,* 2001; Inoue *et al.,* 2002; Duyvestejin *et al.,* 2005; Imazaki *et al.,* 2007). Having said that, a detailed morphological characterization of *snt2* mutants (see below) detected several impaired traits, among them reduced conidia production and growth rate that may be associated with reduced pathogenicity. Correlation between reduced conidiation and pathogenicity was demonstrated in the tomato pathogen, *F. o.* f. sp. *lycopersici* following disruption of *sge1*, encoding a transcription regulator (Michielse *et al.,* 2009), and in the cucumber pathogen, *F. o.* f. sp. *cucumerinum* by disruption of the α subunit G-protein encoded by the *fga1* gene (Jain *et al.,* 2002).

5.2.2. Morphological and genetic differences between D122 and Δ*snt2* mutants of FOM

Several genetic and morphological differences became evident while analyzing the two FOM *snt2* mutants. At the genetic level, the two mutants differ in location of the inserted tag, even though, in both mutants disruption occurred near the 5'-end of the *snt2* gene (Table 6). The D122 BAH domain-encoding conserved region remained intact, while in the Δ*snt2* it was disrupted. Moreover, the D122 mutant was characterized with partial expression of the *snt2* gene, confirmed by RT-PCR amplification of its 5'-end (data not shown). In addition, the two mutants differed in expression levels of at least one gene (*pdc*), even though its transcripts were extremely abundant in the SSH-library. Based on these results, the targeted mutant

Δ*snt2* was chosen for further study of the *snt2* genetic network. Moreover, at the developmental level, the targeted (Δ*snt2*) mutant exhibited a more severely affected phenotype in all tested parameters, compared to the tagged mutant D122. However, plant mortality rate after inoculation with Δ*snt2* was higher than that of D122, even though initial development and appearance of symptoms of wilt disease, caused by both the isolates was identical, until day 8 after inoculation (Fig. 14).

5.2.3. Are the morphological abnormalities, caused by *snt2* disruption, unique for *Fusarium oxysporum*?

A comparative phenotypical characterization of Δ*snt2* mutants of two Ascomycota fungi – FOM and *Neurospora crassa* was performed. In addition to its involvement in pathogenicity on muskmelon plants, *snt2* gene was found to be associated with numerous developmental aspects in the tested fungi. Interestingly, in both the fungi, disruption of *snt2* caused similar sets of morphological abnormalities, including reduction in conidia production, slower vegetative growth and biomass accumulation. Moreover, abnormalities were also observed in hyphal septation and in Congo red staining patterns in FOM and *N. crassa.* An additional trait evident in all the tested *snt2* mutants was increased hyphal cell death. Similar morphological abnormalities were observed in *Podospora anserina* during processes such as vegetative incompatibility, starvation or following treatment with a specific inhibitor of TOR kinase, rapamycin (Pinan-Lucare *et al.*, 2007). An additional trait, linking *snt2* to sexual development was observed in Δ*snt-2 N. crassa* mutants producing only protoperithecia that were unable to mature. Based on these results, it is suggested that *snt2* functions are conserved among ascomycotina and essential for normal fungal development. The genetic basis for all the described morphological abnormalities is presented below (sections 5.2.4 and 5.2.5).

5.2.4. PHD/BAH-containing proteins and SNT2 orthologs

The *snt2* gene encodes a TF-like protein, homologous to SNT2 of *Schizosaccharomyces pombe* (Roguev *et al.*, 2004). In general, fungal SNT2 proteins harbor two types of conserved domains – the bromo-adjacent homeodomain (BAH) and plant homeodomain Zn-fingers (PHD). As a complete genomic DNA sequence of FOM *snt2* was obtained by manual annotation, several differences were found between the sequence in FOM and its closest relative in *F. oxysporum* f. sp. *lycopersici* (FOL). These are evident in different SNT2 domain structures, possibly due to the error in computational annotation of FOL. The PHD domain is a "double zinc finger" with a Cys4HisCy3 motif which binds two zinc ions. The PHD finger is found in a variety of chromatin regulators and transcriptional cofactors including CBP/p300, ATRX, DNMT3, and the KAP1/TIF1β universal repressor protein (reviewed in Pascual *et al*. 2000). Recent studies identified a specific function for PHD fingers, as methyl-lysine effectors involved in recognition and binding of trimethylated lysine (K4) in histone 3 (H3), and by that, triggering an acute gene repression (Mellor, 2006). In *S. pombe*, SNT2 is part of a Lid2 protein complex, which is involved in chromatin regulation (Roguev *et al.*, 2004). It was recently reported that the Lid2 protein is required for coordinating H3K4 and H3K9 methylation of heterochromatin and euchromatin in the fission yeast (Li *et al.*, 2008). Methylation of H3K9, which does not occur in *S. cerevisiae*, but is found in *S. pombe* and in mammals is known to trigger sequential processes leading, ultimately, to transcription repression. Among fungi, over 500 proteins have been identified as containing PHD-finger domains (http://smart.embl-heidelberg.de) most of them identified as putative proteins. Only several were characterized, for example, the Rum1 TF of the corn smut fungus *Ustilago maydis*, a repressor for genes regulated by

the *b* mating type locus (Quadbeck-Seeger *et al.,* 2000). In this study, it was suggested that repress of Rum1 activity could be explained via recruitment of a histone acetylase by direct interaction with PHD. Recently, another PHD-harboring transcription factor of *F. oxysporum* - FoCti6 was found to be involved in fungal pathogenesis (Michielse *et al.,* 2009). Similarly to SNT2, Cti6 was found to participate in chromatin modifications. In *S. cerevisiae*, *cti6* encodes an Rpd3p-Sin3p histone deacetylase-associated protein involved in derepression of promoters which are repressed by Ssn6p-Tup1p complexes, and required for growth in iron deficiency conditions (Puig *et al.,* 2004). The PHD finger is often accompanied by a BAH module and their presence is associated with regulation of gene expression through chromatin modifications (Völkel and Angrand, 2007). Both the domains are found in regulators of gene expression such as histone lysine methyltransferase ASH1 of *Drosophila* (Tanaka *et al.,* 2007) and in *Arabidopsis* where the EBS and SHL proteins regulate a wide range of developmental processes by chromatin remodeling (Piñeiro *et al.,* 2003; Mussig *et al.,* 2000). Furthermore, the SNT2 protein also possesses a similar architecture to a putative transcription factor - ZNF1 (AAN75722) of the human pathogen *Cryptococcus neoformans* that is involved in the pheromone response pathway of the mating-type locus (Lengeler *et al.,* 2002).

5.2.5. Genes with altered expression in FOM *snt2* mutants

In general, study of transcriptional factor networks are often challenging due to the participation of numerous genes/gene products and functional redundancy of some of the downstream targets. Another goal of this study was to detect differentially expressed transcripts between two populations of mRNA, using comparative analysis between the wild type isolate and the tagged *snt2* mutant (D122) of FOM. The global investigation of changes in gene expression in a biological system can be carried out

with a variety of available tools, for example, microarrays, differential display (DD), cDNA-amplified fragment length polymorphism (cDNA-AFLP), representational difference analysis (RDA), and serial analysis of gene expression (SAGE) (Bhadauria *et al.*, 2007). A newly developed, deep sequencing-based expression analysis, provides a major advance in robustness, comparability and richness of expression profiling data and is expected to boost collaborative, comparative and integrative genomics studies (Hoen *et al.*, 2008). Despite the fact that these methods have proven successful in isolation of differentially expressed genes, they all possess some intrinsic drawbacks. In addition to their specific limitations, a common feature is the inability to isolate rare transcripts, i.e., the disproportion of concentrations of differentially expressed genes is maintained in the subtraction. Suppressive subtraction hybridization (SSH) (Diatchenko *et al.*, 1996) enables the construction of subtracted cDNA libraries and is based on hybridization and suppression PCR including normalization and subtraction in a single procedure. It provides a 100-1000-fold enrichment of differentially expressed mRNAs and has been successfully used to compare differences in gene expression between two fungal transcriptomes (Lu *et al.*, 2005). In the current research, the SSH method, combined with QRT-PCR, was used to detect *snt2*-regulated genes and evaluate their expression levels. In order to minimize detection of the indirect target genes of *snt2*, mRNA was extracted at the stage of initial germination. At this stage germination and biomass accumulation did not differ between the wild type and tagged *snt2* mutant, however, as mentioned earlier, biomass accumulation is affected, as the mycelium develops (section 4.3.3). The performed SSH-screen identified fourteen genes that represent functional groups of gene regulation and signal transduction, membrane transport and primary metabolism. The major challenge was to deduce which of the genes are directly

regulated by *snt2* and which are affected in a secondary manner, especially assuming, based on the structure, that SNT2 is a transcriptional repressor involved in chromatin remodeling which is positioned high up in the hierarchy of events (Roguev *et al.*, 2004). Four genes (*idi4*, induced during incompatibility; *pdc*, pyruvate decarboxylase; *msf1*, transporter of the major facilitator family and *eEF1G*, eukaryotic translation elongation factor 1-gamma) out of the fourteen, were previously found to be in association with the TOR kinase pathway in the rice pathogen *F. fujikuroi* (Teichert *et al.*, 2006; Schönig *et al.*, 2008). This shared regulation indicated a possibility that *snt2* might be connected to the Tor or related pathways. The proposed model of shared cellular components between SNT2 and TOR kinase is presented in Appendix 1. The Tor pathway regulates cellular processes such as cell growth and autophagy, as well as expression of multiple genetic pathways, including ribosomal biogenesis, nitrogen catabolite repression (NCR) and stress-response genes (Rohde *et al.*, 2001). The Tor pathway also plays a key role in regulation of autophagy, mitochondrial functioning including respiration and aging (Bonawitz *et al.*, 2007; Yen and Klionsky, 2008). Significant changes of transcript amounts of three genes associated with the Tor pathway were confirmed by QRT-PCR, two of the genes – *idi4* and *pdc* were shown to be over-expressed in Δ*snt2* FOM mutants.

Pyruvate decarboxylase (PDC) catalyses the decarboxylation of pyruvate to acetaldehyde and carbon dioxide in the cytoplasm. In plants and some fungi under anaerobic conditions, PDC is a major determinant in alcoholic fermentation, during which pyruvate is converted to acetataldehyde and then to ethanol. In *F. fujikuroi* expression of the *pdc* and alcohol dehydrogenase (*adh*) downstream of it was affected by rapamycin, suggesting involvement of the Tor pathway in their regulation (Teichert *et al.*, 2006). Moreover, expression of the two genes, *adh* and aldehyde

dehydrogenase (*aldh1*) of the tomato pathogen *C. fulvum*, which participate in carbon metabolism and are positioned downstream to *pdc*, were induced under nitrogen-limiting conditions, as well as *in planta* (Coleman *et al.*, 1997). Even though targeted disruption of the *aldh1* did not affect pathogenicity of *C. fulvum*, the importance of carbon metabolism for fungal pathogenicity was demonstrated by disruption of alcohol oxidase (*aox1*) (Segers *et al.*, 2001). In *A. nidulans*, *pdcA* expression is thought to be regulated by the global nitrogen regulator AreA under nitrogen repressing conditions (Lockington *et al.*, 1997). Although the role of nitrogen-responsive genes in fungal pathogenesis has been extensively explored (reviewed in Bolton and Tomma, 2008), interactions between nitrogen and carbon metabolism during pathogenesis, and all the more so, the role of carbon metabolism in pathogenesis, is not yet clear. Pyruvate is a key intersection in the network of metabolic pathways and can be converted into carbohydrates via gluconeogenesis, to fatty acids or energy through acetyl-CoA, to the amino acid alanine and to ethanol. There are two scenarios that may possibly explain reasons and consequences of *pdc* up-regulation. On the one hand, expression of one of the pyruvate dissimilating enzymes can increase pyruvate dissimilation via the alcohol fermentation pathway, reducing availability of pyruvate for other metabolic pathways. Moreover, over-production of PDC may be toxic, due to increased levels of acetaldehyde (Rahman *et al.*, 2001). On the other hand, if *snt2* does not participate in direct regulation of *pdc*, it shifts the metabolism to a hypoxic (or fermentative) regime, which implies involvement of *snt2* in oxygen sensing. In *A. nidulans*, *pdcA* was found to be involved in anaerobic survival (Lockington *et al.*, 1997). Interestingly, it was proposed that the mammalian TOR kinase may serve as an oxygen sensor by linking decreased oxygen levels with inhibition of protein translation (Ashram *et al.*, 2003). Overall, in this

study, targeted disruption of the pathogenicity-related gene *snt2* caused up-regulation of *pdc*, detecting an additional, probable *pdc* regulatory element, providing evidence for involvement of the gene, in particular, in carbon metabolism and, in general, in fungal pathogenicity and development.

An additional gene, unique to *F. oxysporum*, with unknown functions, designated here as *rbs1*, was identified during the SSH-screen. Its expression was found to be significantly down-regulated in *snt2* mutants of FOM. However, based on SNT2 structure, it is likely to be involved in transcriptional repression, therefore only genes whose expression was induced by *snt2* disruption are likely to be directly controlled by this TF. Thus, it is not yet clear, whether *rbs1* is in fact, directly regulated by *snt2* or its regulation involves an intermediate gene. In order to confirm the link between *snt2* and *rbs1* it is proposed to perform analysis at the protein level, including gel shift assays or tandem affinity purification, enabling evaluation of the proteomic environment.

In the current study it was also found that disruption of *snt2* results in over-expression of an *idi4* gene in both FOM and *N. crassa*. As mentioned above (section 1.4), *idi4* is a stress-responsive gene, also induced during starvation, incompatibility and autophagy in *P. anserina* (Dementhon *et al.,* 2004; Pinan-Lucare *et al.,* 2007) and its expression in *F. fujikuroi* is regulated by the TOR kinase and the AreA TF (Teichert *et al.,* 2006; Schönig *et al.,* 2008). In light of these facts it was decided to examine the involvement of *snt2* in nitrogen metabolism and autophagy.

5.2.6. Is *snt2* involved in regulation of autophagy and nitrogen metabolism?

Autophagy is a conserved catabolic pathway in eukaryotes and is a major mechanism for the removal of damaged cellular structures which is critical for cell survival (Yen and Klionsky, 2008). Autophagy protects a delicate equilibrium

between cell survival and death, and over-induction of autophagy shifts this balance toward cell death as demonstrated by Scherz-Shouval and Elazar (2007). As previously mentioned, autophagy is induced by various stress conditions (section 1.4) and it was suggested that under starvation conditions, autophagy provides a nitrogen source, enabling survival (Kohda *et al.*, 2007). Moreover, both non-selective autophagy and nitrogen metabolism are negatively regulated by TOR kinase. Due to shared regulation between *snt2* and TOR kinase, a nitrogen utilization ability of FOM *snt2* mutants was initially tested, however, utilization of nitrate and ammonia detected no difference between wild type and *snt2* mutants of FOM. Moreover, all the examined isolates were not able to grow on chlorate and were able to grow on hypoxanthine, confirming the apparent absence of defects in the nitrate reduction pathway. The only observed significant delay was during growth on medium containing glutamate as a sole nitrogen source. In fungi, glutamate is processed by glutamine synthetase (*glnA*), nevertheless, expression of three master nitrogen regulators, including *glnA*, *fnr1* (a homolog of *are*A in *F. oxysporum*) and *nit4* (a homolog of pathway-specific nitrogen regulator of *N. crassa*) did not differ significantly in the Δ*snt2* mutant, when compared to the wild type isolate. Therefore, it is likely that *snt2* is not required for utilization of nitrogen and the general delay of hyphal growth in the *snt2* mutants of FOM and *N. crassa* is conveyed through other pathways. For example, a recent research defined a novel function of the *S. cerevisiae* SNT2 TF. The ScSnt2 TF was found to display bias in its promoter affinity towards genes encoding amine transmembrane transporters (Ward and Bussemaker, 2008). It was also found that rapamycin inhibited growth of all the tested FOM isolates in a similar manner and did not affect expression of *snt2*, as identified by QRT-PCR (data

not shown), excluding *snt2* from a long list of TOR kinase downstream targets (i.e., NCR, TCA cycle and ribosomal genes) .

It was previously mentioned that common morphological abnormalities including increased cell death, that were observed in FOM and *N. crassa* as well as in another sodariomycete - *P. anserina*, were accompanied by over-expression of the autophagy-related *idi4* gene (Dementhon *et al.,* 2004). Not surprisingly, in the current study, increased cell mortality, combined with excessive appearance of mature autophagosomes was observed in FOM *snt2* mutants. In *Podospora,* it was observed that both autophagy and expression of *idi-4* are strongly induced by cell death and it was proposed that IDI-4 is one of the transcription factors regulating autophagy and cell fate in *Podospora* **(**Dementhon *et al.,* 2004). Interestingly, in *Podospora*, IDI-4 not only shares structural similarity with the GCN4/cross-pathway control (CPC1) transcription factor, but it was also demonstrated to possess remarkable similarity in binding of promoter sequences, such as the promoter of a putative autophagy gene, *idi-7* (Dementhon and Saupe, 2005). The same authors suggested that IDI-4 could control expression of proteins with pro-survival or pro-death functions. In FOM, increased appearance of mature autophagosomes, that became evident using MDC-staining, along with up-regulation of the autopagy-related TF-encoding gene *idi4* in *snt2* mutants indicated, initially, that *snt2* may be directly involved in autophagy. However, the relative expression of a highly conserved gene, *idi7/agt8*, which regulates initial steps of non-selective autophagy (Meijer *et al.,* 2007) did not differ in *snt2* mutants, therefore it is likely that *snt2* is not involved directly in regulation of non-selective autophagy. Taking into consideration the activation of *idi4* during stress-response, it is proposed that a combination of *idi-4* over-expression with excessive appearance of autophagosomes, cell death, and morphological

abnormalities, such as frequent cell disposition and the patched Congo red-stained pattern of mutant mycelia, resembles a stress-like morphology, similar to starvation-, ROS- or vegetative incompatibility-induced symptoms, observed in different filamentous fungi (Pinan-Lucare *et al.,* 2003; 2007). Autophagy in general, was found to be essential for development and differentiation in fungi, such as *A. nidulans* (Kikuma *et al.,* 2006). Furthermore, inactivation of the vital autophagy genes - *pspA* and *idi-7* led to female sterility in *Podospora* (Pinan-Lucare *et al.,* 2005), linking autophagy to sexual development. In this study, sterility was observed in the *N. crassa* Δ*snt-2* mutant, suggesting a link between *snt-2* disruption, sexual development as well as induction of *idi-4* and cell death of *N. crassa*. Autophagy-defective *S. cerevisiae* mutants were found to be sterile in the absence of environmental nitrogen, whereas supplement of nitrogen enabled normal sexual development (Kohda *et al.,* 2007).

Overall, up-regulation of the autophagy-related *idi4* gene in both FOM and *N. crassa* Δ*snt2* mutants, links *snt2* to a variety of cellular processes and is indicative of the existence of a yet undiscovered, but likely conserved, regulatory link. In the broader biological perspective, non-selective autophagy and nitrogen metabolism are connected and tightly regulated by TOR kinase. Identification of *snt2*, which appears associated with autophagy, but not with nitrogen metabolism in addition to shared genetic regulation between SNT2 and TOR kinase provides additional evidence that "overlapping" of regulatory mechanisms is essential for cell survival.

5.3. *snt2* is important for proper mitochondrial function

Mitochondria are essential and highly dynamic organelles of eukaryotic cells. The fungal mitochondrion, in general, is the center of cellular processes such as life-span control and apoptosis, energy production, aerobic and anaerobic respiration,

denitrification, etc. Impairment of mitochondrial function is highly likely to impose various fitness penalties, including developmental defects, cell death and affected pathogenicity (Yen and Klionsky, 2008). Even though research of mitochondrion-related processes has been of interest for a long time, during the past decade its involvement in aging has attracted increasing scientific interest (Osiewacz, 2002). Because of similarity between filamentous fungi and animals in gene regulation of synthesis of mitochondrial proteins, fungi are considered to be one of the best model systems for investigations of the aging process. In *F. oxysporum*, association between mitochondrial function and pathogenesis was previously demonstrated by disruption of *fow2*, coding a mitochondrial carrier protein (Imazaki *et al.*, 2007). Nevertheless, there are only a few studies dedicated to investigations of mitochondria of filamentous fungi. In spite of the significant progress in understanding of the extremely complicated mechanisms of mitochondrial behavior, much has yet to be learned**.** In the present study it was determined that *snt2* is involved in regulation of several mitochondrial-located processes, such as superoxide dismutase (SOD) activity and oxygen consumption, even thought no obvious morphological defects were observed in mitochondria of FOM *snt2* mutants, when confocal microscopy was utilized (data not shown). Data in this study has emphasized the involvement of mitochondria in fungal pathogenesis and provided a strong basis for comparative research of mitochondria in filamentous fungi.

5.3.1. Is *snt2* involved in regulation of superoxide dismutase activity?

As an initial step in the analysis of the two groups of ROS-responsive enzymes [superoxide dismutases (SODs) and NADPH-oxidases (NOX)], the activities of the mentioned enzyme groups in the FOM wild type and *snt2* mutant isolates were compared. No significant visual difference in NOX activity was detected. Using a

native gel activity assay of SOD enzymes, differences in activity patterns between FOM wild type isolate and the tagged *snt2* mutant (D122), were detected. The D122 mutants displayed increased total Cu,ZnSOD activity of the mycelial proteins when grown on minimal medium, in contrast to the wild type isolate that exhibited higher Fe,MnSOD activity during growth on complete medium. It was previously suggested that expression of different SOD isozymes may be condition-dependent. For example, MnSOD was found to be the predominant SOD in the vegetative mycelium of *F. oxysporum*, while FeSOD was the primary activity detected in chlamydospores. Cu,ZnSOD was not detected in mycelium of *F. oxysporum* grown in liquid culture, but highly aerated cultures that produced bud cells rather than mycelium exhibited significant Cu,ZnSOD activity (Kono *et al.*, 1995). However, the fact that *snt2* disruption caused altered SOD activity in FOM, indicates that the intracellular balance of ROS was affected in *snt2* mutants.

SOD enzymes are important defense players in the reactive oxygen species (ROS) detoxifying system. In particular, Fe,MnSOD enzymes have been of utmost interest due to their location in the cellular ROS production center – mitochondria. Therefore, the responsive SOD activity of *snt2* mutants was examined following oxidative stress. Surprisingly, in contrary to a previous report (Angelova *et al.*, 2005), SOD activity in protein extracts of the FOM and *N. crassa* wild type isolates was found to be induced by hydrogen peroxide. Furthermore, the effect of hydrogen peroxide on expression levels of eight selected putative SOD-coding genes of FOM and *N. crassa* revealed up-regulated expression of the *fe,mn sod* group of genes in the Δ*snt2* mutants. In eukaryotic cells, MnSOD is synthesized in the cytosol and imported posttranslationally into the mitochondrial matrix (Bannister *et al.*, 1987). Having observed that following oxidative stress, *snt2* disruption causes up-regulation of *fe,mn*

sod genes, without visible increase in SOD activity, it is likely that *snt2* is involved in posttranscriptional regulation of Fe,MnSOD. Overall, this research presents an additional angle on regulation of SOD activity, when expression of genes encoding the mitochondrial group of SODs is deregulated and not abolished by knockout. The partial deregulation of ROS-responsive SOD activity is presumed to contribute to the reduced virulence of the *snt2* mutant. In addition, investigation of the role of each separate SOD in *F. oxysporum* pathogenicity is rather difficult due to functional redundancy, caused by presence of seven SOD-encoding genes. Simultaneous suppression of closely related genes can be achieved using the RNA interference (RNAi) technique. The RNAi method was widely introduced in fungal biology, however, to our knowledge, this method has not been used for determining the role of *fe,mnsod* in fungal pathogenicity. Effectiveness of RNAi was recently demonstrated in the lignin-degrading fungus *Phanerochaete chrysosporium*, reducing total enzymatic activity of MnSOD by as much as 70% relative to control levels (Matityahu *et al.*, 2008).

5.3.2. Additional links between *snt2* and mitochondrion-located processes

Two additional genes, related to mitochondrion-located processes, encoding for a formate-nitrite transporter (FNT) and a coproporphyrinogen oxidase III (CPOXIII), were identified using the SSH-screen. The FNT family is composed of integral membrane proteins that possess six to eight α-helical transmembrane domains (Bekcham *et al.,* 2010). Proteins of the FNT family are found widely in prokaryotes and low eukaryotes such as yeasts and fungi. The FNT family contains numerous proteins such as prokaryotic formate efflux transporters (FocA), the formate dehydrogenases (FdhC), the nitrite uptake permeases (NirC) and eukaryotic NitA from *A. nidulans*. Mechanistically, uptake of formate and nitrite are probably coupled

to H^+ symport, and formate efflux may be driven by the membrane potential by a uniport mechanism or by H^+ antiport. In this study, the expression of *fnt* was monitored to determine whether possible changes in H+ transport accompany the deregulation of SOD. Expression of *fnt* in the FOM wild type isolate was highly repressed by hydrogen peroxide, reaching 100-fold reduction after 30 min of oxidative stress, while the FOM Δ*snt2* mutant demonstrated no change in *fnt* expression under the same conditions. These data may indicate the lack of response to oxidative stress, similar to the previously observed lack of SOD activity response, which is caused by *snt2* disruption. In *N. crassa,* however, no significant change in *fnt* expression was detected, suggesting that the reaction observed in FOM could be species-specific and/or regulation of the expression in *N. crassa* is independent of *snt2*. An alternative hypothesis is based on existence of denitrification – a unique metabolic pathway that is activated under hypoxic conditions and typical for *F. oxysporum*, but absent in the obligate anaerobe *N. crassa*, and links between formate-forming catabolic and nitrate respiration pathways (Kuwazaki *et al.,* 2003). Formate is formed from pyruvate by the activity of pyruvate-formate lyase. The FOM FNT protein sequence displayed similarity to numerous fungal and bacterial putative FNT proteins, among which is FdhC of *Desulfobacterium autotrophicum***.** Under hypoxic conditions, *F. oxysporum* is involved in nitrate respiration**,** while Fdh is coupled with ubiquinon-dependent membrane-bound nitrate reductase (Nar) providing electrons for reduction of nitrate (Kobayashi *et al.,* 1996). Fungal denitrification is a unique anaerobic respiration system that is distinct from the bacterial nitrate respiration. It occurs in mitochondria and involves three sequential reactions, which are catalyzed by nitrate reductase (Nar), nitrite reductase (Nir) and cytochrome P450-dependent nitric oxide reductase (Nor), respectively (Kuwazaki *et al.,* 2003**)**. Although the

precise mechanism of the FOM FNT protein is yet unknown, it was assumed that it can contribute to electron transfer and therefore the lack of *fnt* response to oxidative stress, at the transcription level, may be indicative of a general systemic defect. However, the specific activity of denitrifying elements (Nar, Nir, Nor and Nos), under hypoxic conditions, in the FOM *snt2* mutant isolate is yet to be determined.

Expression of an additional gene, *cpoxIII*, previously detected by SSH-screening, was also assessed. Even though, the expression of *cpoxIII* in *snt2* mutant strains was not different from that of the wild type isolates in both FOM and *N. crassa*, the link between *snt2* and *cpoxIII* was established yet requires additional assessment. The *cpoxIII* gene encodes a coproporphyrinogen oxidase III (CPOXIII), which is located in the intermembrane space of the mitochondrion and catalyzes the third step of heme biosynthesis. Heme serves a prosthetic group in many enzymes, including flavohemoglobins (Fgh) involved in electron transport and protection against oxygen radicals. Fungal Fgh along with cytochrome P450 play an important role in protection against nitrosative stress, detoxifying nitrous oxide (NO), produced by Nir (Takaya, 2003). In the same report it was also stated that this NO degrading system is essential for *F. oxysporum* growth.

5.3.3. Role of *snt2* in fungal oxygen consumption

One of the major functions of the mitochondrion is energy production, which is mediated by an electron transduction chain, prone to electron leakage. Electron leakage gives rise to ROS that at higher concentrations damage cellular components and can lead to cellular dysfunction. Thus, the mitochondrial respiratory chain can be perceived as a potential "cellular achilles heel" (Osiewacz, 2002). In light of the observed dysfunction of FeMnSOD in FOM and *N. crassa* Δ*snt2* mutant isolates, it was assumed that mitochondrial functions, in general, are impaired. Indeed, using gas

chromatography (GC) analysis, Δ*snt2* mutants of FOM and *N. crassa* demonstrated reduced total oxygen consumption. Use of specific respiration inhibitors – cyanide and salicylhydroxamic acid (SHAM), located possible defects in the cytochrome oxidase respiratory pathway of the *snt2* disrupted mutants. In addition, both Δ*snt2* mutants appear to be less responsive to cyanide, displaying insignificant reduction in oxygen consumption compared to the respective wild type isolates. Reduced respiration is usually observed in aging filamentous fungi, which has been extensively studied in the senescence model fungus *P. anserina* (reviewed by Osiewacz, 2002). Senescent wild type strains of *P. anserina*, displaying gross mitochondrial (mt) DNA rearrangements inevitably lead to impairment of cytochrome oxidation machinery and respiratory decline, and to increased ROS production (Borghouts *et al.*, 2002). In general, relationships between mitochondrial respiration and ROS production are complicated mechanisms which are poorly understood (Bonawitz *et al.*, 2007). Transcription of mtDNA regulated, among others, by the Tor pathway, whose disruption led to increased longevity (Schieke and Finkel, 2006). For example, in *S. cerevisiae, tor1* null mutants were characterized by increased oxygen consumption, lower cellular ROS and extended life span however, these differences were also dependent on presence of glucose (Bonawitz *et al.*, 2007). In this study, FOM and *N. crassa snt2* disruption affected activity of cytochrome-dependent oxidation leading to reduced oxygen consumption, probably linking this transcription factor-encoding gene to regulation of fungal aerobic respiration.

Evaluation of an alternative oxidase (AOX) respiratory pathway using GC analysis, in the presence of SHAM, did not detect changes in oxygen consumption in the Δ*snt2* mutants. This is probably due to the relatively small contribution of this pathway to oxygen consumption, even though expression of the AOX-coding gene

(*aod1*) in both FOM and *N. crassa* Δ*snt2* mutants was found to be significantly up-regulated, suggesting the presence of a compensatory mechanism, or even a potential direct link between *snt2* and regulation of alternative oxidation. Study of the *P. anserina* "long-lived" *grisea* mutant that was impaired in a copper-activated transcription factor GRISEA and was also defective in activity of cytochrome-oxidase complex (COX) IV, determined that (Pa)AOX levels are reversely dependent on COX activity (Borghouts *et al.,* 2002). The *grisea* mutant was also characterized by excessive COX-dependent oxygen uptake, lack of respiratory response to cyanide and up-regulated AOX activity (Osiewacz *et al.,* 2002).

The most extensive study of regulation of AOX expression has been performed in plants. In tobacco, it was proposed that two separate pathways for mitochondria-to-nucleus signaling of *AOX1* may exist, one involving ROS and the other organic acids, such as pyruvate (Gray *et al.,* 2004). The signal transduction pathway for regulation of *aod1* transcription in filamentous fungi is not yet clear. Involvement of a retrograde mechanism in AOX regulation was implied, since it is encoded in the nucleus, but functions in mitochondria (Chae *et al.,* 2007). A recent study on the effect of strobilurin fungicides on AOX in the wheat blight pathogens *F. graminearum* and *Microdonchium nivale* suggests that AOX activity is regulated at the transcriptional level (Kaneko and Ishii, 2009). Fungal alternative oxidase was also found to be stimulated by succinate rather than pyruvate. In the cephalosporin C-producer fungus *Acermonium chrysogenum*, AOX activity was found to be growth-rate dependent and a high metabolic rate can stimulate it even under glucose limitation (Sandor *et al.,* 2003). In *N. crassa*, alternative oxidase (*aod-1*) expression is regulated by two zinc-cluster transcription factors (Chae *et al.,* 2007). A number of functions have been suggested for the AOX pathway. In plants, the enzyme may prevent the accumulation

of ROS, prevent programmed cell death, and/or ensure proper energy and biosynthetic equilibrium during growth (Chae *et al.,* 2007). In fungi, the alternative oxidase is generally induced by conditions that impair the function of the normal electron transport chain and/or increase ROS levels, but constitutive expression has also been reported. However, in the obligate aerobe *P. anserina*, the major role of *PaAox* expression was to protect cells from respiration deficiencies and not to reduce the amounts of ROS (Borghouts *et al.,* 2002). In *M. grisea*, *aox* expression is induced by hydrogen peroxide and it was proposed that mitochochondria-originated ROS could be involved in regulation of signaling for *aox* expression (Yukioka *et al.,* 1998). In this study, an additional gene - *snt2* was identified that appears to affect COX-dependent respiration as well as *aod* expression in at least two filamentous fungi – FOM and *N. crassa*. A hypothesis is proposed, which is intended to clarify the mechanistic relation between *snt2* and aerobic respiration, in the case of direct regulation. Decreased oxygen consumption by the Δ*snt2* mutants may indicate direct, positive regulation of the COX-dependent respiration by *snt2*. The increase of *aod* expression in Δ*snt2* mutants contributes to ATP synthesis that is impaired due to malfunction of the COX respiratory pathway. Reduction in respiration increases levels of cellular ROS (Schieke and Finkel, 2006) that is known to trigger autophagy and cell death, which was also observed in Δ*snt2* mutants of FOM and *N. crassa.* In order to confirm this hypothesis a comparative functional analysis of intact mitochondria in both FOM and *N. crassa*, including estimation of transmembrane potential and level of oxidative phosphorylation, should be performed.

5.4. A probable mode of SNT2 action

On the basis of previous characterization of SNT2 of *S. pombe* it can be proposed that in *F. oxysporum* the homologous transcription factor (TF) functions as a

part of a large protein Lid2-like complex and is involved in regulation of transcription repression. Based on a literature review, a resemblance was found between the mode of action of TOR kinase and *S. pombe* SNT2. In general, Tor pathway-regulated gene expression occurs by linking between nutrient sensing to histone acetylation (Rohde and Cardenas, 2003). In *S. cerevisiae*, TOR regulates association of Rpd3–Sin3 histone deacetylase (HDAC) with rDNA chromatin, leading to site-specific deacetylation of histone H4 (Tsang *et al.*, 2003). It was also postulated that SNT2 is a budding yeast homolog of mammalian SMTR/N-Co (Yoon *et al.*, 2005). In higher eukaryotes the SMTR/N-Co is associated with HDAC3 in large protein complexes involved in transcriptional repression via histone acetylation (Li *et al.*, 2000). The recruitment of HDAC by SMRT/N-Co is performed through interaction with mSin3A and mSin3B, which are homologs of the yeast Sin3 protein (Heinzel *et al.*, 1997), the same protein that is necessary for TOR-controlled response in *S. cerevisiae*. In a recent report on the tumor suppressor protein ING2, it was postulated that its PHD domain is necessary for linking between mSin3a-HDAC1 and methylated H3K4 (Shi *et al.*, 2006). This model however, is rather provisional and needs confirmation, especially with regard to its relevance to fungal growth, development and pathogenesis. Nonetheless, the proposed model provides a basis for additional hypothesis-driven experiments that may lead to the elucidation of the mode of action of SNT2 in filamentous fungi.

6. Concluding remarks and future prospects

The current study was conducted in order to identify and characterize genes of *Fusarium oxysporum* involved in pathogenicity on muskmelon. As a result, three novel pathogenicity-related genes (*cdc48, pex7* and *snt2*) of *F. oxysporum* on muskmelon plants were identified, suggesting involvement of programmed cell death (*cdc48*) and peroxisome metabolism (*pex7*) in fungal pathogenesis. Moreover, an involvement of the adenine biosynthetic pathway in pathogenesis of *F. oxysporum* f. sp. *melonis* (FOM) was demonstrated using a UV-induced non-pathogenic isolate.

Efforts were focused on detailed characterization of reduced pathogenicity isolate (D122), impaired in the *snt2* gene, coding a novel fungal transcription factor, homologous to SNT2, a functional component of the Lid2 complex of *S. pombe*. SNT2 harbors two types of conserved functional domains - BAH and the PHD finger found in a variety of chromatin regulators and transcriptional cofactors, involved mostly in gene repression. Performed targeted disruption of *snt2* confirmed its requirement for invasive growth and full pathogenicity of *F. oxysporum* on muskmelon. Evaluation of *snt2* transcript levels in the infected host tissue, demonstrated its necessity for early pathogenesis. Phenotypical characterization of Δ*snt2* mutants of two Ascomycota clade fungi – FOM and *Neurospora crassa* identified similar developmental defects. In *N. crassa*, *snt-2* was found to be essential for sexual development, indicating an additional regulatory aspect of this gene. Analysis of differential gene expression between the wild type and tagged *snt2* mutant of FOM was conducted by utilizing suppressive subtraction hybridization (SSH) analysis, identifying fourteen putative genes, four of which (*idi4*, induced during incompatibility; *pdc*, pyruvate decarboxylase; *msf1*, transporter of the major facilitator family and *eeF1G*, eukaryotic translation elongation factor 1-gamma) were previously

found in association with the highly conserved target of rapamycin (TOR) serine/threonine kinase (Teichert *et al.*, 2006) and the global nitrogen regulator AreA (Schönig *et al.*, 2008). Using qRT-PCR analysis it was found that *snt2* represses an autophagy-related TF-coding *idi4* and *pdc*. Even though the SNT2 transcription factor shares regulation with AreA and TOR kinase, it does not appear to be involved in regulation of nitrogen metabolism. Schematic representation of the current *snt2* genetic network and proposed model of shared cellular components between *snt2* and TOR kinase is summarized in Fig. 25.

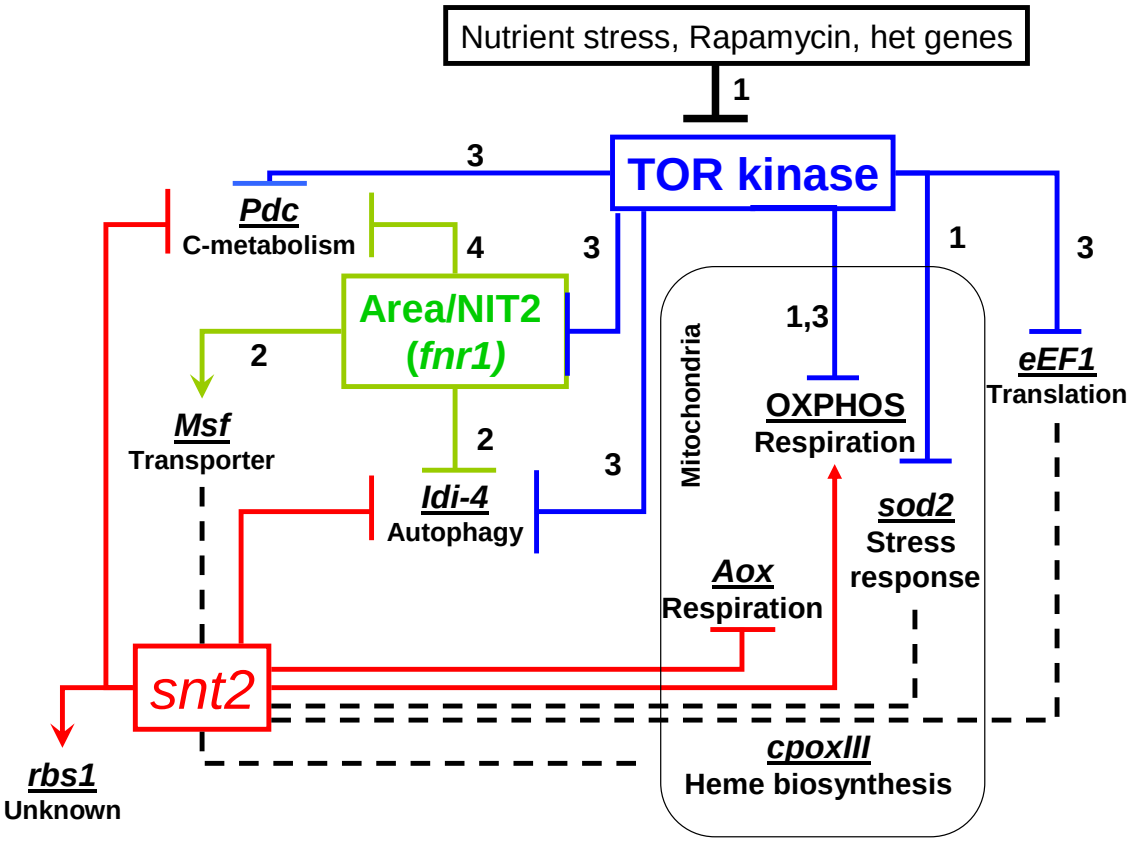

Fig. 25. Proposed model of shared cellular components between the *snt2* and TOR kinase. Red-marked and dashed links were identified in the current study. Other links were identified in the following studies: 1 - Bonawitz et al., 2007; 2 - Schonig, et al., 2008; 3 – Teichert, et al., 2006; 4 – Lockington, et al., 1997.

In view of the fact that elimination of *snt2* led to increased appearance of mature autophagosomes and cell death, it is hypothesized that *snt2* might be an additional TOR kinase independent regulatory element controlling a shift between

normal autophagy, functioning as a survival mechanism and autophagy-induced cell death. This hypothesis is supported by increased cell death, observed in mycelium of FOM and *N. crassa*. However, to confirm this hypothesis, autophagosome biogenesis has to be thoroughly monitored, via direct fluorescence microscopy, applying ATG8-GFP-tagging, which more sensitive than the currently applied MDC-staining method. An alternative hypothesis suggests that the observed morphological abnormalities are indicative of stress-related symptoms in *snt2* mutants, therefore leading to up-regulation of *idi4* gene and increased appearance of autophagosomes, as a part of survival mechanism. Thus, the increased appearance of autophagosomes belongs to a secondary phenotype and is not regulated directly by *snt2*.

Susceptibility to stress was evaluated by monitoring the reactive oxygen species (ROS) scavenging ability of Δ*snt2* mutants. Results of superoxide dismutases (SOD) enzymatic activity tests, combined with qRT-PCR analysis of SOD-encoding genes not only emphasized a posttranscriptional nature for *fe,mn sod* regulation, but also indicated a possible defect in mitochondria functioning caused by *snt2* disruption. Indeed, it was detected that *snt2* disruption affected activity of mitochondria-located cytochrome-dependent oxidation leading to reduced oxygen consumption, probably linking this transcription factor-encoding gene to regulation of fungal aerobic respiration. Detected up-regulation of the *aod1* gene, coding for an alternative oxidase pathway suggests the presence of a compensatory mechanism, or even a potential direct link between *snt2* and regulation of alternative oxidation. Interestingly, decreased respiration was demonstrated to give rise to ROS that at higher concentrations can lead to cellular dysfunction and cell death (Schieke and Finkel, 2006).

Here, a hypothesis of *snt2* involvement in cellular functioning is presented:

1) Based on comparative proteomic analysis, SNT2 is part of a large protein complex that is involved in transcriptional repression.

2) Reduced ability to adequately detoxify naturally produced ROS in mitochondria leads to mitochondrial and cell damage, and to up-regulation of stress-related genes, such as *idi4*, decreased respiration, which can lead to further ROS accumulation and cell death, while autophagy plays a protective role.

3) *snt2* displayed shared regulation with TOR kinase, representing a possible additional regulatory element for several TOR-controlled cellular functions, such as cytochrome-dependent oxidation (Fig. 25).

4) The partial deregulation of ROS-responsive SOD activity suggests a reduction in defense against oxidative burst and is presumed to contribute to reduced virulence of the FOM *snt2* mutant.

Among future prospects of studying SNT2 TF several research directions can be suggested. Since modular architecture of SNT2 proteins is conserved among fungi, the use of microarray analyses using cross-species hybridization with the available Affymetrix GeneChip of *F. graminearum*, similar to that performed by Schönig *et al* (2008), may assist in detecting additional SNT2 target genes. A link between SNT2 TF and proteins coded by SSH-detected genes and gel-mobility shift assay may be utilized. To shed light on the proteomic environment of SNT2, a wide range of biochemical techniques may be applied, including co-immunoprecipitation of the LID complex using tandem affinity purification-tagged SNT2 analysis and bimolecular fluorescence complementation assay.

7. REFERENCES

Allen, T.D. and Nuss, D.L. 2004. Linkage between mitochondrial hypovirulence and viral hypovirulence in the chestnut blight fungus revealed by cDNA microarray assay. *Eucar. Cell*, **3:** 1227-1232.

Angelova, M.B., Pashova, S.B., Spasova, B.K., Vassiliev, S.V. and Slokoska, L.S. 2005. Oxidative stress response of filamentous fungi induced by hydrogen peroxide and paraquat. *Mycol. Research***, 109:**150-158.

Asakura, M., Okuno, T. and Tanako, Y. 2006. Multiple contributions of peroxisomal metabolic function to fungal pathogenicity in *Colletotrichum lagenarium*. *Appl Envron Microbiol***, 72**: 6345-6354.

Arsham, A.M., Howell, J.J. and Simon, M.C. 2003. A novel hypoxia-inducible factor-independent hypoxic response regulating mammalian target of rapamycin and its targets. *J. Biol. Chem.* **278:** 29655–29660.

Balhadère, P.V., Foster, A.J. and Talbot, N.J. 1999. Identification of pathogenicity mutants of the rice blast fungus *Magnaporthe grisea* by insertional mutagenesis. *Mol. Plant-Microbe Interact.* **12**:129-142.

Bannister, J.V., Bannister, W.H. and Rotilio, G**.** 1987. Aspects of the structure, function, and applications of superoxide dismutase. *CRC Crit. Rev. Biochem*. **22:**111-180.

Beauchamp, C. and Fridovich, I. 1971. Superoxide dismutase: Improved assays and an assay applicable to acrylamide gels. *Anal. Biochem*. **44:** 276-287.

Beckman, C.H. 1987. The nature of wilt diseases of plants. The American Phytopathological Society Press, New York.

Bhadauria, V., Popescu, K., Zhao, W-S. and Peng, Y-L., 2007. Fungal transcriptomics. *Microbiol. Res*. 162: 285—298.

Biederbick, A., Kern, H.F. and Elsässer, H.P. 1995. Monodansylcadaverine (MDC) is a specific *in vivo* marker for autophagic vacuoles. *Eur. J. Cell Biol.* **66**:3-14.

Bolton, M.D. and Thomma, B.P.H.J. 2008. The complexity of nitrogen metabolism and nitrogen-regulated gene expression in plant pathogenic fungi. *Physiol. Mol. Plant. Pathol.* 72:101-110.

Bonawitz, N.D., Chatenay-Lapointe, M., Pan, Y. and Shadel, G.S. 2007. Reduced TOR signaling extends chronological life span via increased respiration and upregulation of mitochondrial gene expression. *Cell Metab.* **5**:265-77.

Bonnet, C., Espagne, E., Zickler, D., Boisnard, S., Bourdais, A. and Berteaux-Lecellier, V. 2006. The peroxisomal import proteins PEX2, PEX5 and PEX7 are differently involved in *Podospora anserina* sexual cycle. *Mol. Microbiol,* **62**: 157-169.

Borghouts, C., Scheckhuber, C.Q., Werner, A. and Osiewacz, H.D. 2002. Respiration, copper availability and SOD activity in *P. anserina* strains with different lifespan. *Biogerontol.* **3**: 143–153

Bosch, H., Schutgens, R.B., Wanders, R.J. and Tager, J.M. 1992. Biochemistry of peroxisomes. *Annu. Rev. Biochem.* **61:**157-197.

Brotman, Y., Silberstein, L., Kovalski, I., Perin, C., Dogimont, C., Pitrat, M., Klingler, J., Thompson, A. and Perl-Treves, R. 2002. Resistance gene homologues in melon are linked to genetic loci conferring disease and pest resistance. *Theor. Appl. Genet.* **104:**1055-1063.

Calero-Nieto, F., Di Pietro, A., Roncero, M.I.G. and Hera, C. 2007. Role of the transcriptional activator XlnR of *Fusarium oxysporum* in regulation of xylanase genes and virulence. *Mol. Plant-Microbe Interact.* **20**:977-985.

Caracuel, Z., Roncero, M.I.G., Espeso, E.A., Gonzalez-Verdejo, C.I., Garcia-Maceira, F.I. and Di Pietro, A. 2003. The pH response transcription factor PacC controls virulence in the plant pathogen *Fusarium oxysporum. Mol. Microbiol*. **48**:765-779.

Chae, M.S., Nargang, C.E., Cleary, I.A., Lin, C.C., Todd, A.T. and Nargang, F.E. 2007. Two zinc-cluster transcription factors control induction of alternative oxidase in *Neurospora crassa*. *Genet*, **177**: 1997-2006.

Chang, S., Puryear, J. and Cairney, J. 1993. Simple and efficient method for isolating RNA from pine trees. *Plant Mol Biol Rep*. **11**: 113-116.

Chary, P., Dillon, D., Schroeder, A.L. and Natvig, D.O. 1994. Superoxide dismutase (*sod-1*) null mutants of *Neurospora crassa*: oxidative stress sensitivity, spontaneous mutation rate and response to mutagens. *Genet*, **137**: 723–730.

Cohen, R., Katan, T., Katan, J. and Cohn, R. 1989. Occurrence of *Fusarium oxysporum* f. sp. *melonis* race 1,2 on muskmelon in Israel. *Phytoparasit.* **17:** 319-322.

Coleman, M., Henricot, B., Arnau, J. and Oliver, R.P. 1997. Starvation-induced genes of tomato-pathogen *Cladosporium fulvum* are also induced during growth in planta. *Mol. Plant-Microbe Interact*. **10**: 1106-1109.

Correll J.C., Klittich, C.J.R. and Leslie, J.F. 1987. Nitrate non-utilizing mutants of *Fusarium oxysporum* and their use in vegetative compatibility tests. *Phytopathol*, **77**: 1640–1646.

Davis, R.H. and de Serres, F.J. 1970. Genetic and microbiological research techniques for *Neurospora crassa. Method. Enzymol.* **17:** 79-143.

Dementhon, K., Paoletti, M., Pinan-Lucarré, B., Loubradou-Bourges, N., Sabourin, M., Saupe, S.J. and Clavé, C. 2003. Rapamycin mimics the incompatibility reaction in the fungus *Podospora anserina. Eukaryot. Cell.* **2**: 238–246.

Dementhon, K., Saupe, S.S. and Clavé, C. 2004. Characterization of IDI-4, a b-ZIP transcription factor inducing autophagy and cell death in the fungus *Podospora anserina*. *Mol. Microbiol.* **53**: 1625-1640.

Dementhon, K. and Saupe, S.S. 2005. DNA-binding specificity of the IDI-4 basic leucine zipper factor of *Podospora anserina* defined by systematic evolution of ligands by exponential enrichment (SELEX). *Eukaryot. Cell*, **4***:* 476-483.

Denisov, Y., Yarden, O. and Freeman, S. 2005. Impaired purine biosynthesis affects pathogenicity of *Fusarium oxysporum* f. sp. *melonis*. *Eur. J. Plant Pathol*, **112**: 293–297.

Di Pietro, A. and Roncero, M.I.G. 1996. Endopolygalacturonase from *Fusarium oxysporum* f. sp. *lycopersici*: purification, characterization, and production during infection of tomato plants. *Phytopathol*. **86**: 1324-1330

Di Pietro, A., Garcia-Maceira, F.I., Meglecz, E. and Roncero, M.I.G. 2001. A MAP kinase if the vascular wilt fungus *Fusarium oxysporum* is essential for root penetration and pathogenesis. *Mol. Microbiol.* **39**: 1140-1152.

Diatchenko, L., Lau, Y-F.C., Campbell, A.P., Chenchik, A., Moqadqm, F., Huang, B., Lukyanov, S., Lukyanov, K., Gurskaya, N., Sverdlov. E.D. and Siebert, P.D. 1996. Suppression subtractive hybridization: A method for generating differentially regulated or tissue-specific cDNA probes and libraries. *Proc. Natl. Acad. Sci. USA*. **93**: 6025-6030.

Divon, H.H., Ziv, C., Davydov, O., Yarden, O. and Fluhr, R. 2006. The global nitrogen regulator, FNR1, regulates nitrogen-genes and fitness during *Fusarium oxysporum* pathogenesis. *Mol. Plant-Microbe Interact*. **7**: 485-497.

Dufresne, M., Bailey, J.A., Dron, M. and Langin T. 1998. *Clk*1, a serine/threonine protein kinase-encoding gene, is involved in pathogenicity of *Colletotrichum lindemuthianum* on common bean. *Mol. Plant-Microbe Interact*. **11**: 99-108.

Duttaroy, A., Paul, A., Kundu, K. and Belton, A. 2003. A *sod2* null mutation confers severely reduced adult life span in *Drosophila*. *Genet*, **165**: 2295-2299.

Duyvesteijn, R.G.E., Wijk, R. van Boer, Y., Rep, M., Cornelissen, B.J.C. and Haring, M.A. 2005. Frp1 is a *Fusarium oxysporum* F-box protein required for pathogenicity on tomato. *Mol. Microbiol.* **57:** 1051-1063.

Eshel, D., Ben-Arie, R., Dinoor, A. and Prusky, D. 2000. Resistance of gibberellin-treated persimmon fruit to *Alternaria alternata* arises from the reduced ability of the fungus to produce endo-1,4-β-glucanase. *Phytopathol*, **90**:1256-1262.

Fang, G.C., Hanau, R.M. and Vaillancourt, L.J. 2002. The SOD2 gene, encoding a manganese-type superoxide dismutase, is up-regulated during conidiogenesis in the plant-pathogenic fungus *Colletotrichum graminicola*. *Fung. Genet. Biol*. **36**: 155–165.

Fedorova, N.D., Badger, J.H., Robson, G.D., Wortman, J.R. and Nierman, W.C. 2005. Comparative analysis of programmed cell death pathways in filamentous fungi. *BMC Genom*. **6**:177-191.

Feiler, H.S., Desprez, T., Santoni, V., Kronenberger, J., Caboche, M. and Traas, J. 1995. The higher plant *Arabidopsis thaliana* encodes a functional CDC48 homologue which is highly expressed in dividing and expanding cells. *EMBO J.* **14:** 5626-2637.

Forman, H.J. and Boveris, A. 1982. Superoxide radical and hydrogen peroxide in mitochondria. In: W.A. Pryor, Editor, *Free Radicals in Biology* Vol. V, Academic Press, New York, NY, pp. 65–90.

Fréalle, E., Noël, C., Viscogliosi, E., Camus, D., dei-Cas, E. and Delhaes, L. 2005. Manganese superoxide dismutase in pathogenic fungi: an issue with pathophysiological and phylogenetic involvements. *FEMS Imm. Med. Research.* **45:** 411-422.

Freeman, S., and Rodriguez, R.J. 1993. Genetic conversion of a fungal plant pathogen to a nonpathogenic, endophypic mutualist. *Science,* **260**: 75-78.

Freeman, S., Zveibil, A., Vintal, H. and Maymon, M. 2002. Isolation of nonpathogenic mutants of *Fusarium oxysporum* f. sp. *melonis* for biocontrol of Fusarium wilt in cucurbits. *Phytopathol,* **92**: 164-168.

Fuchs, F., Prokisch, H., Neupert, W. and Westermann, B. 2002. Interaction of mitochondria with microtubules in the filamentous fungus *Neurospora crassa*. *J Cell Sci*. **115:** 1931-1937.

Galagan, J.E., Calvo, S. E., Borkovich, K.A., Selker, E.U., Read, N.D., FitzHugh, W., Ma, L-J., Smirnov, S., Purcell, S., Rehman, B., Elkins, T., Engels, R., Wang, S., Nielsen, C.B., Butler, J., Jaffe, D., Endrizzi, M., Qui, D., Ianakiev, P., Bell-Pedersen, D., Nelson, M.A., Werner-Washburne, M., Selitrennikoff, C.P., Kinsey, J.A., Braun, E.L., Zelter, A., Schulte, U., Kothe, G.O., Jedd, G., Mewes, W., Staben, C., Marcotte, E., Greenberg, D., Roy, A., Foley, K., Naylor, J., Stange-Thomann, N., Barrett, R., Gnerre, S., Kamal, M., Kamvysselis, M., Bielke, C., Rudd, S., Frishman, D., Krystofova, S., Rasmussen, C., Metzenberg, R.L., Perkins, D.D., Kroken, S., Catcheside, D., Li, W., Pratt, R.J., Osmani, S.A., DeSouza, C.P.C., Glass, L., Orbach, M.J., Berglund, J.A., Voelker, R., Yarden, O., Plamann, M., Seiler, S., Dunlap, J., Radford, A., Aramayo, R., Natvig, D.O., Alex, L.A., Mannhaupt, G., Ebbole, D.J., Freitag, M., Paulsen, I., Sachs, M.S., Lander, E.S.,

Nusbaum, C. and Birren, B. 2003. The genome sequence of the filamentous fungus *Neurospora crassa*. *Nature*, **422**: 859-868.

Gray, G., Maxwell, D., Villarimo, A. and McIntosh, L. 2004. Mitochondria/nuclear signaling of alternative oxidase gene expression occurs through distinct pathways involving organic acids and reactive oxygen species. *Plant Cell Rep*, **23**: 497-503.

Grune, T., Merker, K., Sandig, G. and Davies, K.J.A. 2003. Selective degradation of oxidatively modified protein substrates by the proteasome. *Biochem. Biophys. Res. Commun.* **305:** 709-718.

Hahnenberger, K.M., Jia, Z. and Young, P.G. 1996. Functional expression of the *Schizosaccharomyces pombe* Na+/H+ antiporter gene, *sod2*, in *Saccharomyces cerevisiae*. *PNAS*, **93**: 5031–5036.

Heinzel, T., Lavinsky, R.M., Mullen, T.M., Söderstrom, M., Laherty, C.D., Torchia, J., Yang, W.M., Brard, G., Ngo, S.D., Davie, J.R., Seto, E., Eisenman, R.N., Rose, D.W., Glass, C.K. and Rosenfeld, M.G. 1997. A complex containing N-CoR, mSin3 and histone deacetylase mediates transcriptional repression. *Nature*, **387**: 43-48.

Hoen, P.A.C., Ariyurek, Y., Thygesen, H.H., Vreugdenhil, E., Vossen, R.H.A.M., de Menezes, R.X., Boer, J.M., van Ommen, G-J.B. and den Dunnen, J.T. 2008. Deep sequencing-based expression analysis shows major advances in robustness, resolution and inter-lab portability over five microarray platforms. *Nucl. Acid. Res*. doi:10.1093/nar/gkn705.

Horowitz, S., Freeman, S., Zveibil, A. and Yarden, O. 2006. A defect in *nir1*, a *nirA*-like transcription factor, confers morphological abnormalities and loss of pathogenicity in *Colletotrichum acutatum*. *Mol. Plant Pathol.* **7**: 341-354.

Inoue, I., Ohara, T., Namiki, F. and Tsuge, T. 2001. Isolation of pathogenicity mutants of *Fusarium oxysporum* f. sp. *melonis* by insertional mutagenesis. *J. Gen. Plant Pathol.* **67**:191-199.

Inoue, I., Namiki, F. and Tsuge, T. 2002. Plant colonization by the vascular wilt fungus *Fusarium oxysporum* requires FOW1, a gene encoding a mitochondrial protein. *Plant Cell*, **14**: 1869-1883.

Imazaki, I., Kurahashi, M., Iida, Y. and Tsuge, T. 2007. Fow2, a Zn(II)2Cys6-type transcription regulator, controls plant infection of the vascular wiltfungus *Fusarium oxysporum*. *Mol. Microbiol*. **63**: 737-753.

Jain, S., Akiyama, K., Mae, K., Ohguchi, T. and Takata, R. 2002. Targeted disruption of a G protein a subunit gene results in reduced pathogenicity in Fusarium oxysporum. *Curr. Genet*. **41**: 407–413.

Joobeur, T., King, J.J., Nolin, S.J., Thomas, C.E. and Dean, R.A. 2004. The Fusarium wilt resistance locus Fom-2 of melon contains a single resistance gene with complex features. *Plant J*, **39**: 283-297.

Kaneko, I. and Ishii, H. 2009. Effect of azoxystrobin on activities of antioxidant enzymes and alternative oxidase in wheat head blight pathogens *Fusarium graminearum* and *Microdochium nivale. J Gen Plant Pathol*. **75**: 388–398.

Kershaw, M.J. and Talbot, N.J. 2009. Genome-wide functional analysis reveals that infection-associated fungal autophagy is necessary for rice blast disease. *Proc. Natl. Acad. Sci. USA.* **109:** 15967–15972.

Khang, C.H., Park, S.Y., Lee, Y.H. and Kang, S. 2005. A dual selection based, targeted gene replacement tool for *Magnaporthe grisea* and *Fusarium oxysporum*, *Fungal Genet. Biol.* **42**: 483–492.

Kiffin, R., Bandyopadhyay, U. and Cuervo, A.M. 2006. Oxidative stress and autophagy. *Antioxid. Redox Sig*, **8:**152-162.

Kiel, J.A.K.W., Veenhuis, M. and van der Klei, I.J. 2006. PEX genes in fungal genomes: common, rare or redundant. *Traff*, **7**: 1291–1303.

Kikuma, T., Ohneda, M., Arioka, M. and Kitamoto, K. 2006. Functional analysis of the *ATG8* homologue *Aoatg8* and role of autophagy in differentiation and germination in *Aspergillus oryzae*. *Eukar. Cell*, **8**:1328-1336.

Kim, H. and Woloshuk, C.P. 2008. Role of AREA, a regulator of nitrogen metabolism, during colonization of maize kernels and fumonisin biosynthesis in *Fusarium verticillioides*. *Fung. Genet. Biol.* **45**: 947-53.

Kim, K.S., Min, J.Y. and Dickman, M.B. 2008. Oxalic acid is an elicitor of plant programmed cell death during Sclerotinia sclerotiorum disease development. *Mol. Plant-Microbe Interact.* **21**: 605-12.

Kimura, A., Takano, Y. Furusawa, I. and Okuno. T 2001. Peroxisomal metabolic function is required for appressorium-mediated plant infection by *Colletotrichum lagenarium*. *Plant Cell*, **13**:1945-1957.

Kirkinezosa, I.G. and Moraes, C.T. 2001. Reactive oxygen species and mitochondrial diseases. *Semin Cell Dev Biol*, **12**: 449–457.

Kobayashi, M., Matsuo, Y., Tanimoto, A., Suzuki, S., Maruo, F. and Shoun, H. 1996. Denitrification, a novel type of respiratory metabolism in fungal mitochondrion. *J Biol Chem*, **271**: 16263–16267.

Kohda, T.A., Tanaka, T., Konomi, M., Sato, M., Osumi, M. and Yamamoto, M., 2007. Fission yeast autophagy induced by nitrogen starvation generates a nitrogen source that drives adaptation processes. *Genes. Cells*, **12**: 155-170.

Kono, Y., Yamamoto, H., Takeuchi, M. and Komada, H. 1995. Alterations in superoxide dismutase and catalase in *Fusarium oxysporum* during starvation-induced differentiation. *Bioch. Bioph. Act*, **1268**: 35-40.

Kuwazaki, S., Takaya, N., Nakamura, A. and Shoun, H. 2003. Formate-forming fungal catabolic pathway to supply electrons to nitrate respiration. *Biosci. Biotechnol. Biochem.* **67:** 937-939.

Lee, Y.H., Lin, Q., Boelsterli, U.A. and Chung, M.C. 2010. The Sod2 mutant mouse as a model for oxidative stress: A functional proteomics perspective. *Mass Spectrom. Rev*. **29**: 179-96.

Lengeler, K.B., Fox, D.S., Fraser, J.A., Allen, A., Forrester, K., Dietrich, F.S. and Heitman, J. 2002. Mating-type locus of *Cryptococcus neoformans:* a step in the evolution of sex chromosomes. *Eukaryot. Cell,* **1**: 704-718.

Levine, B. and Klionsky, D.J. 2004. Development by self-digestion: molecular mechanisms and biological functions of autophagy. *Develop.Cell*. **6:** 463-477.

Li, J., Wang, J., Wang, J., Nawaz, Z., Liu, J.M., Qin, J. and Wong, J. 2000. Both corepressor proteins SMRT and N-CoR exist in large protein complexes containing HDAC3. *EMBO J.* **19**: 4342-4350.

Li, F., Huarte, M., Zaratiegui, M., Vaughn, M.W., Shi, Y., Martienssen, R. and Cande, W.Z. 2008. Lid2 is required for coordinating H3K4 and H3K9 methylation of heterochromatin and euchromatin. *Cell*, DOI 10.1016.

Lin, C-H., Yang, S.L. and Chung, K-R. 2009. The YAP1 homolog–mediated oxidative stress tolerance is crucial for pathogenicity of the necrotrophic fungus *Alternaria alternata* in citrus. *Mol. Plant-Microbe Interact.* **22:** 942-952.

Liu, X.F., Elashvili, I., Gralla, E.B., Valentine, J.S., Lapinskas. P. and Culotta, V.C. 1992. Yeast lacking superoxide dismutase. *J Biol Chem*. **267**: 18298-18302.

Liu, X.H., Lu, J.P. and Lin, F.C. 2007. Autophagy during conidiation, conidial germination and turgor generation in *Magnaporthe grisea*. *Autophagy*, 3: 472-473.

Liu, Y.G. and Whittier, R.F. 1995. Thermal asymmetric interlaced PCR: automatable amplification and sequencing of insert end fragments from P1 and YAC clones for chromosome walking. *Genom*, **25**: 674-81.

Lockington, R.A., Borlace, G.N. and Kelly, J.M. 1997. Pyruvate decarboxylase and anaerobic survival in *Aspergilus nidulans*. *Gene*, **191**: 61-67.

Lopez-Berges, M.S., Di Pietro, A., Daboussi, M.-J., Wahab, H.A., Vasnier, C., Roncero, M.I.G. and Dufresne, M.H. 2009. Identification of virulence genes in *Fusarium oxysporum* f. sp. *lycopersici* by large-scale transposon tagging. *Mol Plant Pathol.* **10**: 95-107.

Lopez-Huertas, E., Corpas, J.F., Sandalio, M.L. and del Rio, A.L. 1999. Characterization of membrane polypeptides from pea leaf peroxisomes involved in superoxide radical generation. *Biochem. J*. **337**: 531-536.

Lu, B.C.K. 2006. Programmed cell death in fungi. In: Growth, differentiation and sexuality, 2nd edition. Springer Berlin Heidelberg Press. 167-187 pp.

Lu, J.P., Liu, T.B. and Lin, F.C. 2005. Identification of mature appressorium-enriched transcripts in *Magnaporthe grisea*, the rice blast fungus, using suppression subtractive hybridization. *FEMS Microbiol Lett*. **245**: 131–7.

Ma, L.J., van der Does, H.C., Borkovich, K.A., Coleman, J.J., Daboussi, M.J., Di Pietro, A., Dufresne, M., Freitag, M., Grabherr, M., Henrissat, B., Houterman, P.M., Kang, S., Shim, W.B., Woloshuk, C., Xie, X., Xu, J.R., Antoniw, J., Baker, S.E., Bluhm, B.H., Breakspear, A., Brown, D.W, Butchko, R.A., Chapman, S., Coulson, R., Coutinho, P.M., Danchin, E.G., Diener, A., Gale, L.R., Gardiner, D.M., Goff, S., Hammond-Kosack, K.E., Hilburn, K., Hua-Van, A., Jonkers, W.,

Kazan, K., Kodira, C.D., Koehrsen, M., Kumar, L., Lee, Y.H., Li, L., Manners, J.M., Miranda-Saavedra, D., Mukherjee, M., Park, G., Park, J., Park, S.Y., Proctor, R.H., Regev, A., Ruiz-Roldan, M.C., Sain, D., Sakthikumar, S., Sykes, S., Schwartz, D.C., Turgeon, B.G., Wapinski, I., Yoder, O., Young, S., Zeng, Q., Zhou, S., Galagan, J., Cuomo, C.A., Kistler, H.C. and Rep, M. 2010. Comparative genomics reveals mobile pathogenicity chromosomes in Fusarium. *Nature*, 464, 367-73.

Madden, L.V. and Wheelis, M. 2003. The threat of plant pathogens as weapons against U.S. crops. *Ann Rev Phytopathol*, **41**: 155-176.

Matityahu, A., Hadar, Y., Dosoretz, C.G. and Belinky, P.A. 2008. Gene silencing by RNA interference in the white rot fungus *Phanerochaete chrysosporium*. *App. Environ. Microbiol***, 74:** 5359-5365**.**

Meijer, W.H., van der Klei, I.J., Veenhuis, M. and Kiel, J.A.K.W. 2007. ATG genes involved in non-selective autophagy are conserved from yeast to man. *Autophagy*, **3:** 106-116.

Mellor, J. 2006. It takes a PHD to read the histone code. *Cell*, **126**: 22-24.

Michielse, C.B., Hooykaas, P.J., Cees A.M.J.J., van den Hondel, C.A. and Ram, A.F.J. 2005. *Agrobacterium*-mediated transformation as a tool for functional genomics in fungi. *Curr. Genet.* **48**: 1-17.

Michielse, C.B. and Rep, M. 2009. Pathogen profile update: *Fusarium oxysporum*. *Mol. Plant Pathol.*, **10**, 311-324.

Michielse, C.B., van Wijk, R., Reijnen, L., Cornelissen, B.J.C. and Rep, M. 2009. Insight into the molecular requirements for pathogenicity of *Fusarium oxysporum* f. sp. *lycopersici* through large-scale insertional mutagenesis. *Genome Biol*, 10:R4 (doi:10.1186/gb-2009-10-1-r4).

Miller, R.V., Ford, E.J., Zidack, N.J. and Sands, D.C. 1989. A pyrimidine auxotroph of *Sclerotinia sclerotiorum* for use in biological weed control. *J. Gen. Microbiol.* **135**: 2085-2091.

Möller, E.M., Bahnweg, G., Sanderman, H. and Geiger, H.H. 1992. A simple and efficient protocol for isolation of high molecular weight DNA from filamentous fungi, fruit bodies and infected plant tissues. *Nucl. Acid. Research,* **20**: 6115-6116.

Moore, S., De Vries, O.M.H. and Tudzynski, P. 2002. The major Cu,Zn SOD of the phytopathogen *Claviceps purpurea* is not essential for pathogenicity. *Mol Plant Pathol*. **3**: 9 –22.

Mullins, E.D., Chen, X., Romanie, P., Raina, R., Geiser, D.M. and Kang, S. 2001. *Agrobacterium*-mediated transformation of *Fusarium oxysporum*: An efficient tool for insertional mutagenesis and gene transfer. *Phytopathol,* **91**: 173-180.

Müssig, C., Kauschmann, A., Clouse, S.D. and Altmann, T. 2000. The *Arabidopsis* PHD-finger protein SHL is required for proper development and fertility. *Mol Gen Genet.* **264**: 363-70.

Namiki, F., Matsunaga, M., Okuda, M., Inoue, I., Fujita, Y. and Tsuge, T. 2001. Mutation of an arginine biosynthesis gene causes reduced pathogenicity in *Fusarium oxysporum* f. sp. *melonis. Mol. Plant-Microb. Interact*. **14**: 580-584.

Narasipura, S.D., Chaturvedi, V. and Chaturvedi, S. 2005. Characterization of *Cryptococcus neoformans* variety *gattii SOD2* reveals distinct roles of the two superoxide dismutases in fungal biology and virulence. *Mol. Microbiol*. **55**: 1782–1800.

Nelson, N. 1945. A photometric adaptation of the Somogyi method for the determination of glucose. *Biol. Chem.* **153**: 375-380.

Nelson, P.E., Toussoun, T.A. and Cook, R.J. 1981. Fusarium: disease, biology and taxonomy. Pennsylvania State University Press: University Park, Pennsylvania. 457 pp.

Nir-Paz, R., Strahilevitz, J., Shapiro, M., Keller, N., Goldschmied-Reouven, A., Yarden, O., Block, C. and Polacheck, I. 2004. Clinical and epidemiological aspects of infections caused by *Fusarium* species: a collaborative study from Israel. *J Clin. Microbiol.* **42**: 3456-3461.

Pascual, J., Martinez-Yamout, M., Dyson, H.J. and Wright, P.E. 2000. Structure of the PHD zinc finger from human Williams–Beuren syndrome transcription factor, *J. Mol. Biol.* **304**: 723–729.

Perchepied, L. and Pitrat, M. 2004. Polygenic inheritance of partial resistance to *Fusarium oxysporum* f.sp. *melonis* race 1.2 in melon. *Phytopathol*, **94**: 1331-1336.

Perfect, J.R., Toffaletti, D.L. and Rude, T.H. 1993. The gene encoding phosporibosylaminoimidazole carboxylase (ADE2) is essential for growth of *Cryptococcus neoformants* in cerebrospinal fluid. *Inf Imm*, **6**1: 4446-4451.

Perkins, D.D., Radford, A. and Sachs, M.S. 2001. *The Neurospora Compendium: Chromosomal Loci*. Academic Press, San Diego.

Pinan-Lucarré, B., Balguerie, A. and Clavé, C. 2005. Accelerated cell death in *Podospora* autophagy mutants. *Eukaryot Cell*, **4**: 1765–1774.

Pinan-Lucarré, B., Paoletti, M., Dementhon, K., Coulary-Salin, B. and Clavé, C. 2002. Autophagy is induced during cell death by incompatibility and is essential for differentiation in the filamentous fungus *Podospora anserina*. *Mol. Microbiol*. **47**: 321-333.

Pinan-Lucarré, B., Paoletti, M. and Clavé, C. 2007. Cell death by incompatibility in the fungus *Podospora*. *Seminar. Cancer Biol*. **17**: 101-111.

Piñeiro, M., Gómez-Mena, C., Schaffer, R., Martínez-Zapater, J. M. and Coupland, G. 2003. EARLY BOLTING IN SHORT DAYS is related to chromatin remodeling factors and regulates flowering in Arabidopsis by repressing FT. *Plant Cell***, 15:** 1552-1562**.**

Pollack, J.K., Harris, S.D. and Marten, M.R. 2009. Autophagy in filamentous fungi. *Fungal Genet. Biol.* **46**: 1-8.

Pfaffl, M.W., Horgan G.W. and Demfie, L. 2002. Relative expression software tool (REST©) for group-wise comparison and statistical analysis of relative expression results in real-time PCR. *Nucl. Acid. Research,* **30**: 36-44.

Prusky, D., Gold, S. and Keen, N.T. 1989. Purification and characterization of an endopolygalacturonase produced by *Colletotrichum gloeosporioides*. *Physiol. Mol. Plant Pathol.* **35**: 121-133.

Puig, S., Lau, M. and Thiele, D.J. 2004. Cti6 Is an Rpd3-Sin3 histone deacetylase-associated protein required for growth under iron-limiting conditions in *Saccharomyces cerevisiae*. *J Biol. Chem,* **279**: 30298-30306.

Ortoneda, M., Guarro, J, Madrid, M.P., Caracuel, Z., Roncero, M.I.G., Mayayo, E. and Di Pietro, A. 2004. *Fusarium oxysporum* as a multihost model for the genetic dissection of fungal virulence in plants and mammals. *Inf. Immun*. **72**: 1760-1766.

Osiewacz, H.D. 2002. Genes, mitochondria and aging in filamentous fungi. *Age. Res. Rev.* **1**: 425-442.

Quadbeck-Seeger, C., Wanner, G., Huber, S., Kahnmann, R. and Kämper, J. 2000. A protein with similarity to the human retinoblastome binding protein 2 acts scecifically as a repressor for genes regulated by the *b* mating type locus in *Ustilago maydis*. *Mol. Microbiol.* **38:** 154-166.

Raha, S. and Robinson, B.H. 2000. Mitochondria, oxygen free radicals, disease and aging. *Trends Biochem. Sci.* **25**: 502–508.

Rahman, M., Groverc, A., Peacock, W.J., Dennis, E.S. and Ellis, M.H. 2001. Effects of manipulation of pyruvate decarboxylase and alcohol dehydrogenase levels on the submergence tolerance of rice. *Aust. J. Plant Physiol.*, **28**: 1231–1241.

Ramos, B., Alves-Santos, F.M., García-Sánchez, M.A., Martín-Rodrigues, N., Eslava, A.P. and Díaz-Mínguez, J.M. 2007. The gene coding for a new transcription factor (ftf1) of *Fusarium oxysporum* is only expressed during infection of common bean. *Fungal Genet. Biol.* **44**: 864-876.

Ramos-Pamplona, M. and Naqvi, N.I. 2006. Host invasion during rice-blast disease requires carnitine-dependent transport of peroxisomal acetyl-CoA. *Mol Microbiol*. **61**: 61-75.

Rep, M., Meijer, M., Houterman, P.M., van der Does, H.C. and Cornelissen, B.J.C. 2005. *Fusarium oxysporum* evades I-3-mediated resistance without altering the matching avirulence gene. *Mol. Plant-Microbe Interact*. **18**: 15-23.

Risser, G., Banhishemi, Z. and Davis, D.V. 1976. A proposed nomenclature of *Fusarium oxysporum* f. sp. *melonis* races and resistance genes in *Cucumis melo. Phytopathol,* **66**: 1105-1106.

Rohde, J.R. and Cardenas, M.E. 2003. The Tor pathway regulates gene expression by linking nutrient sensing to histone acetylation. *Mol. Cell Biol.* **23**: 629-635.

Rohde, J.R., Heitman, J. and Cardenas, M.E. 2001.The TOR kinases link nutrient sensing to cell growth. *J. Biol. Chem*. **276**: 9583-9586.

Roguev, A., Shevchenko, A., Schaft, D., Thomas, H., Stewart, A.F. and Shevchenko, A. 2004. A comparative analysis of an orthologous proteomic environment in the

yeasts *Saccharomyces cerevisiae* and *Schizosaccharomyces pombe*. *Mol. Cell. Proteom*. **3**:125-32.

Sambrook, J., Fritsch, E.F. and Maniatis, T. 1989. Molecular Cloning: A laboratory manual. 2nd ed. Cold Spring Harbor Laboratory, Cold Spring Harbor, NY.

Sandor, E., Fekete, E. and Karaffa, L. 2003. Regulation of the cyanide-resistant alternative respiratory pathway in the fungus *Acremonium chrysogenum*. *Food Technol. Biotechnol.* **47**: 43-47.

Saraste, M. 1999. Oxidative Phosphorylation at the *fin de siècle*. *Science*, **283:** 1488-1493.

Scandalios, J.G. 1993. Oxygen stress and superoxide dismutases. *Plant Phisiol.* **101:**7-12.

Scherz-Shouval, R. and Elazar, Z. 2007. ROS, mitochondria and the regulation of autophagy. *Trend Cell Biol.* **17**: 422-7.

Schönig, B., Brown, D.W., Oeser, B. and Tudzynski, B. 2008. Cross-species hybridization with *Fusarium verticillioides* microarrays reveals new insights into *Fusarium fujikuroi* nitrogen regulation and the role of AreA and NMR. *Eukaryot. Cell.* **7**:1831-1846**.**

Segers, G., Bradshaw, N., Archer, D., Blissett, K. and Oliver, R.P. 2001. Alcohol oxidase is a novel pathogenicity factor for *Cladosporium fulvum*, but aldehyde dehydrogenase is dispensable. *Mol. Plant-Microbe Interact*. **14**: 367–377.

Schieke, S.M. and Finkel, T. 2006. Mitochondrial signaling, TOR, and life span. *Biol Chem*, **387:** 1357-1361.

Shi, X., Hong, T., Walter, K.L., Ewalt, M., Michishita, E., Hung, T., Carney, D., Peña, P., Lan, F., Kaadige, M.R., Lacoste, N., Cayrou, C., Davrazou, F., Saha, A., Cairns, B.R., Ayer, D.E., Kutateladze, T.G., Shi, Y., Côté, J., Chua, K.F. and

Gozani, O. 2006. ING2 PHD domain links histone H3 lysine 4 methylation to active gene repression. *Nature*. **442**: 96-9.

St. Clair, D. 2004. Manganese Superoxide Dismutase: Genetic Variation and Regulation. *J. Nutr*. **134**: 3190S–3191S.

Stade, C. and Brambl, R. 1981. Mitochondrial biogenesis during fungal spore germination: respiration and cytochrome c oxidase in *Neurospora crassa*. *J Bacteriol.* **147:** 757–767.

Sweigard, J.A., Carroll, A.M., Farrall, L, Chumley F.G. and Valent, B. 1998. *Magnaporthe grisea* pathogenicity genes obtained through insertional mutagenesis. *Mol. Plant-Microbe Interact*. **11**: 404-412.

Takemoto, D., Tanaka, A. and Scott, B. 2007. NADPH oxidases in fungi: Diverse roles of reactive oxygen species in fungal cellular differentiation. *Fung Gen Biol.* 44: 1065–1076.

Tanaka, Y., Katagiri, Z., Kawahashi, K., Kioussis, D. and Kitajima, S. 2007. Trithorax-group protein ASH1 methylates histone H3 lysine 36. *Gene,* **397**:161-168.

Takaya, N., Kuwazaki, S., Adachi , Y., Suzuki, S., Kikuchi, T., Nakamura, H., Shiro, Y. and Shoun, H. 2003. Hybrid respiration in the denitrifying mitochondria of *Fusarium oxysporum*. *J Biochem.* **133**: 461-465.

Thannickal, V.J. and Fanburg, B.L., 2000. Reactive oxygen species in cell signaling. *Am J Physiol Lung Cell Mol Physiol.* **279**: L1005– L1028.

Tsang, C.K., Bertram, P.G., Ai, W., Drenan, R. and Zheng X.F.S. (2003) Chromatin-mediated regulation of nucleolar structure and RNA Pol I localization by TOR. *EMBO J.* **22**:6045-6056.

Teichert, S., Wottawa, M., Schönig, B. and Tudzynski, B. 2006. Role of the *Fusarium fujikuroi* TOR kinase in nitrogen regulation and secondary metabolism. *Eukaryot. Cell*, **5**: 1807-1819. T

Torres, M.A., Jones, J.D.G. and Dangl, J.L. 2006. Reactive oxygen species signaling in response to pathogens. *Plant Physiol*, **141**: 373-378.

Tshijimoto, Y. and Shimizu, S. 2005. Another way to die; autophagic programmed cell death. *Cell Death Diff.* **12**: 1528-1534.

Veneault-Fourrey, C., Barooah, M., Egan, M., Wakley, G. and Talbot, N.J. 2006. Autophagic fungal cell death is necessary for infection by the rice blast fungus. *Science*, **312**: 580-583.

Völkel, P. and Angrand, P.O. 2007. The control of histone lysine methylation in epigenetic regulation. *Biochimie,* **89**: 1–20.

Ward, L.D. and Bussmaker, H.J. 2008. Predicting functional transcription factor binding througn alignment-free and affinity-based analysis of orthologous promoter sequences. *Bioinformatics*, **24:** 165-171.

Weld, R.J., Plummer, K.M., Carpenter, M.A. and Ridgway, H.J. 2006. Approaches to functional genomics in filamentous fungi. *Cell Research*, **16:** 31–44.

Wheeler, M.D., Nakagami, M., Bradford, B.U., Uesugi, T., Mason, R.P., Connor, H.D., Dikalova, A., Kadiiska, M. and Thurman, R.G. 2001. Overexpression of manganese superoxide dismutase prevents alcohol-induced liver injury in the rat. *J Biol. Chem.* **276:** 36664–36672.

Wojtaszek, P. 1997. Oxidative burst: an early plant response to pathogen infection. *Biochem. J.* **322**: 681–692.

Yen, W.-L. and Klionsky, D.J. 2008. How to live long and prosper: autophagy, mitochondria, and aging. *Physiol*, **23**: 248-262.

Yoon, H-G., Choi, Y., Cole P.A. and Wong, J. 2005. Reading and function of a histone code involved in targeting corepressor complexes for repression. *Mol. Cell. Biol.* **25**: 324–335.

Yukioka, H., Inagaki, S., Tanaka, R., Katoh, K., Miki, N., Mizutani, A. and Masuko, M. 1998. Transcriptional activation of the alternative oxidase gene of the fungus *Magnaporthe grisea* by a respiratory-inhibiting fungicide and hydrogen peroxide. *Biochim Biophys Acta*, **1442**: 161–169.

Zhou, Z., Takaya, N., Nakamura, A., Yamaguchi, M., Takeo, K. and Shoun, H. 2002. Ammonia fermentation, a novel anoxic metabolism of nitrate by fungi. *J Biol. Chem.* **277:** 1892-1896.

Zvirin, T., Herman, R., Brotman, Y., Denisov, Y., Belausov, E., Freeman, S. and Perl-Treves, R. 2010. Differential colonization and defence responses of resistant and susceptible melon lines infected by *Fusarium oxysporum* race 1,2. *Plant Pathol*. Doi: 10.1111/j.1365-3059.2009.02225.